AD 284 659

DISCLAIMER NOTICE

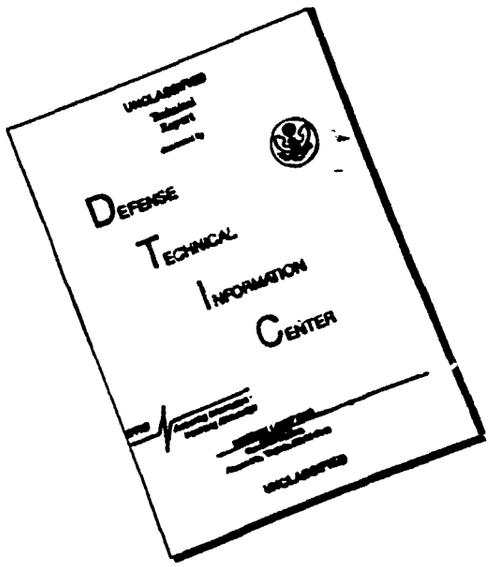

THIS DOCUMENT IS BEST QUALITY AVAILABLE. THE COPY FURNISHED TO DTIC CONTAINED A SIGNIFICANT NUMBER OF PAGES WHICH DO NOT REPRODUCE LEGIBLY.

HYDRODYNAMICS & STABILITY & CONTROL OF A TANDEM PROPELLER SUBMARINE

Prepared for:
OFFICE OF NAVAL RESEARCH
MATHEMATICAL SCIENCES DIVISION
DEPARTMENT OF THE NAVY
WASHINGTON, D.C.

FINAL REPORT - PHASE I
By: D.C. Clark and F. Dell'Amico
CAL Report No. AG-1634-V-2
August 1962

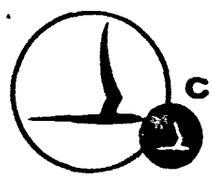

CORNELL AERONAUTICAL LABORATORY, INC.
OF CORNELL UNIVERSITY, BUFFALO 21, N Y

CORNELL AERONAUTICAL LABORATORY, INC.
Buffalo, New York

PHASE I - FINAL REPORT
ON THE
HYDRODYNAMICS & STABILITY & CONTROL
OF A
TANDEM PROPELLER SUBMARINE

CAL REPORT NO. AG-1634-V-2
August 1962

Prepared for
Office of Naval Research
Mathematical Sciences Division
Department of the Navy
Washington, D. C.

Prepared by: D. C. Clark
D. C. Clark
Research Engineer

Prepared by: F. Dell'Amico
F. Dell'Amico
Section Head
Vehicle Dynamics Dept.

Approved by L. Segel
L. Segel
Assistant Dept. Head
Vehicle Dynamics Dept.

FOREWORD

This report describes the work performed by the Cornell Aeronautical Laboratory, Inc. under Contract Nonr-3659(00)(FBM), sponsored by the Office of Naval Research of the Department of the Navy. The time period of the contract ran from 16 October 1961 to 20 August 1962. The program is being conducted under the general direction of Cdr. F. R. Haselton, Code 466, and R. Cooper, Code 438, of the Office of Naval Research.

The authors wish to express their gratitude to Messrs. E. F. Schroeder and L. Segel (Vehicle Dynamics Department, CAL) for their contributions to the stability and control studies, and to Messrs. C. Tufts, F. DuWaldt and E. Sullivan (Applied Mechanics Department, CAL) for valuable assistance in the hydrodynamic studies.

ABSTRACT

Hydrodynamic and stability and control characteristics are investigated for a novel submarine configuration employing tandem, large hub-to-diameter ratio propellers whose blades can be pitched both collectively and cyclicly. The propulsion and lateral control forces which can be produced by the propellers at very low forward speeds (including zero) are defined by means of simple blade-element theory that includes, however, the effects of propeller-induced, axial inflow velocity. The resulting analysis is employed to investigate the problem of trimming the submarine at hovering speeds.

An earlier analysis of stability and control at high speeds was continued and extended. The analysis indicates that the TPS can be stabilized and controlled at high speeds. Maneuvering performance in the pitch-plane is equivalent to that of a conventional submarine except that a higher percentage of the total available control effectiveness must be used in performing diving maneuvers. It is found that the minimum turning radius of the TPS, when operating at high speeds, is approximately five times greater than that of a conventional submarine, as a result of the requirement for using part of the control effectiveness for stabilization purposes. As operating speeds are decreased, however, the turning performance of the TPS becomes markedly superior to that of the conventional submarine.

In addition to two-propeller operation, stability and control is investigated for off-design conditions, with either the fore or aft propeller operating as the active control element

TABLE OF CONTENTS

LIST OF FIGURES

LIST OF TABLES

I

INTRODUCTION

In October 1961 the Cornell Aeronautical Laboratory, Inc. undertook to investigate the hydrodynamic and stability and control aspects of a novel submarine configuration utilizing variable-pitch, large hub-to-diameter-ratio propellers. The configuration, invented by Cdr. F. R. Haselton of the Office of Naval Research, employs two propellers mounted circumferentially (forward and aft) on a neutrally buoyant body of revolution, to produce any combination of forces and moments. By means of this arrangement, which has been called a Tandem Propeller Submarine (TPS), it is possible to produce control forces in three degrees of freedom, or control moments in three degrees of freedom, as well as combinations of these forces and moments.

The work undertaken by the Cornell Aeronautical Laboratory has as its basic objectives (a) the theoretical determination of the hydrodynamic characteristics of the tandem-propeller configuration, (b) an investigation of the trim and stability and control characteristics of the controlled submarine, and (c) a comparison between the TPS and a conventional submarine with respect to stability and control characteristics and handling qualities.

Certain of these objectives were partially achieved and reported upon in Reference 1, entitled "First Interim Report on the Hydrodynamics and Stability and Control of a Tandem Propeller Submarine." Reference 1 contains a large portion of the general results of the entire program and will be frequently referred to in what follows. The present report covers work accomplished since the publication of Reference 1 and should be treated as a continuation of that report, since it has not been considered practical to attempt to repeat herein the bulk of the material presented in the earlier document. (It should be noted however that some of the key figures and the terminology are repeated in Section III.) Accordingly, the reader will profit by reviewing Reference 1, especially the section on stability and control (Section VII). For those who cannot, the section entitled "Summary of Conclusions" is taken verbatim from Reference 1 and repeated below in the hope that it will help bridge the gap between Reference 1 and this report.

(1) Analysis of the stability coefficients for the high-speed case shows that, in comparison with conventional submarines, the gains in control effectiveness achieved at low and zero speeds (plus the gain in control flexibility) are obtained at a sacrifice of high-speed control effectiveness.

(2) The TPS is dynamically unstable in pitch, unless control forces and moments are applied to modify and eliminate this instability. The instability arises primarily from the large unstable pitching moment due to angle-of-attack (M_w) relative to the levels of damping in pitch (M_q) possessed by the TPS.

(3) The divergence in pitch motion, due to instability, is sufficiently severe to require automatic stabilization in contrast to manual stabilization.

(4) Although other types of stabilizing feedbacks were investigated for use in an automatic pitch-control system, simple pitch-rate and pitch-angle feedbacks were found to be effective. Well-

damped pitch-angle responses to pitching moment control inputs can be obtained in about 60 seconds. Corresponding steady-state dive or climb rates of about 6 ft/sec are easily achieved. These figures do not represent maximum achievable performance.

(5) An analog computer investigation shows that the level of the command control inputs must be limited to keep the propeller blade angles of attack within their stall limits when cyclic and collective pitch are used for automatic stabilization. Computed feedback-loop gains that originally appeared to be so large that continual saturation of the cyclic-pitch control would result, were found to be acceptable, provided limits were placed on maneuver demands.

(6) Although an investigation of the yaw-plane dynamics has not been completed it is probable that conclusions, similar to those given above for pitch, will eventually be reached.

(7) It has been shown that within certain speed limits it is possible to trim the TPS in high-speed, straight and level flight, with one propeller fixed and one operating. Speeds of about 15 knots can be achieved with a single propeller operating at 50 rpm. (An investigation of the problem of maneuvering the TPS with one propeller operating remains to be completed. It is anticipated that this control mode will present a serious problem.)

(8) With respect to the overall stability and control problems, the tentative conclusion is reached that automatic control of the TPS submarine is feasible. Comparison with a conventional submarine has not yet been made nor has the question of handling qualities been examined fully.

The present report is devoted, in the main, to the following topics:

(a) A theoretical development (started in Ref. 1) of the hydrodynamic forces/moments produced by the tandem propellers in low-speed flight, including hovering (inflow velocity is taken into consideration, but cascade effects, swirl and propeller interaction are not).

(b) A brief investigation of trim operation at low-speed.

(c) Stability and control studies of the pitch and yaw plane dynamics at high speed. (This work is comparable to the pitch-plane studies reported in Reference 1 and, in fact, is a logical continuation of that work.)

(d) A discussion of the predicted handling qualities (limited to unpiloted, controlled-vehicle performance) of a TPS configuration, including a comparison between a TPS and a conventional submarine.

(e) A brief investigation of the influence of hovering and high-speed maneuvers on control linkage resolution.

A summary of the results that have been obtained and of the conclusions drawn to date for the entire program is given in Section II. Recommendations for future work are discussed in Section VIII.

II

SUMMARY OF RESULTS AND CONCLUSIONS

Results and conclusions based on work performed prior to 25 March 1962 were reported in Reference 1 and repeated in the Introduction (Section I). Results and conclusions, based on work accomplished since the publication of Reference 1 are given below.

(1) The previously presented hydrodynamic analysis for the low-speed (and hovering) case has been refined and brought into conformity with the nomenclature and symbology of Reference 1 and this report. The complete set of equations describing the forces/moments produced by the propellers on the hull are given in Table 4.1-1. These equations include the effects of propeller-induced axial-inflow velocity, but not the effects of blade cascading, swirl and propeller interaction. The validity of the equations in Table 4.1-1 is subject to these limitations.

(2) The above equations have been reduced to a set of approximate force/moment coefficients (see Table 4.1-2) that yield the propeller forces/moments, at zero speed, as a function of the motion variables v, w, p, q, r and the blade-angle components δ_0, δ_1, and δ_2 (collective, sine-cyclic, and cosine-cyclic pitch respectively). These coefficients are subject to further limitation that δ_0 be small ($\leq$ about 0.1 rad) and that δ_1 and δ_2 be small relative to δ_0.

(3) Trim operation at zero and nearly zero forward speeds was investigated in connection with the production of pure sideforce under these conditions. It appears that the production of pure sideforce, at zero forward speed, cannot be accomplished with zero collective pitch in the propellers and that counter-thrusting collective pitch must be used. Under the restrictions given in (2) above $\dot{y}$ and $\dot{z}$ velocities of about 0.1 ft/sec ($\Omega \cong 1$ rad/sec) and .5 ft/sec ($\Omega \cong 5$ rad/sec) can be achieved. In performing pure translational maneuvers at very low speed, coupled forces/moments exist, but they are generally quite small and it should be possible to null them out by proper control action.

(4) It has not been possible to accomplish any significant work in the general area of six-degree-of-freedom stability and control at low (and very low) forward speeds. It is anticipated that this work will be accomplished at some future date, with the aid of an analog computer simulation (see Section VIII).

(5) At high forward speeds, the proposed TPS configuration is capable of maximum diving rates comparable to a conventional submarine of the Albacore class. These large depth rates, however, require about 22% of the available control power compared with about 8% in the case of the Albacore.

(6) At high forward speeds direct-axis feedback stabilization is desirable in both yaw and pitch plane maneuvers. Pitch angle and depth rate are most effectively controlled by ordered pitching moment control (δ_{mc}). Yaw rate is most effectively controlled by ordered yawing moment control (δ_{nc}). Z-force and Y-force commands (δ_{zc} and δ_{yc}) require excessive propeller blade angles.

(7) Nonlinear control coupling effects are negligible in the yaw and pitch planes at high forward speeds.

(8) The yawing moment due to roll rate and sideforce due to roll rate derivatives (N_p and Y_p respectively) are negligibly small, thus eliminating yaw plane stability dependence on roll coupling and separating the yaw plane from the roll plane in all stability calculations at high forward speeds. Conversely, the rolling moment due to yaw rate and side velocity derivatives (K_r and K_v) are not negligible and the roll behavior of the submarine is affected by yaw plane motions.

(9) Stable, easily controlled, submarine yaw plane motions result from single propeller operation at high forward speeds when the forward propeller is disabled. Conversely, when the aft propeller is disabled, yaw plane instability occurs for feedback gains that produce well-behaved, two-propeller submarine responses. Very large feedback signals are necessary to achieve static stability when the aft propeller is disabled, and the dynamic response of the submarine is totally unsatisfactory. Additional stability augmentation through feedback control is not possible in this case, requiring modification of stability derivatives (through the use of auxiliary control surfaces, for example).

(10) Gyroscopic coupling between the pitch and yaw planes, resulting from unbalanced propeller operation, is negligible at high forward speeds.

(11) With respect to overall stability and control problems the general conclusion is reached that automatic control of the TPS submarine is feasible. Limited comparisons with a conventional submarine have been made and no drastic differences in pitch-plane maneuvering performance have been found for the high forward speed case. There is, however, a significant difference in the percentage of total available hydrodynamic forces available which must be used to perform certain maneuvers, the TPS requiring higher percentages than a conventional submarine. As a consequence maximum yaw-plane responses are somewhat less than those of

a conventional submarine. These high-speed limitations on TPS maneuverability are not serious, however, because the operation of the TPS is such that turning maneuvers can be performed at low speeds, where the propeller forces and moments can be used to greatest advantage.

(12) A preliminary investigation of the influence of maneuvering requirements on blade-pitch angle resolution reveals that the high speed case will probably determine resolution. For example, in order to change forward speed by one ft/sec a resolution on collective pitch, δ_0 , of about 1° is needed. To change steady-state dive angle by 1° a resolution on sine-cyclic pitch, δ_1 , of about 0.2° is needed. The requirement on the resolution of cosine-cyclic pitch, δ_2 , does not appear to be as stringent as that on sine-cyclic pitch.

III

SYMBOLS AND NOMENCLATURE

The symbols and nomenclature used in this report are, for the most part, those used in Reference 1. For convenience these are repeated here, along with new symbols, in Table 3-1.

The postulated TPS configuration, the blade pitch-angle geometry, and the physical constants associated with the postulated configuration are also those of Reference 1. These data are repeated in Figures 3-1 and 3-2 and Table 3-2.

TABLE 3-1 Symbols and Nomenclature

Symbol		Description	Units
d	=	Max. hull diameter (or drag coefficient)	ft (dimensionless)
f	=	Fineness ratio = ℓ/d	
ℓ	=	Length of submarine	ft
ℓ_1	=	Distance, fore point to c.g.	ft
ℓ_2	=	Distance, prop. plane to c.g. (ℓ_2 carries no sign)	ft
$\overline{gb}$	=	Metacentric height	ft
Δ	=	Submerged displacement (= Weight)	lbs
R	=	Average propeller radius	ft
D	=	Average propeller diameter	ft
N	=	Number of blades per propeller	
A	=	Blade area	ft^2
Ω	=	Blade angular velocity (Ω carries no sign)	rad/sec
n	=	Blade angular velocity (n carries no sign)	rev/sec
C_{L_α}	=	Lift coefficient (the symbol C is sometimes used)	
C_{d_o}	=	Profile drag coefficient (the symbol d is sometimes used)	
f_i	=	Induced drag coefficient	
γ	=	Flight path angle of the blade (see Fig. 3-2)	rad
α	=	Blade angle-of-attack (see Fig. 3-2)	rad
δ	=	Total instantaneous blade pitch (see Fig. 3-2)	rad
δ_o	=	Collective pitch (see Fig. 3-2)	rad
$\Delta\delta$	=	Change in collective pitch (see Fig. 3-2)	rad

Symbol		Description	Units
b_o	=	Blade angle of attack due to collective pitch ($b_o = \delta_o + \Delta\delta - \gamma_o$)	rad
σ	=	Blade azimuth angle in plane of prop. (see Fig. 3-2)	rad
$\delta_1 \sin\sigma$	=	Sine component of cyclic pitch (see Fig. 3-2)	rad
$\delta_2 \cos\sigma$	=	Cosine component of cyclic pitch (see Fig. 3-2)	rad
a, b	=	Dimensionless constants used to define inflow velocity	
U	=	Total velocity of c.g. ($U^2 = u^2 + v^2 + w^2$)	ft/sec
u	=	x -component of velocity (perturbation = $\bar{u}$)	ft/sec
v	=	y -component of velocity (perturbation = $\bar{v}$)	ft/sec
w	=	z -component of velocity (perturbation = $\bar{w}$)	ft/sec
p	=	x-component of total angular velocity (perturbation = ϕ)	rad/sec
q	=	y -component of total angular velocity (perturbation = $\dot{\theta}$)	rad/sec
r, γ	=	z -component of total angular velocity (perturbation = $\dot{\psi}$)	rad/sec
V	=	Blade velocity relative to water (see Fig. 3-2)	ft/sec
v_t	=	Tangential component of V	ft/sec
v_a	=	Axial component of V	ft/sec
i, λ	=	Propeller-induced (axial) inflow velocity	ft/sec
$K_1 - K_2 - K_3$	=	Coefficients of accession to mass along $x - y - z$	dimensionless
$K_4 - K_5 - K_6$	=	Coefficients of accession to inertia around $x - y - z$	dimensionless

Symbol		Description	Units
m	=	Mass of submarine	$\#\text{-sec}^2/\text{ft}$
m_1	=	Virtual mass along $x = m(1+K_1)$	$\#\text{-sec}^2/\text{ft}$
m_2	=	Virtual mass along $y = m(1+K_2)$	$\#\text{-sec}^2/\text{ft}$
m_3	=	Virtual mass along $z = m(1+K_3)$	$\#\text{-sec}^2/\text{ft}$
I_{xo}-I_{yo}-I_{zo}	=	Submerged moments of inertia about x-y-z	$\#\text{-ft-sec}^2$
I_{xx}	=	Virtual moment of inertia about $x = I_{xo}(1+K_4)$	$\#\text{-ft-sec}^2$
I_{yy}	=	Virtual moment of inertia about $y = I_{yo}(1+K_5)$	$\#\text{-ft-sec}^2$
I_{zz}	=	Virtual moment of inertia about $z = I_{zo}(1+K_6)$	$\#\text{-ft-sec}^2$
H	=	Propeller angular momentum	#-ft-sec
ρ	=	Water density	$\#\text{-sec}^2/\text{ft}^4$
F_{xo}	=	Trim thrust available from one propeller	#
M_{xo}	=	Trim moment of one propeller	ft-#
P_o	=	Trim propeller power	hp
M_θ	=	Metacentric pitching moment coefficient $= mgz_b$	ft-#/rad
X_c-Y_c-Z_c	=	Control (propeller) forces (hi-speed)	#
K_c-M_c-N_c	=	Control (propeller) moments (hi-speed)	#-ft
ΣX-ΣY-ΣZ	=	Combined propeller and hull hydrodynamic and hydrostatic forces (hi-speed)	#
ΣK-ΣM-ΣN	=	Combined propeller and hull hydrodynamic and hydrostatic moments (hi-speed)	#-ft
X_p-Y_p-Z_p	=	Total propeller x-y-z forces (low-speed)	#
K_p-M_p-N_p	=	Total propeller x-y-z moments (low-speed)	ft-#

Symbol		Description	Units
X'_u	=	Dimensionless x -force derivative* due to $\bar{u}$	
Y'_v	=	Dimensionless y -force derivative due to $\bar{v}$	
Y'_r	=	Dimensionless y -force derivative due to $\dot{\psi}$	
Y'_p	=	Dimensionless y -force derivative due to $\dot{\phi}$	
Z'_w	=	Dimensionless z -force derivative due to $\bar{w}$	
Z'_q	=	Dimensionless z -force derivative due to $\dot{\theta}$	
K'_v	=	Dimensionless x -moment derivative due to $\bar{v}$	
K'_p	=	Dimensionless x -moment derivative due to $\dot{\phi}$	
K'_r	=	Dimensionless x -moment derivative due to $\dot{\psi}$	
M'_w	=	Dimensionless y -moment derivative due to $\bar{w}$	
M'_q	=	Dimensionless y -moment derivative due to $\dot{\theta}$	
N'_v	=	Dimensionless z -moment derivative due to $\bar{v}$	
N'_r	=	Dimensionless z -moment derivative due to $\dot{\psi}$	
N'_p	=	Dimensionless z -moment derivative due to $\dot{\phi}$	
X^P_u	=	Dimensional x-force derivative due to $\bar{u}_p$ **	#/ft per sec
X^P_p	=	Dimensional x-force derivative due to $\dot{\phi}_p$	#/rad per sec
Y^P_r	=	Dimensional y-force derivative due to $\bar{v}_p$	#/ft per sec
Y^P_q	=	Dimensional y -force derivative due to $\dot{\theta}_p$	#/rad per sec
Z^P_w	=	Dimensional z-force derivative due to $\bar{w}_p$	#/ft per sec
Z^P_r	=	Dimensional z-force derivative due to $\dot{\psi}_p$	#/rad per sec

---

* All of the primed derivatives and the P superscripted derivatives apply to the high-speed case only. These are hull and propeller derivatives respectively.

** The P subscript denotes perturbations with respect to propeller axes. Propeller axes are parallel to body axes but with origin at $x = \ell_2$, forward and aft.

Symbol		Description	Units
$K_p^{\dot{p}}$	=	Dimensional x-moment derivative due to $\dot{\phi}_p$	#-ft/rad per sec
$K_u^{\bar{u}_p}$	=	Dimensional x-moment derivative due to $\bar{u}_p$	#-ft/ft per sec
$M_\theta^{\dot{\theta}_p}$	=	Dimensional y-moment derivative due to $\dot{\theta}_p$	#-ft/rad per sec
$M_v^{\bar{v}_p}$	=	Dimensional y-moment derivative due to $\bar{v}_p$	#-ft/ft per sec
$N_w^{\bar{w}_p}$	=	Dimensional z-moment derivative due to $\bar{w}_p$	#-ft/ft per sec
$N_\psi^{\dot{\psi}_p}$	=	Dimensional z-moment derivative due to $\dot{\psi}_p$	#-ft/rad per sec
F_x-F_y-F_z	=	x-y-z components of lift and drag, prop. axes	#
F_T	=	Tangential force at average radius R	#
M_x-M_y-M_z	=	x-y-z components of moment, prop. axes	#-ft
L-D	=	Lift and drag forces	#
$X_{\Delta\delta}$	=	Dimensional x-force propeller coefficient* due to $\Delta\delta$	#/rad
$X_{(\Delta\delta)^2}$	=	Dimensional x-force propeller coefficient due to $(\Delta\delta)^2$	#/rad^2
X_{δ^2}	=	Dimensional x-force propeller coefficient due to δ_1^2 or δ_2^2	#/rad^2
Y_δ	=	Dimensional y-force propeller coefficient due to δ_2	#/rad
$Y_{\Delta\delta\cdot\delta}$	=	Dimensional y-force propeller coefficient due to $\Delta\delta\cdot\delta_2$	#/rad^2
Z_δ	=	Dimensional z-force propeller coefficient due to δ_1	#/rad
$Z_{\Delta\delta\cdot\delta}$	=	Dimensional z-force propeller coefficient due to $\Delta\delta\cdot\delta_1$	#/rad^2

* All of the propeller coefficients given in this table apply to the high-speed case.

Symbol		Description	Units
$K_{\Delta\delta}$	=	Dimensional χ -moment propeller coefficient due to $\Delta\delta$	#/rad
K_{δ^2}	=	Dimensional χ -moment propeller coefficient due to δ_1^2 or δ_2^2	#/rad^2
$K_{(\Delta\delta)^2}$	=	Dimensional χ -moment propeller coefficient due to $(\Delta\delta)^2$	#/rad^2
M_δ	=	Dimensional γ-moment propeller coefficient due to δ_1	#/rad
M_{δ_2}	=	Dimensional γ-moment propeller coefficient due to δ_2	#/rad
$M_{\Delta\delta\cdot\delta_2}$	=	Dimensional γ-moment propeller coefficient due to $\Delta\delta\cdot\delta_2$	#/rad^2
N_δ	=	Dimensional γ-moment propeller coefficient due to δ_2	#/rad
N_{δ_1}	=	Dimensional γ-moment propeller coefficient due to δ_1	#/rad
$N_{\Delta\delta\cdot\delta_1}$	=	Dimensional γ-moment propeller coefficient due to $\Delta\delta\cdot\delta_1$	#/rad^2
λ_T	=	Propeller thrust parameter	nondimensional
λ_Q	=	Propeller torque parameter	nondimensional
λ_P	=	Propeller power parameter	nondimensional
P	=	Power	ft-#/sec
P_{HP}	=	Power	hp
$\mathcal{P}$	=	Nondimensional power	
$\mathcal{T}$	=	Propeller thrust coefficient	nondimensional
μ	=	Propeller torque coefficient	nondimensional
f	=	tan γ (used in Ref. 1 only)	nondimensional

The symbols given below are used only in Section 7.2 and are consistent with the terminology of Reference 1. Terms not defined in Reference 1 are defined below.

Symbol		Description	Units
$K_{\dot{y}}$	=	Direct-axis side-force equation feedback gain	sec/ft
$\bar{K}_{\dot{\psi}}$	=	Direct-axis yawing moment equation feedback gain	sec
$\bar{K}_{\dot{\phi}}$	=	Direct-axis rolling moment equation rate feedback gain	sec
$\bar{K}_{\phi}$	=	Direct-axis rolling moment equation position feedback gain	
$K_{\dot{\psi}}$	=	Yaw rate into sideslip velocity decoupling feedback gain	sec
$K_{\dot{\phi}}$	=	Roll rate into sideslip velocity decoupling feedback gain	sec
$\bar{K}_{\dot{y}}$	=	Side slip velocity into yaw rate decoupling feedback gain	sec/ft
$\bar{K}_{\dot{\phi}}$	=	Roll rate into yaw rate decoupling feedback gain	sec
$\bar{K}_{\dot{\psi}}$	=	Yaw rate into roll position decoupling feedback gain	sec
$\bar{K}_{\dot{y}}$	=	Sideslip velocity into roll position decoupling feedback gain	sec/ft
I_p	=	Propeller inertia	lb ft sec^2
s	=	Laplace transform variable	rad/sec

Symbol	Description
$\lvert\ \rvert$	absolute value

Dots over symbols signify time derivatives

Subscripts:

a	aft
f	forward
c	ordered or commanded value
ss	steady-state
C	propeller control forces/moments (high speed)

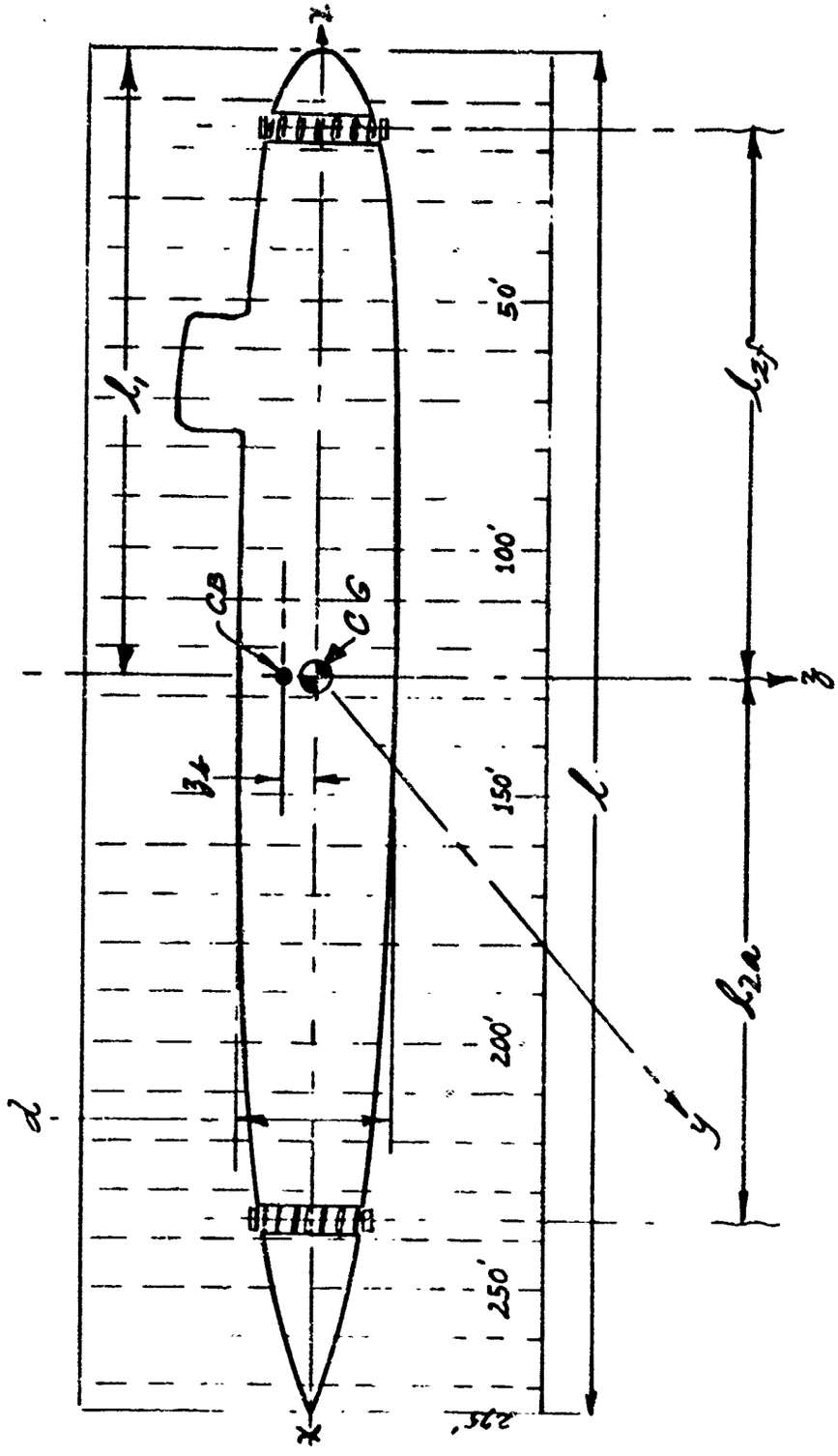

FIGURE 3-1 - Tandem Propeller Submarine

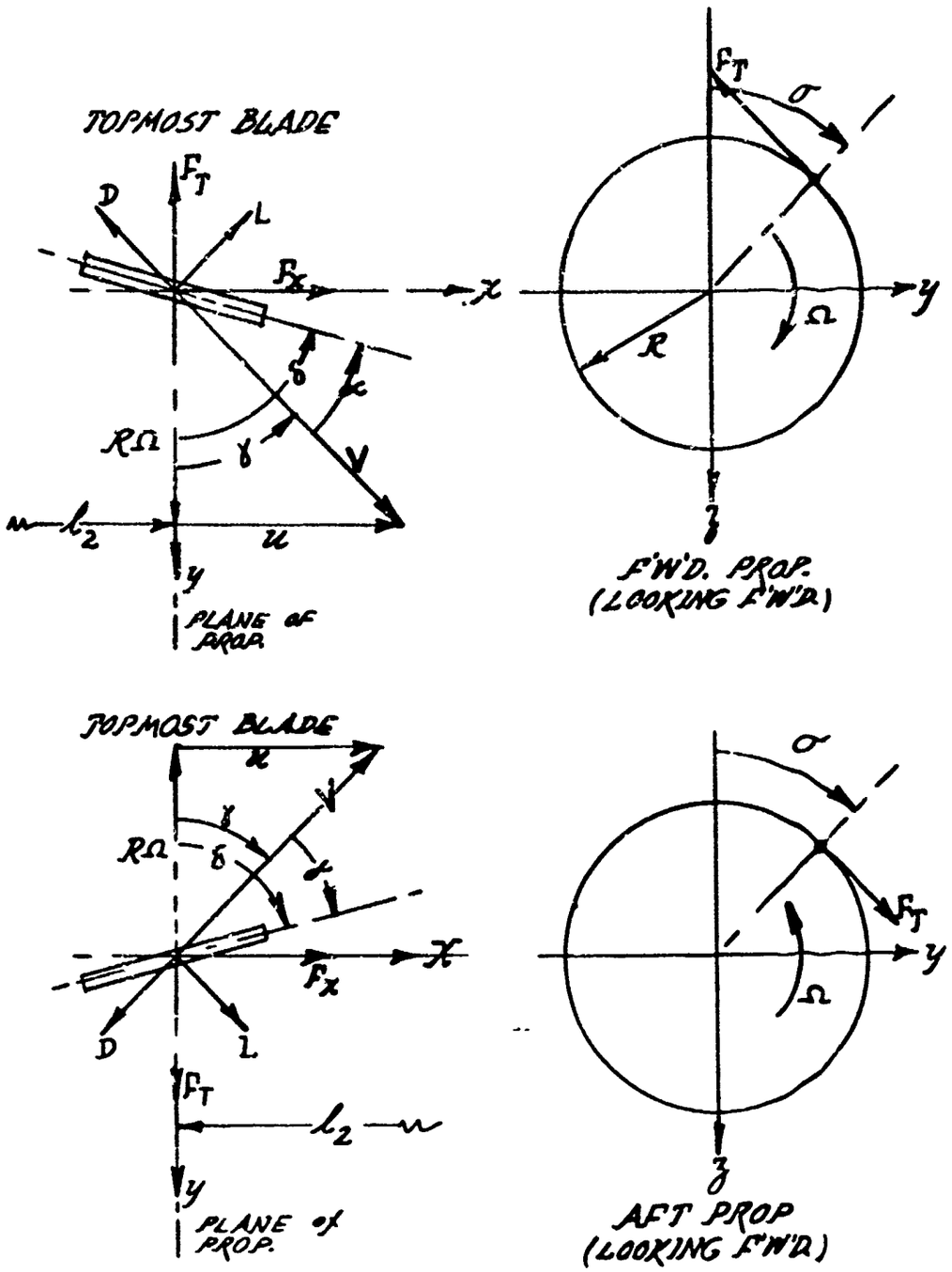

$\delta = \delta_0 + \Delta\delta + \delta_1 \sin\sigma + \delta_2 \cos\sigma$

δ_0 = TRIM COLLECTIVE PITCH

$\Delta\delta$ = CHANGE IN COLLECTIVE PITCH

$b_0 = \delta_0 + \Delta\delta - \gamma_0$

$\delta_1 \sin\sigma$, $\delta_2 \cos\sigma$ } CYCLIC COMPONENTS OF PITCH

$\alpha = \delta - \gamma$

FIGURE 3-2 - Propeller Sign Conventions

TABLE 3-2 Physical Properties of the Postulated TPS

		Symbol
Hull		
Submerged displacement	4300 long tons (= weight)	$\Delta = W$
Length	275 ft	ℓ
Maximum diameter	32 ft	d
Fineness ratio	8.6	f
Distance, forepoint to c.g.	125 ft	ℓ_1
Distance, propeller plane to c.g.	110 ft fore and aft	ℓ_2
Metacentric height	-1.0 ft	z_b
Propellers		
Hub diameter	20 ft	
Tip diameter	24 ft	
Number of blades	16	N
Maximum rpm	50	
Blade area	3 ft^2	A
Average radius	11 ft	R
Average diameter	22 ft	D

Other Physical Data (see list of symbols)

$m = 299.3 \times 10^3$ #-sec^2/ft

$M_\Theta = -9.63 \times 10^6$ ft-#/rad

$m_1 = m(1 + K_1) = m(1.026) = 307.1 \times 10^3$ #-sec^2/ft

$m_2 = m(1 + K_2) = m(1.95) = 583.7 \times 10^3$ #-sec^2/ft

$m_3 = m(1 + K_3) = m(1.95) = 583.7 \times 10^3$ #-sec^2/ft

$I_{xo} = m\ell^2/10f^2 = 30.61 \times 10^6$ #-ft-sec^2

$I_{yo} = m(.23\ell)^2 = 1197 \times 10^6$ #-ft-sec^2

$I_{zo} = m(.23\ell)^2 = 1197 \times 10^6$ #-ft-sec^2

$I_{xx} = I_{xo}(1 + K_4) = I_{xo}(1) = 30.61 \times 10^6$ #-ft-sec^2

Other Physical Data (continued)

$I_{yy} = I_{yo}(1 + K_5) = I_{yo}(1.86) = 2227 \times 10^6$ #-ft-sec^2

$I_{zz} = I_{zo}(1 + K_6) = I_{zo}(1.86) = 2227 \times 10^6$ #-ft-sec^2

C_{d_o} (high-and low-speed) = .015

C_{L_α} (high-speed only) = 3.59

C_{L_α} (low-speed only) = 5.7

Ω = 5.24 rad/sec (= 50 rpm), high-speed case

$\gamma_o \cong 35°$ (high-speed trim)

V = 70.5'/sec (high-speed trim)

Note: Numerical values for high-speed hull derivatives, propeller stability derivatives, and propeller control force and moment coefficients may be found in Reference 1.

IV

HYDRODYNAMIC ANALYSIS--LOW-SPEED FLIGHT

4.1 THE HYDRODYNAMIC CHARACTERISTICS OF TANDEM PROPELLERS

Expressions for the hydrodynamic forces and moments due to the propellers were derived in Section 5.2.2.2 of Reference 1 for the low-speed case. Unlike the theoretical development for the high-speed case, propeller-induced inflow velocity was taken into consideration. The analysis in Reference 1 was developed in the terminology of Reference 11 and, in addition, was considered tentative and preliminary. It is proposed here to set down the propeller hydrodynamics in somewhat more detail and in the nomenclature adopted in Reference 1 and in this report. The resulting equations may be considered as superseding those presented in Reference 1.

In Figure 4.1-1, we define:

$v_t(\sigma)$ = local tangential blade velocity (in the plane of the propeller, perpendicular to the average radius R) relative to the water.

$v_a(\sigma)$ = local axial blade velocity (perpendicular to the plane of the propeller) relative to the water.

$V(\sigma)$ = total blade velocity relative to the water.

i = propeller-induced (axial) inflow velocity.

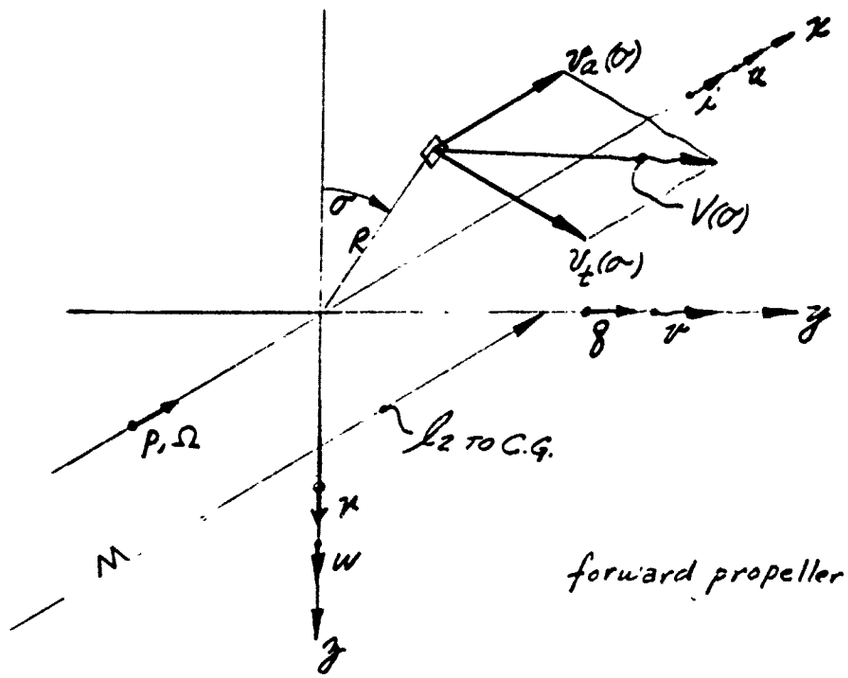

Figure 4.1-1 Blade Kinematics

For the forward propeller:*

$$v_t(\sigma)]_f = R(\Omega + p) + (v + x\ell_2)\cos\sigma + (w - q\ell_2)\sin\sigma \qquad (4.1\text{-}1)$$

$$v_a(\sigma)]_f = u + i - qR\cos\sigma - xR\sin\sigma \qquad (4.1\text{-}2)$$

---

* Hull interference effects on v and w are taken into account later.

Similarly, for the aft propeller (counterclockwise rotation, looking forward):

$$v_t(\sigma)]_a = R(\Omega - p) - (v + \ell_2)\cos\sigma - (w + q\ell_2)\sin\sigma \qquad (4.1\text{-}3)$$

$$v_a(\sigma)]_a = u + \dot{\ell} - qR\cos\sigma + \ell R\sin\sigma \qquad (4.1\text{-}4)$$

Since (4.1-3) and (4.1-4) differ from (4.1-1) and (4.1-2) only in a negative sign pre-fixing p, v, and w, the first pair of equations may be used to derive results for the forward propeller, with the understanding that a sign change in p, v, and w must be made in order to apply these expressions to the aft propeller.

The lift and drag produced by one blade is:

$$L(\sigma) = \tfrac{1}{2}\rho A V^2 C_{L_\alpha}(\delta - \gamma) \qquad (4.1\text{-}5)$$

$$D(\sigma) = \tfrac{1}{2}\rho A V^2 [C_{d_0} + f_1 C_{L_\alpha}^2 (\delta - \gamma)^2] \qquad (4.1\text{-}6)$$

in which it is understood that V, δ and γ are functions of the propeller azimuth angle σ. Thus: (see Figure 3-2 *)

$$\gamma(\sigma) = TAN^{-1}\frac{v_a(\sigma)}{v_t(\sigma)} \qquad (4.1\text{-}7)$$

$$\delta(\sigma) = \gamma(\sigma) + \alpha(\sigma) = \delta_0 + \delta_1 \sin\sigma + \delta_2 \cos\sigma \qquad (4.1\text{-}8)$$

$$V^2(\sigma) = v_t^2(\sigma) + v_a^2(\sigma) \qquad (4.1\text{-}9)$$

---

* In order to simplify the analysis, change in collective pitch $\Delta\delta$ is no longer used.

It should be noted that the numerical value of the lift curve slope, C_{L_α}, used in this development should be the two-dimensional section value (approximately 5.7/radian) since the induced velocity will appear explicitly in the hydrodynamic angle of attack. Use of this value, unmodified for unsteady effects, also implies the assumption that $\sigma_0 > \sqrt{\sigma_1^2 + \sigma_2^2}$.

Before proceeding to develop the appropriate expressions for forces and moments, it will be useful to define a number of approximations and linearizations that will be used in the derivations to follow. For convenience, the parenthetic notation (σ), signifying "a function of sigma" is discarded.

From (4.1-1):

$$v_t = R\Omega\left[1 + \frac{p}{\Omega} + \frac{(v + r\ell_2)}{R\Omega}\cos\sigma + \frac{(w - q\ell_2)}{R\Omega}\sin\sigma\right] \qquad (4.1\text{-}10)$$

and

$$v_t^2 \cong R^2\Omega^2\left[1 + \frac{2p}{\Omega} + \frac{2(v + r\ell_2)}{R\Omega}\cos\sigma + \frac{2(w - q\ell_2)}{R\Omega}\sin\sigma\right] \qquad (4.1\text{-}11)$$

For small motions and all but very low propeller speeds* it appears that the second order terms in the motion variables p, v, and w, can properly be ignored in Equation (4.1-11).

Also, Equation (4.1-2) can be rewritten as:

$$v_a = R\Omega\left[\frac{u + i'}{R\Omega} - \frac{q\cos\sigma}{\Omega} - \frac{r\sin\sigma}{\Omega}\right] \qquad (4.1\text{-}12)$$

and v_a is assumed to be small relative to v_t so that:

$$V \cong v_t \qquad (4.1\text{-}13)$$

---

* Minimum propeller speed is believed to be of the order of 1 rad/sec, so that $R\Omega$ (min) $\cong$ 11 ft/sec.

Other approximations are:

$$\sin\gamma = \frac{v_a}{V} \cong \frac{v_a}{v_t} \cong \gamma \qquad (4.1\text{-}14)$$

$$\cos\gamma = \frac{v_t}{V} \cong 1 \qquad (4.1\text{-}15)$$

$$\tan\gamma = \frac{v_a}{v_t} \cong \gamma \qquad (4.1\text{-}16)$$

$$v_a v_t \cong R^2\Omega^2\left[\frac{u+a'}{R\Omega} - \frac{p}{\Omega}\cos\sigma - \frac{r}{\Omega}\sin\sigma\right] \qquad (4.1\text{-}17)$$

$$\frac{v_a}{v_t} \cong \frac{u+a}{R\Omega}\left\{1 - \frac{p}{\Omega} - \left[\frac{Rq}{u+a} + \frac{v+rh_2}{R\Omega}\right]\cos\sigma + \left[\frac{Rr}{u+a} + \frac{w-qh_2}{R\Omega}\right]\sin\sigma\right\} \qquad (4.1\text{-}18)$$

The propeller forces and moments, written in propeller axes, are obtained by resolving the lift and drag forces along Z and tangent to the average blade circle to obtain the axial force F_Z, and the tangential force F_T. The remaining forces and moments follow from the geometry of the situation. The complete set of expressions, for N blades, comparable to Equations (5-7) through (5-13) of Reference 1 (the high-speed case), are:

$$F_Z = N\tfrac{1}{2}\rho A N V^2\left\{C_{L_\alpha}(\delta-\gamma)\cos\gamma - C_{d_0}\sin\gamma - f_1 C_{L_\alpha}^2(\delta-\gamma)^2\sin\gamma\right\} \qquad (4.1\text{-}19)$$

$$F_T = \tfrac{1}{2}\rho A N V^2 \left\{ C_{L_\alpha}(\delta-\gamma)\sin\gamma + C_{d_0}\cos\gamma + f_i C_{L_\alpha}^2 (\delta-\gamma)^2 \cos\gamma \right\} \quad (4.1\text{-}20)$$

$$F_y = -/+ \; F_T \cos\sigma \quad (4.1\text{-}21)$$

$$F_z = -/+ \; F_T \sin\sigma \quad (4.1\text{-}22)$$

$$m_x = -/+ \; F_T R \quad (4.1\text{-}23)$$

$$m_y = -/- F_x R \cos\sigma \quad (4.1\text{-}24)$$

$$m_z = -/- F_x R \sin\sigma \quad (4.1\text{-}25)$$

As has been used previously, the notation -/+ denotes forward/aft propeller.

4.1.1 Axial Force

On substituting (4.1-11), (4.1-8), (4.1-7) and (4.1-13) into (4.1-19) and using the approximations (4.1-14) through (4.1-18), the instantaneous axial force becomes:

$$F_x = +/+ \tfrac{1}{2}\rho A N \Big\{ v_t^2 C_{L_\alpha} \left[\delta_0 + \delta_1 \sin\sigma + \delta_2 \cos\sigma - \frac{v_a}{v_t}\right] - v_t^2 C_{d_0} \frac{v_a}{v_t}$$

$$- v_t^2 f_1 C_{L_\alpha}^2 \left[\delta_0^2 + 2\delta_0\delta_1 \sin\sigma + 2\delta_0\delta_2 \cos\sigma + \delta_1^2 \sin^2\sigma + 2\delta_1\delta_2 \sin\sigma\cos\sigma \right.$$

$$\left. + \delta_2^2 \cos^2\sigma\right] \frac{v_a}{v_t}$$

$$+ v_t^2 f_1 C_{L_\alpha}^2 \left[2\delta_0 \frac{v_a}{v_t} + 2\delta_1 \sin\sigma \frac{v_a}{v_t} + 2\delta_2 \cos\sigma \frac{v_a}{v_t} - \frac{v_a^2}{v_t^2}\right] \frac{v_a}{v_t} \Big\}$$

(4.1-26)

The average axial force is obtained by integrating (4.1-26) over one cycle and dividing by 2π . The result is*:

$$F_x = +/+ Q\Big\{ C_{L_\alpha}\Big[(1+\tfrac{2\mu}{\pi})\delta_0 + \Big(\tfrac{\pi+\pi l_2}{R\pi}\Big)\delta_2 + \Big(\tfrac{W-ql_3}{R\pi}\Big)\delta_1 - \Big(\tfrac{u+\dot{\iota}}{R\Omega}\Big)\Big]$$

$$-C_{d_0}\Big[\tfrac{u+\dot{\iota}}{R\Omega}\Big]$$

$$-f_1 C_{L_\alpha}^2\Big[\Big(\tfrac{u+\dot{\iota}}{R\Omega}\Big)\Big(\delta_0^2 + \tfrac{\delta_1^2}{2} + \tfrac{\delta_3^2}{2} + \tfrac{2\delta_2 q}{\Omega} + \tfrac{2\delta_1 \pi}{\Omega}\Big)$$

$$-\Big(\tfrac{u+\dot{\iota}}{R\Omega}\Big)^2(2\delta_0)$$

$$+\Big(\tfrac{u+\dot{\iota}}{R\Omega}\Big)^3\Big(1-\tfrac{p}{\Omega}\Big)$$

$$-\Big(\delta_0\delta_2\tfrac{q}{\pi} + \tfrac{\delta_0\delta_1\pi}{\Omega}\Big)\Big]\Big\}$$

(4.1-27)

---

* See Appendix A for details of the integration and some remarks relative to their validity. $\varphi = \frac{1}{2}\rho A N R^2 \Omega^2$

4.1.2 Tangential Force

Using Equation (4.1-20) for F_T and making the same kind of substitutions as was done for F_Z, we have:

$$F_T = \left(\tfrac{1}{2}\rho AN/2\pi\right)\Big\{\int_0^{2\pi} v_a v_t C_{L_\alpha}\left[\delta_0 + \delta_1 \sin\sigma + \delta_2 \cos\sigma\right] d\sigma$$

$$- \int_0^{2\pi} v_a^2 C_{L_\alpha} d\sigma$$

$$+ \int_0^{2\pi} v_t^2 C_{d_o} d\sigma$$

$$+ \int_0^{2\pi} v_t^2 f_1 C_{L_\alpha}^2 \left[\delta_0^2 + 2\delta_0\delta_1 \sin\sigma + 2\delta_0\delta_2 \cos\sigma + \delta_1^2 \sin^2\sigma\right.$$

$$\left. + 2\delta_1\delta_2 \cos\sigma \sin\sigma + \delta_2^2 \cos^2\sigma\right] d\sigma$$

$$- \int_0^{2\pi} v_a v_t f_1 C_{L_\alpha}^2 \left[2\delta_0 + 2\delta_1 \sin\sigma + 2\delta_2 \cos\sigma\right] d\sigma$$

$$+ \int_0^{2\pi} v_a^2 f_1 C_{L_\alpha}^2 d\sigma \Big\}$$

(4.1-28)

On integrating over one cycle, and neglecting the resulting four terms in r^2 and q^2

$$F_T = Q\left\{C_{L_\alpha}\left[\left(\frac{u+i}{R\Omega}\right)\left(\delta_0 - \frac{u+i}{R\Omega}\right) - \frac{q}{\Omega}\cdot\frac{\delta_2}{2} - \frac{r}{\Omega}\cdot\frac{\delta_1}{2}\right]\right.$$

$$+C_{d_0}\left[1+\frac{2p}{\Omega}\right]$$

$$+f_1 C_{L_\alpha}{}^2\left[\left(1+\frac{2p}{\Omega}\right)\left(\delta_0^2+\frac{\delta_1^2}{2}+\frac{\delta_2^2}{2}\right)+\frac{2(r+rl_2)}{R\Omega}\delta_0\delta_2\right.$$

$$\frac{+2(w-ql_2)\delta_0\delta_1}{R\Omega} - \left(\frac{u+i}{R\Omega}\right)\left(2\delta_0 - \frac{u+i}{R\Omega}\right)$$

$$\left.\left. + \frac{q\delta_2}{\Omega} + \frac{r\delta_1}{\Omega}\right]\right\} \qquad (4.1\text{-}29)$$

4.1.3 Lateral Forces

The lateral forces, in propeller axes, are given by Equations (4.1-21) and (4.1-22)

$$F_y = -/+ \tfrac{1}{2}\rho A N V^2 \{ C_{L_\alpha} (\delta - \gamma) \sin\gamma \cos\sigma + C_{d_o} \cos\gamma \cos\sigma + f_1 C_{L_\alpha}^2 (\delta - \gamma)^2 \cos\gamma \cos\sigma \} \quad (4.1\text{-}30)$$

$$F_z = -/+ \tfrac{1}{2}\rho A N V^2 \{ C_{L_\alpha} (\delta - \gamma) \sin\gamma \sin\sigma + C_{d_o} \cos\gamma \sin\sigma + f_1 C_{L_\alpha}^2 (\delta - \gamma)^2 \cos\gamma \sin\sigma \} \quad (4.1\text{-}31)$$

Making the required substitutions and integrating over one cycle, the average lateral forces are:

$$F_y = -/+ Q \Big\{ C_{L_\alpha} \Big[\frac{\delta_2}{2} \Big(\frac{u + \iota}{R\Omega} \Big) - \frac{\delta_0}{2} \frac{q}{\Omega} + \Big(\frac{u + \iota}{R\Omega} \Big) \frac{q}{\Omega} \Big] + C_{d_o} \Big[\frac{u + x l_2}{R\Omega} \Big] + f_1 C_{L_\alpha}^2 \Big[\Big(1 + \frac{2p}{\Omega} \Big) \Big(\delta_0 \delta_2 \Big) + \Big(\frac{u + x l_2}{R\Omega} \Big) \Big(\delta_0^2 + \frac{\delta_1^2}{4} + \frac{3}{4} \delta_2^2 \Big) + \Big(\frac{w - q l_2}{R\Omega} \Big) \frac{\delta_1 \delta_2}{2} - \Big(\frac{u + \iota}{R\Omega} \Big) \delta_2 + \frac{q}{\Omega} \delta_0 - \Big(\frac{u + \iota}{R\Omega} \Big) \frac{q}{\Omega} \Big] \Big\} , \quad (4.1\text{-}32)$$

and:

$$F_z = \bar{q}Q\left\{C_{L\alpha}\left[\frac{\delta_1}{2}\left(\frac{u+\ell'}{R\Omega}\right) - \frac{\delta_0}{2}\frac{r}{\Omega} + \left(\frac{u+\ell'}{R\Omega}\right)\frac{w}{\Omega}\right]\right.$$
$$+ C_{d_0}\left[\frac{W-q\ell_2}{R\Omega}\right]$$
$$+ f_1 C_{L\alpha}^2\left[\left(1+\frac{2p}{\Omega}\right)\delta_0\delta_1 + \left(\frac{W-q\ell_2}{R\Omega}\right)\left(\delta_0^2 + \frac{\delta_2^2}{4} + \frac{3}{4}\delta_1^2\right)\right.$$
$$+ \left(\frac{v+r\ell_2}{R\Omega}\right)\frac{\delta_1\delta_2}{2} - \left(\frac{u+\ell'}{R\Omega}\right)\delta_1 + \frac{w}{\Omega}\delta_0$$
$$\left.\left. - \left(\frac{u+\ell'}{R\Omega}\right)\frac{r}{\Omega}\right]\right\} \qquad (4.1\text{-}33)$$

It should be noted that no terms have been discarded in Equations (4.1-32) and (4.1-33).

4.1.4 Moments (Propeller Axes)

On combining (4.1-24) and (4.1-25) with (4.1-19), the instantaneous propeller moments become:

$$M_y = -\tfrac{1}{2}\rho ANRV^2\left\{C_{L_\alpha}(\delta-\gamma)\cos\gamma\cos\sigma - C_{d_0}\sin\gamma\cos\sigma - f_1 C_{L_\alpha}^2(\delta-\gamma)^2\sin\gamma\cos\sigma\right\}$$

$$M_z = -\tfrac{1}{2}\rho ANRV^2\left\{C_{L_\alpha}(\delta-\gamma)\cos\gamma\sin\sigma - C_{d_0}\sin\gamma\sin\sigma - f_1 C_{L_\alpha}^2(\delta-\gamma)^2\sin\gamma\sin\sigma\right\}$$

Making the proper substitution and integrating over one cycle the average moments become:

$$\begin{aligned} M_y = -\tfrac{1}{2}QR\Bigg\{ & C_{L_\alpha}\left[\left(1+\frac{2p}{\Omega}\right)\frac{\delta_2}{2} + \left(\frac{v+rl_2}{R\Omega}\right)\delta_0 + \frac{q}{2\Omega}\right] \\ & + C_{d_0}\left[\frac{q}{2\Omega}\right] \\ & + f_1 C_{L_\alpha}^2\left[\left(\frac{u+l}{R\Omega}\right)\left(-\delta_0\delta_2 + \delta_2\frac{u+l}{R\Omega} - 2\delta_0\frac{q}{\Omega}\right)\right. \\ & \left. + \frac{q}{\Omega}\left(\frac{\delta_0^2}{2} + \frac{3}{8}\delta_2^2 + \frac{1}{8}\delta_1^2\right)\right. \\ & \left. + \frac{r}{\Omega}\,\frac{\delta_1\delta_2}{4}\right. \\ & \left. + \left(\frac{u+l}{R\Omega}\right)^2\left(\frac{q}{\Omega}\left[1-\frac{p}{\Omega}\right] + \frac{q}{2\Omega}\right) + \left(\frac{u+l}{R\Omega}\right)^3\left(\frac{v+rl_2}{2R\Omega}\right)\right]\Bigg\} \end{aligned}$$

(4.1-34)

and,

$$M_y = \tfrac{1}{2}QR\Big\{C_{L_\alpha}\Big[\Big(1+\frac{2p}{\pi}\Big)\frac{\delta_1}{2}+\Big(\frac{w-ql_2}{R\pi}\Big)\delta_0+\frac{\alpha}{2\pi}\Big]$$

$$+C_{d_0}\Big[\frac{\alpha}{2\pi}\Big]$$

$$+f_1 C_{L_\alpha}{}^2\Big[\Big(\frac{u+\iota'}{R\pi}\Big)\Big(-\delta_0\delta_1+\delta_1\frac{u+\iota'}{R\pi}-2\delta_0\frac{\alpha}{\pi}\Big)$$

$$+\frac{\alpha}{\pi}\Big(\frac{\delta_0^2}{2}+\frac{3}{8}\delta_1^2+\frac{1}{8}\delta_2^2\Big)+\frac{q}{\pi}\frac{\delta_1\delta_2}{4}$$

$$+\Big(\frac{u+\iota'}{R\pi}\Big)^2\Big(\frac{\alpha}{\pi}\Big[1-\frac{p}{\pi}\Big]+\frac{1}{2}\frac{\alpha}{\pi}\Big)$$

$$+\Big(\frac{u+\iota'}{R\pi}\Big)^3\Big(\frac{w-ql_2}{2R\pi}\Big)\Big]\Big\} \qquad (4.1\text{-}35)$$

In (4.1-34) and (4.1-35) all terms containing second and third powers of q or α and terms containing $q\alpha$ products are discarded.

4.1.5 Force/Moment Summation (Body Axes)

The forces/moments produced by the propellers with respect to body axes, are related to the propeller forces/moments of Equations (4.1-19) through (4.1-25) by the following set of equations:

$$\left.\begin{aligned} X &= F_x & K &= M_x \\ Y &= F_y & M &= M_y \mp Z\ell_z \\ Z &= F_z & N &= M_z \pm Y\ell_z \end{aligned}\right\} \quad (4.1\text{-}36)$$

Note that the distance from the plane of the propellers to the c.g., ℓ_z, carries no sign. The body forces/moments of (4.1-36) are presented in Table 4.1-1. In this table, the two parts of M and N in Equation (4.1-36) have been combined into one expression for each. Also the hull interference effect discussed in Reference 1 (pg 26) has been taken into account by multiplying all terms containing $\frac{v+r\ell_z}{R\Omega}$ and $\frac{w-q\ell_z}{R\Omega}$ by a factor of 2.

At this point it is desirable to review the assumptions, approximations and linearizations that have been made in deriving the expressions set forth in Table 4.1-1, as well as reviewing some of the limitations on their use.

(1) The effects of swirl (tangential component of induced velocity) and of interaction between fore and aft propellers have been neglected. Swirl is neglected on the grounds that the component of swirl due to cyclic pitch is small relative to that due to collective pitch. The latter component would normally be "compensated" for by slightly increased rpm or δ_0 (over "design" values). Fore and aft propeller interaction is neglected because it is nonlinear and lacks axial symmetry for any maneuver other than pure rolling or axial acceleration at zero angle of attack of the hull. It is also believed

TABLE 4.1-1

PROPELLER EQUATIONS - LOWSPEED

$(\Omega_f = \Omega_a = \Omega)$

$$X_p = \tfrac{1}{4}\rho Q\left\{C_{L_\alpha}\left[\left(1+\frac{2\rho}{\Omega}\right)\delta_0 + 2\left(\frac{v+rl_2}{R\Omega}\right)\delta_2 + 2\left(\frac{w-ql_2}{R\Omega}\right)\delta_1 - \left(\frac{u+i}{R\Omega}\right)\right] - C_{d_0}\left[\frac{u+i}{R\Omega}\right]\right.$$
$$\left. - f_1 C_{L_\alpha}^2\left[\left(\frac{u+i}{R\Omega}\right)\left(\delta_0^2 + \frac{\delta_1^2}{2} + \frac{\delta_2^2}{2} + 2\delta_2\frac{q}{\Omega} + 2\delta_1\frac{r}{\Omega}\right) - \left(\frac{u+i}{R\Omega}\right)^2 2\delta_0 + \left(\frac{u+i}{R\Omega}\right)^3\left(1-\frac{\rho}{\Omega}\right) - \frac{q}{\Omega}\delta_0\delta_2 - \frac{r}{\Omega}\delta_0\delta_1\right]\right\}$$

$$Y_p = \tfrac{1}{4}\rho Q\left\{C_{L_\alpha}\left[\left(\frac{u+i}{R\Omega}\right)\left(\frac{\delta_2}{2}+\frac{q}{\Omega}\right) - \frac{q}{\Omega}\frac{\delta_0}{2}\right] + 2C_{d_0}\left[\frac{v+rl_2}{R\Omega}\right]\right.$$
$$\left. + f_1 C_{L_\alpha}^2\left[\left(1+\frac{2\rho}{\Omega}\right)\delta_0\delta_2 + 2\left(\frac{v+rl_2}{R\Omega}\right)\left(\delta_0^2 + \frac{\delta_1^2}{4} + \frac{3}{4}\delta_2^2\right) + 2\left(\frac{w-ql_2}{R\Omega}\right)\frac{\delta_1\delta_2}{2} - \left(\frac{u+i}{R\Omega}\right)\left(\delta_2 + \frac{q}{\Omega}\right) + \frac{q}{\Omega}\delta_0\right]\right\}$$

$$Z_p = \tfrac{1}{4}\rho Q\left\{C_{L_\alpha}\left[\left(\frac{u+i}{R\Omega}\right)\left(\frac{\delta_1}{2}+\frac{r}{\Omega}\right) - \frac{r}{\Omega}\frac{\delta_0}{2}\right] + 2C_{d_0}\left[\frac{w-ql_2}{R\Omega}\right]\right.$$
$$\left. + f_1 C_{L_\alpha}^2\left[\left(1+\frac{2\rho}{\Omega}\right)\delta_0\delta_1 + 2\left(\frac{w-ql_2}{R\Omega}\right)\left(\delta_0^2 + \frac{\delta_2^2}{4} + \frac{3}{4}\delta_1^2\right) + 2\left(\frac{v+rl_2}{R\Omega}\right)\frac{\delta_1\delta_2}{2} - \left(\frac{u+i}{R\Omega}\right)\left(\delta_1 + \frac{r}{\Omega}\right) + \frac{r}{\Omega}\delta_0\right]\right\}$$

$$K_p = \tfrac{1}{4}\rho QR\left\{C_{L_\alpha}\left[\left(\frac{u+i}{R\Omega}\right)\delta_0 - \frac{q}{\Omega}\frac{\delta_2}{2} - \frac{r}{\Omega}\frac{\delta_1}{2} - \left(\frac{u+i}{R\Omega}\right)^2\right] + C_{d_0}\left[1+\frac{2\rho}{\Omega}\right]\right.$$
$$\left. + f_1 C_{L_\alpha}^2\left[\left(1+\frac{2\rho}{\Omega}\right)\left(\delta_0^2 + \frac{\delta_1^2}{2} + \frac{\delta_2^2}{2}\right) + 4\left(\frac{v+rl_2}{R\Omega}\right)\delta_0\delta_2 + 4\left(\frac{w-ql_2}{R\Omega}\right)\delta_0\delta_1 - \left(\frac{u+i}{R\Omega}\right)2\delta_0 + \left(\frac{u+i}{R\Omega}\right)^2 + \frac{q}{\Omega}\delta_2 + \frac{r}{\Omega}\delta_1\right]\right\}$$

$$M_p = \tfrac{1}{4}\rho QR\left\{C_{L_\alpha}\left[\left(\frac{u+i}{R\Omega}\right)\frac{l_2}{R}\left(\frac{\delta_1}{2}+\frac{r}{\Omega}\right) - \frac{rl_2}{R\Omega}\frac{\delta_0}{2} - \left(1+\frac{2\rho}{\Omega}\right)\frac{\delta_2}{2} - 2\left(\frac{v+rl_2}{R\Omega}\right)\delta_0 - \frac{q}{2\Omega}\right] + C_{d_0}\left[\frac{2(w-ql_2)l_2}{R^2\Omega} - \frac{q}{2\Omega}\right]\right.$$
$$+ f_1 C_{L_\alpha}^2\left[\left(1+\frac{2\rho}{\Omega}\right)\frac{l_2}{R}\delta_0\delta_1 + 2\left(\frac{w-ql_2}{R\Omega}\right)\left(\delta_0^2 + \frac{\delta_2^2}{4} + \frac{3}{4}\delta_1^2\right)\frac{l_2}{R} + \left(\frac{v+rl_2}{R\Omega}\right)\frac{l_2}{R}\delta_1\delta_2\right.$$
$$- \left(\frac{u+i}{R\Omega}\right)\left(\frac{l_2}{R}\delta_1 + \frac{rl_2}{R\Omega} - \delta_0\delta_2 - 2\frac{q}{\Omega}\delta_0\right) - \left(\frac{u+i}{R\Omega}\right)^2\left(\delta_2 + \frac{q}{\Omega}\left[1-\frac{\rho}{\Omega}\right] + \frac{q}{2\Omega}\right)$$
$$\left.\left. - \left(\frac{u+i}{R\Omega}\right)^3\left(\frac{v+rl_2}{R\Omega}\right) + \frac{rl_2}{R\Omega}\delta_0 - \frac{q}{\Omega}\left(\frac{\delta_0^2}{2} + \frac{3}{8}\delta_2^2 + \frac{\delta_1^2}{8}\right) - \frac{r}{4\Omega}\delta_1\delta_2\right]\right\}$$

$$N_p = \tfrac{1}{4}\rho QR\left\{C_{L_\alpha}\left[\left(\frac{u+i}{R\Omega}\right)\frac{l_2}{R}\left(\frac{\delta_2}{2}+\frac{q}{\Omega}\right) - \frac{ql_2}{R\Omega}\frac{\delta_0}{2} + \left(1+\frac{2\rho}{\Omega}\right)\frac{\delta_1}{2} + 2\left(\frac{w-ql_2}{R\Omega}\right)\delta_0 + \frac{r}{2\Omega}\right] + C_{d_0}\left[\frac{2(v+rl_2)l_2}{R^2\Omega} + \frac{r}{2\Omega}\right]\right.$$
$$+ f_1 C_{L_\alpha}^2\left[\left(1+\frac{2\rho}{\Omega}\right)\frac{l_2}{R}\delta_0\delta_2 + 2\left(\frac{v+rl_2}{R\Omega}\right)\left(\delta_0^2 + \frac{\delta_1^2}{4} + \frac{3}{4}\delta_2^2\right)\frac{l_2}{R} + \left(\frac{w-ql_2}{R\Omega}\right)\frac{l_2}{R}\delta_1\delta_2\right.$$
$$- \left(\frac{u+i}{R\Omega}\right)\left(\frac{l_2}{R}\delta_2 + \frac{ql_2}{R\Omega} + \delta_0\delta_1 + \frac{2r}{\Omega}\delta_0\right) + \left(\frac{u+i}{R\Omega}\right)^2\left(\delta_1 + \frac{r}{\Omega}\left[1-\frac{\rho}{\Omega}\right] + \frac{r}{2\Omega}\right)$$
$$\left.\left. + \left(\frac{u+i}{R\Omega}\right)^3\left(\frac{w-ql_2}{R\Omega}\right) + \frac{ql_2}{R\Omega}\delta_0 + \frac{r}{\Omega}\left(\frac{\delta_0^2}{2} + \frac{3}{8}\delta_1^2 + \frac{\delta_2^2}{8}\right) + \frac{q}{4\Omega}\delta_1\delta_2\right]\right\}$$

that neglect of propeller interaction is consistent with the neglect of the effects of the propeller slipstreams on the hydrodynamic characteristics of the body.

(2) The influence of the hull on the velocities induced at the propellers has been neglected with the exception of the cross-flow velocity. The neglect of body-induced changes in axial velocity is based on classical slender-body theory.

(3) The important assumptions and linearizations made in the mathematical development are stated in Equations (4.1-11) and (4.1-13) through (4.1-18). In deriving the expressions for forces/moments in propeller axes the equations were carried out to completion and terms discarded only at the end. Discarded terms include those containing squares, cubes and products of the motion variables q and r.

(4) The propeller equations of Table 4.1-1 are valid within the limitations reviewed above and provided that the inflow velocity, λ', is defined properly for the operating conditions being examined. The proper definition of λ' is discussed further in the next section.

4.1.6 The Propeller Equations in Coefficient Form

Subject to the limitations discussed in the previous section, the propeller forces/moments for the general case of low speed flight are given by the equations of Table 4.1-1. These equations are explicit in the blade-angle variables δ_0, δ_1, and δ_2, the inflow velocity λ', and the motion variables u, v, w, p, q, r. It is possible to place these equations in coefficient form, in somewhat the same manner as was done for the high-speed case, in which a force or moment is expressed as the product of a dimensional coefficient multiplied by functions of the blade-angle variables and/or multiplied by the motion variables. The ease with which this can be done depends markedly on the nature of the theoretical expression for λ', the inflow velocity. For

the special case that satisfies the condition,

$$\frac{u}{R\Omega} << \frac{\lambda}{\varrho R\Omega} \qquad (4.1\text{-}37)$$

the expression for λ given in Reference 1 (pg 37) is valid. This expression,

$$\lambda \cong R\Omega\,(a\delta_0 + b\delta_0|\delta_0|), \qquad (4.1\text{-}38)$$

is based on a combined lifting-line and propeller momentum analysis.* For the postulated configuration of the TPS, the constants a and b have the approximate values .95 and -1.0 respectively. By limiting δ_0 to less than about 0.1 rad in magnitude, Equation (4.1-38) can be simplified to

$$\lambda \cong R\Omega a\delta_0, \qquad (4.1\text{-}39)$$

with a loss in accuracy of about 12%.

If (4.1-39) is substituted into the equations of Table 4.1-1, the inflow velocity, λ, can be eliminated and the equations can be further reduced without difficulty to a "coefficient" form (a form which has been called a "force matrix"). Such a substitution has been carried out to derive Table 4.1-2, "Zero Speed Force and Moment Coefficients". Note that the derivation of this table and its further application are influenced by the following considerations:

(a) Balanced operation of the forward and aft propellers is assumed, that is, $\Omega_f = \Omega_a = \Omega$. For convenience, the following symbol changes are made:

$$C_{L_\alpha} = C$$
$$C_{d_0} = d$$

(b) As will be shown in Section VI, the constraint (4.1-37) cannot be satisfied even at very low forward speeds. For this reason the matrix is limited in practical application to the zero forward speed case (e.g. fore and aft propellers counter-thrusting). For non-zero forward speeds (see Section 6.2), an expression for λ, somewhat more complicated than (4.1-39), will be given, and substituted directly into the general equations listed in Table 4.1-1.

* See Appendix C for a discussion of the inflow velocity equation.

(c) The matrix form of the propeller equations (Table 4.1-2) contain the inflow velocity definition (4.1-39). In (4.1-39) the effects of cyclic pitch on λ have been neglected.* This assumption requires that δ_1 and δ_2 be much smaller than δ_0, a condition which is adhered to in all of the zero and low speed work in this report. The effect of appreciable cyclic pitch, relative to δ_0, where the cyclic frequency is one cycle per revolution (as it is in the present case) is to reduce the available forces due to cyclic pitch by a significant factor. According to the two-dimensional analysis of Reference 5, this multiplying factor is approximately equal to $1/1+\frac{CkN\Omega}{4(N+1)}$, where CR is the blade chord. In addition, the inclusion of finite-span effects (see Reference 6, for example) would involve the use of large scale digital computer.

A meaningful analysis of the extreme operating condition, corresponding to $\sqrt{\delta_1^2+\delta_2^2} > \delta_0$ and low forward speed, would be most difficult for the propeller configurations being considered herein, since individual blades would be intersecting the vortical wake of preceding blades in certain azimuth positions. Practical consideration of high oscillatory stresses that would probably be encountered under these conditions tend to rule out the possibility of operating in this mode.

(d) On taking due account of the sign notation prefixing the equations of Table 4.1-1 (e.g. $+/+$ for the X-force) and also of the sign change required for the aft-propeller terms involving p, v, and w, the two-propeller forces/moments are expressed in terms of specific combinations of blade-pitch angle. These combinations are listed in the first column of Table 4.1-2 and are denoted "δ inputs". Thus the X-force due to the propellers is given by**

---

* This is also true of the less restrictive definition of λ given in 6.2.

** Note that all of the $X - Y - Z - K - M - N$ entries are multiplied by a common factor QC/Ω (not shown).

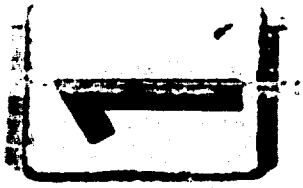

TABLE 4.1-2
ZERO SPEED FORCE/MOMENT COEFFICIENTS

LINE	δ INPUTS	EQUIVALENT NO-SPEED INPUT	X-COEFFICIENT	Y-COEFFICIENT	Z-COEFFICIENT	M-COEFFICIENT	N-COEFFICIENT
1	$\delta_{es}+\delta_{as}$	δ_e	$[Q(1-a-a^2/2)]$	0	0	0	$\left[-\frac{\rho}{2}I_y+I_{yz}a(1+A_1C)+\frac{\rho}{2}\right.$
2	$\delta_{es}-\delta_{as}$	δ_a	$[Z]p$	$[-(a-\frac{1}{2})-A_1C(1-a)]q$	$[-(a-\frac{1}{2})-A_1C(1-a)]r$	0	$[-Z]v$
3	$\delta_{er}-\delta_{ar}$	δ_r	$[-2I_y/R]q$	0	0	0	0
4	$\delta_{er}-\delta_{ar}$	δ_f	$[Z/R]w$	0	$[-(\frac{1}{2}-A_1C)\frac{L}{R}]u$	$[\frac{L}{R}(1-2A_1C]r$	0
5	$\delta_{es}+\delta_{as}$	δ_w	$[2I_y/R]r$	0	0	0	$[-\frac{L}{R}\Omega\sigma]$
6	$\delta_{er}-\delta_{ar}$	δ_f	$[Z/R]v$	0	0	$[\frac{L}{R}(1-2A_1C]r$	$[-R]p$
7	$\delta_{es}^2-\delta_{as}^2$	$\delta_e^2-\delta_a^2/2$	0	$[-2A_1C/R]w$	$[-2A_1C/R]w$	$[-2RA_1C]p$	$\left[\sigma A_1C(\delta\frac{L}{R}+\frac{L}{R}-\frac{L}{R}\sigma^2-\right.$
8	$\delta_{es}^2-\delta_{as}^2$	$\delta-\delta_a$	0	$[-2A_1C(L_f/R]r$	$[2A_1C(L_f/R]q$	$[-\Omega RA_1C(a-1)^2$ $-\Omega Ra(1-a)]$	$\left[\frac{2A_1C/R}{\rho}\right]w+\left[\frac{\sigma A_1C\sigma}{2}\right.\sigma$
9	$\delta_{es}\delta_{er}+\delta_{as}\delta_{ar}$	$\delta_e\delta_r+\delta_a\delta_f/2$	$[-A_1C(2a-1)]r$	0	$[-2A_1C]p$	$[-4A_1C]w$	$[\frac{1}{2}\Omega I_{xz}a+\Omega A_1C(L_f(1-a$
10	$\delta_{es}\delta_{ar}+\delta_{as}\delta_{er}$	$\delta_e\delta_f+\delta_a\delta_r/2$	0	0	$[-\Omega A_1C(1-a)-\frac{1}{2}\Omega a]$	$[wA_1C_{l_f}]q$	$[2A_1C_{l_f}]p$
11	$\delta_{es}\delta_{ar}+\delta_{as}\delta_{er}$	$\delta_e\delta_r+\delta_a\delta_f/2$	$[-A_1C(2a-1)]q$	$[-2A_1C]p$	0	$[-4A_1C]v$	0
12	$\delta_{es}\delta_{ar}+\delta_{as}\delta_{er}$	$\delta_e\delta_f+\delta_a\delta_r/2$	0	$[-\Omega A_1C(1-a)-\frac{1}{2}\Omega a]$	0	$[-4A_1C_{l_f}]r$	0
13	$\delta_{es}^2+\delta_{as}^2$	$\delta_f^2+\delta_w^2/2$	0	$[-\frac{L}{R}A_1C/R]w$	$[-\frac{L}{R}A_1C/R]w$	$[-RA_1C]p$	$[-RA_1C(\frac{L}{R}\frac{I_{xz}}{I_z}+\frac{L}{R})]q$
14	$\delta_{es}^2-\delta_{as}^2$	$\delta_f\delta_w$	0	$[-\frac{L}{R}A_1C_{l_f}/R]r$	$[\frac{L}{R}A_1C_{l_f}/R]q$	$[-\frac{L}{R}\Omega RA_1C]$	$[\frac{L}{R}\frac{I_{xz}}{I_z}C_{l_f}]w$
15	$\delta_{es}^2+\delta_{ar}^2$	$\delta_e^2+\delta_r^2/2$	0	$[-\frac{L}{R}A_1C/R]w$	$[-\frac{L}{R}A_1C/R]w$	$[-RA_1C]p$	$[-RA_1C(\frac{L}{R}\frac{I_{xz}}{I_z}+\frac{L}{R})]q$
16	$\delta_{es}^2-\delta_{ar}^2$	$\delta_e\delta_r$	0	$[-\frac{L}{R}A_1C_{l_f}/R]r$	$[\frac{L}{R}A_1C_{l_f}/R]q$	$[-\frac{L}{R}\Omega RA_1C]$	$[\frac{L}{R}\frac{I_{xz}}{I_z}C_{l_f}]w$
17	$\delta_{es}\delta_{er}+\delta_{as}\delta_{ar}$	$\delta_e\delta_r+\delta_a\delta_f/2$	0	$[-A_1C/R]w$	$[-A_1C/R]w$	0	$[\sigma A_1C(\frac{L}{R})^2\sigma^2-\frac{L}{R}]\sigma$
18	$\delta_{es}\delta_{ar}+\delta_{as}\delta_{er}$	$\delta_e\delta_f+\delta_a\delta_r/2$	0	$[A_1C_{l_f}/R]q$	$[-A_1C_{l_f}/R]r$	0	$[A_1C_{l_f}\sigma]v$
19	$\delta_{es}^2+\delta_{as}^2$		$[-\Omega A_1C\sigma(1+a^2$	0	0	0	$[-A_1C_{l_f}a^2]r$
20	$\delta_{es}^2-\delta_{as}^2$		$[A_1C\sigma a^2]p$	0	0	0	$[A_1C\sigma a^2]v$
21	$\delta_{es}\delta_{ar}+\delta_{as}\delta_{er}$		0	0	0	0	
22	$\delta_{es}\delta_{ar}+\delta_{as}\delta_{er}$	$\delta_e\delta_r+\delta_a\delta_f/2$		0	0	0	
23	$\delta_{es}+\delta_{ar}+\delta_{as}$		$-\frac{L}{R}A_1C_{l_f}a$	0	0		
24	$\delta_{es}+\delta_{ar}+\delta_{as}$		$-\frac{L}{R}A_1C_{l_f}a$		0		
25			0	$[A_1C\sigma a]w$	$[-A_1C\sigma a]w$	$[A_1C\sigma a]p$	

AG-1[illegible]-2

TABLE 4.1-2
ZERO SPEED FORCE/MOMENT COEFFICIENTS

INPUTS	EQUIVALENT ZERO-SPEED INPUT	X-COEFFICIENT	Y-COEFFICIENT	Z-COEFFICIENT	M-COEFFICIENT	W-COEFFICIENT	N-COEFFICIENT
	δ_0	$[\Omega(1-a-a^2/6)]$	0	0	0	$[-\frac{1}{2}l_1+l_2a(1-4_1C)+l_3l_1C]r$	$[\frac{1}{2}l_2-l_2a(1-4_1C)-l_3l_1C]q$
	δ_a	$[2]p$	$[-(a-\frac{1}{2})-4_1C(1-a)]q$	$[-(a-\frac{1}{2})-4_1C(1-a)]r$	0	$[2]v$	$[-2]w$
	δ_w	$[-2l_1/R]q$	0	0	0	0	$[-\frac{1}{2}\Omega a]$
	δ_q	$[2/R]w$	0	$[-\frac{1}{2}-4_1C)\frac{1}{2}]u$	$[\frac{a}{2}(1-2l_1C]r$	0	$[-a]p$
	δ_w	$[2l_1/R]r$	0	0	0	$[-\frac{1}{2}\Omega a]$	0
	δ_r	$[2/2]v$	0	0	$[\frac{a}{2}(1-2l_1C]r$	$[-a]p$	C
	$\delta_e^2-\delta_a^2/2$	0	$[-2l_1C/R]v$	$[-2l_1C/R]w$	$[-2R4_1C]p$	$[-a4_1C(2\frac{l_1}{R}a+\frac{1}{2}-\frac{1}{2}a^2-2\frac{l_1}{R}a)]q$	$[-a4_1C(\frac{l_1}{R}a^2-\frac{1}{2}-\frac{1}{2}a^2+2a)]r$
	$\delta\cdot\delta_w$	0	$[-2l_1Cl_2/R]r$	$[2l_1Cl_2/R]q$	$[-\Omega R4_1C(a-1)^2-\Omega R_a(1-a)]$	$[\frac{2l_1Cl_2}{R}]w+[\frac{a4_1Ca}{2}]w$	$[\frac{2l_1Cl_2}{R}]v+[\frac{a4_1Ca}{2}]w$
$\delta_e\delta_w$	$\delta_e\delta_w+\delta_e\delta_r/2$	$[-4_1C(2a-1)]r$	0	$[-2l_1C]p$	$[-a4_1C]w$	$[\frac{1}{2}\Omega l_2a+\Omega l_1Cl_2(1-a)]$	0
δ_{ew}	$\delta_e\delta_q+\delta_e\delta_w/2$	0	0	$[-\Omega l_1C(1-a)-\frac{1}{2}\Omega a]$	$[a4_1Cl_2]q$	$[2l_1Cl_2]r$	0
δ_{ew}	$\delta_w\delta_w+\delta_e\delta_w/2$	$[-4_1C(2a-1)]q$	$[-2l_1C]p$	0	$[-a4_1C]v$	0	$[-\frac{1}{2}\Omega l_2a-a4_1Cl_2(1-a)]$
δ_{ew}	$\delta_w\delta_q+\delta_e\delta_w/2$	0	$[-\Omega l_1C(1-a)-\frac{1}{2}\Omega a]$	0	$[-a4_1Cl_2]r$	0	$[-2l_1Cl_2]p$
	$\delta_q^2+\delta_w^2/2$	0	$[-\frac{1}{2}l_1C/R]v$	$[-\frac{1}{2}l_1C/R]w$	$[-R4_1C]p$	$[-R4_1C(\frac{1}{2}\frac{l_2^2}{R^2}+\frac{1}{8})]q$	$[-R4_1C(\frac{1}{2}\frac{l_2^2}{R^2}-\frac{1}{8})]r$
	$\delta_q\delta_w$	0	$[-\frac{1}{2}l_1Cl_2/R]r$	$[\frac{1}{2}l_1Cl_2/R]q$	$[-\frac{1}{2}\Omega R4_1C]$	$[\frac{1}{2}\frac{l_2}{R}\frac{l_1Cl_2}{R}]w$	$[-\frac{1}{2}\frac{l_2}{R}\frac{l_1Cl_2}{R}]v$
	$\delta_r^2-\delta_w^2/2$	0	$[-\frac{1}{2}l_1C/R]v$	$[-\frac{1}{2}l_1C/R]w$	$[-R4_1C]p$	$[-a4_1C(\frac{1}{2}\frac{l_2^2}{R^2}+\frac{1}{8})]q$	$[-a4_1C(\frac{1}{2}\frac{l_2^2}{R^2}-\frac{1}{8})]r$
	$\delta_r\delta_w$	0	$[-\frac{1}{2}l_1Cl_2/R]r$	$[\frac{1}{2}l_1Cl_2/R]q$	$[-\frac{1}{2}\Omega R4_1C]$	$[\frac{1}{2}\frac{l_2}{R}\frac{l_1Cl_2}{R}]w$	$[-\frac{1}{2}\frac{l_2}{R}\frac{l_1Cl_2}{R}]v$
$\delta_e\delta_w$	$\delta_e\delta_r+\delta_w\delta_w/2$	0	$[-l_1C/R]w$	$[-l_1C/R]v$	0	$[-a4_1C(\frac{1}{2}l_2^2R^2-\frac{1}{8})]r$	$[a4_1C(\frac{1}{2}l_2^2R^2-\frac{1}{8})]q$
δ_{ew}	$\delta_q\delta_w+\delta_e\delta_w/2$	C	$[l_1Cl_2/R]q$	$[-l_1Cl_2/R]r$	0	$[-l_1Cl_2a]v$	$[l_1Cl_2a]w$
		$[-2l_1Cl_2(1-a)^2]$	0	0	0	$[-l_1Cl_2a^2]r$	$[l_1Cl_2a^2]q$
		$[l_1Cl_2a^2]p$	0	0	0	$[-l_1Cl_2a^2]v$	$[l_1Cl_2a^2]w$
		0	0	0	0		
	$\delta_e^2\delta_w+\delta_w^2\delta_w+\delta_e^2\delta_w+\delta_w^2\delta_w$	0	0	0	0		
		$-\frac{1}{2}\Omega l_1Cl_2$	0	0			
		$[-2l_1Cl_2]$	0	0			
		0	$[-l_1Cl_2]w$	$[-l_1Cl_2]w$	$[-l_1Cl_2]p$	$[-l_1Cl_2a]r$	$[l_1Cl_2a]q$

$$X_p = \frac{QC}{\Lambda}\Big\{(\delta_{of}+\delta_{oa})\left[\Lambda\left(1-a-\frac{ad}{c}\right)\right]$$

$$+(\delta_{of}-\delta_{oa})[2p]$$

$$+ \cdots\cdots$$

$$\vdots$$

$$+\left(\delta_{oa}\left\{\delta_{1a}^2+\delta_{2a}^2\right\}\right)\left[-\tfrac{1}{2}\Lambda f_i C a\right],$$

in which terms in parentheses ( ) are δ inputs, and terms in brackets $[\,]$ are the corresponding χ -force coefficients for the δ inputs.

(e) Because of the linearization of the inflow velocity expression (4.1-38), certain entries in Table 4.1-2 will contain larger errors than others. The entry, line $1-\chi$ is a good example. It contains a term $1-a$ which is large, relative to the neglected part of the inflow expression $b\,\delta_o/\delta_o$, but not so large as to preclude a large error, depending on the size of δ_o. In these entries, it is suggested that an equivalent a be used, say a', such that $a' = a + b/\delta_o$. If a' is evaluated for a particular δ_o, the entries in question will be fairly accurate and values of δ_o larger than the suggested limit ($\delta_o = 0.1$) may be used.

4.2 HULL HYDRODYNAMICS

Representation of the hull forces (given in dimensional coefficient form in Table 4.2-1) for the low-speed case is complicated by the absence of a dominant velocity component on which a linearized theory could be based. The hull forces are therefore nonlinear in form. A simplification is obtained by assuming that the forces depend on the individual velocity components.

The axial drag coefficient (.00102) was based on results presented in Reference 7 and is open to question for very low Reynolds numbers (that prevail at low forward speeds). Forces arising from lateral velocity components were obtained by considering the hull to consist of a series of right circular cylinders. The drag on each segment was estimated from data given in Reference 8, including the effects of Reynolds numbers. The cubic terms in Y_r and Z_q arise from these cross-flow Reynolds number variations along the hull.

Flat plate drag data were used to estimate the cross-flow forces on the sail and a linear lateral velocity profile was assigned to account for yawing and rolling motions.

The above treatment of hull forces is admittedly crude. Greatest percentage errors occur when the hull is moving very slowly, and the propellers are operating at high thrust levels (and, hence, have large slipstream velocities). In this situation, however, it can be anticipated that the propeller forces will be very much larger than those due to the hull and the absolute errors introduced by poorly defined hull hydrodynamics will not be significant.

Table 4.2-1 Hull Forces and Moments - Low-Speed

$X_u = -\frac{1}{2}\rho\ell^2 u\,|u|(.00102)$ $\quad X_p = 0$

$X_v = 0$ $\quad X_q = 0$

$X_w = 0$ $\quad X_r = 0$

$Y_u = 0$ $\quad Y_p = -\frac{1}{2}\rho\ell^4 p\,|p|(.0000311)$

$Y_v = -\frac{1}{2}\rho\ell^2 v\,|v|(.0809)$ $\quad Y_q = 0$

$Y_w = 0$ $\quad Y_r = -\frac{1}{2}\rho\ell^4 r\,(.000325|r| + .062 r^2)$

$Z_u = 0$ $\quad Z_p = 0$

$Z_v = 0$ $\quad Z_q = -\frac{1}{2}\rho\ell^4 q\,(.000097|q| + .062 q^2)$

$Z_w = -\frac{1}{2}\rho\ell^2 w\,|w|(.0762)$ $\quad Z_r = 0$

$K_u = 0$ $\quad K_p = -\frac{1}{2}\rho\ell^5 p\,|p|(.00000375)$

$K_v = -\frac{1}{2}\rho\ell^3 v\,|v|(.000395)$ $\quad K_q = 0$

$K_w = 0$ $\quad K_r = -\frac{1}{2}\rho\ell^5 r\,|r|(.0000187)$

$M_u = 0$ $\quad M_p = 0$

$M_v = 0$ $\quad M_q = -\frac{1}{2}\rho\ell^5 q\,(.00217|q| + .214 q^2)$

$M_w = -\frac{1}{2}\rho\ell^3 w\,|w|(.00109)$ $\quad M_r = 0$

$N_u = 0$ $\quad N_p = -\frac{1}{2}\rho\ell^5 p\,|p|(.00000701)$

$N_v = +\frac{1}{2}\rho\ell^3 v\,|v|(.00004)$ $\quad N_q = 0$

$N_w = 0$ $\quad N_r = -\frac{1}{2}\rho\ell^5 r\,(.00217|r| + .214 r^2)$

V

SIX-DEGREE-OF-FREEDOM EQUATIONS OF MOTION

LOW-SPEED FLIGHT

The six-degree-of-freedom equations of motion* for low-speed operation are written in the same way as the high-speed equations. The total propeller forces/moments, defined in Table 4.1-1 are designated by subscript P. The hull forces/moment of Table 4.2-1 are designated by the subscript H. Their sum is then equated to the mass/inertia reaction terms. Thus**:

$$\left.\begin{aligned}
&m_1\dot{u} - m_2 r v + m_3 q w = X_P + X_H \\
&m_2\dot{v} + m_1 r u - m_3 p w = Y_P + Y_H \\
&m_3\dot{w} - m_1 q u + m_2 p v = Z_P + Z_H \\
&I_{xx}\dot{p} + (I_{zz} - I_{yy}) q r = K_P + K_H \\
&I_{yy}\dot{q} + (I_{xx} - I_{zz}) p r = M_P + M_H \\
&I_{zz}\dot{r} + (I_{yy} - I_{xx}) p q = N_P + N_H
\end{aligned}\right\} \quad (5\text{-}1)$$

---

* In total form, as contrasted to a perturbation form.

** Gyroscopic terms are added to the propeller and hull terms if applicable.

VI

TRIMMED HOVERING FLIGHT

Attention is confined in this section to: (1) the required trim settings of collective pitch for very low (i.e., hovering) forward speeds and, (2) the generation of pure translational forces by means of cyclic pitch and the translational velocities which result from these forces*.

The range of forward speeds is arbitrarily taken to be $0 \leq u \leq 1$ ft/sec. Of interest is the capability of a tandem-propeller configuration to perform "creeping" maneuvers in a single plane. This operational mode may be of some practical importance in submerged rendezvous, search, escape or docking operations.

As noted in Reference 1, it is possible to operate at zero or very low forward speeds in a number of different ways, each of which entails a specific combination of forward and aft propeller settings, either rotating (thrusting or counter-thrusting) or locked. In the hovering case it will be assumed that it is desirable to achieve translational motions without rotation, and that operation of the forward and aft propellers is balanced (i.e., $\Omega_f = \Omega_a = \Omega$). Three modes of operation will be considered

---

*The question of blade angle resolution is treated in Section 7.3.

(1) Zero forward speed - zero collective pitch forward and aft.

(2) Zero forward speed - counter-thrusting collective pitch forward and aft.

(3) Very low forward speed - thrusting collective pitch forward and aft.

6.1 ZERO FORWARD SPEED - ZERO COLLECTIVE PITCH

At zero forward speed, with zero collective and cyclic pitch, forward and aft, the neutrally-buoyant submarine will remain stationary. It would be desirable to be able to predict whether or not it is possible to generate pure sideforce under these conditions, by the exclusive application of cyclic pitch. Unfortunately, the approximate propeller equations presented in Section IV cannot be used when δ_1 or $\delta_2 > \delta_o$ (see Section 4.16). Accordingly, no strictly valid conclusions can be drawn relative to the zero collective pitch case on the basis of the developed equations. Nevertheless, it is of interest to note that there is only one uncoupled* Y (or Z) coefficient, listed in Table 4.1-2, accounting for the generation of a sideforce, and it is δ_o-dependent. The tentative conclusion is that pure sideforce cannot be developed when the collective pitch setting is zero.

6.2 ZERO FORWARD SPEED - COUNTER-THRUSTING COLLECTIVE PITCH

In this mode of balanced operation, forward and aft collective pitch are equal in magnitude but oppositely signed. (i.e., $\delta_f = +\delta_o$, $\delta_a = -\delta_o$**). Net thrust, forward velocity, and net roll moment are zero. From Table 4.1-2, the uncoupled Y and Z forces are given in lines 12 and 10 respectively as:

---

*An uncoupled coefficient is taken to mean one which is independent of all of the motion variables but dependent only on control inputs.

**A δ symbol without the forward or aft subscript carries no inherent sign.

$$Y_p = QC/\Omega(\delta_{2f}+\delta_{2a})\delta_0\left[-\Omega f_1 C(1-a) - \tfrac{1}{2}\Omega a\right] \text{ lbs.} \qquad (6.2\text{-}1)$$

$$Z_p = QC/\Omega(\delta_{1f}+\delta_{1a})\delta_0\left[-\Omega f_1 C(1-a) - \tfrac{1}{2}\Omega a\right] \text{ lbs.} \qquad (6.2\text{-}2)$$

If we focus our attention on the y-axis, and let $\delta_{2f} = \delta_{2a} = +\delta_2$, (6.2-1) becomes:

$$Y_p = -2QC\,\delta_0\delta_2\left[f_1 C(1-a) + \frac{a}{2}\right] \qquad (6.2\text{-}3)$$

For the postulated configuration:

$$Q = \tfrac{1}{2}\rho A N R^2\Omega^2 \cong 5820\Omega^2$$
$$C \cong 6$$
$$f_1 \cong .1$$
$$a \cong .9$$

Thus:

$$Y_p \cong -QC\,\delta_0\delta_2 a \cong -31400\Omega^2\delta_0\delta_2 \text{ lbs.} \qquad (6.2\text{-}3a)$$

If δ_2 is restricted to a maximum of $0.2\,\delta_0$, in keeping with the assumption that $\delta_2 < \delta_0$, and if δ_0 is limited to about 0.1, in keeping with the linear approximation of the expression for inflow velocity (refer to Equation 4.1-39) the available sideforce is then:

$$|Y_p|_{max} \cong 62\Omega^2 \text{ lbs} \qquad (6.2\text{-}4)$$

At high propeller speeds, say 5 rad/sec, the available force is about 1500 lbs.*

---

*For the same cyclic control input about 11,000 lbs are available in the high speed case.

Before proceeding to compute the side velocity, v , which may be obtained with this sideforce, it is interesting to draw an analogy between the previously developed expression for sideforce in the high-speed case and Equation (6.2-3).

The sideforce expression in the high-speed case is given by Equation (5-15), Reference 1 (with change in collective pitch, $\Delta\delta$, equal to zero):

$$Y_C = \text{CONTROL FORCE} = Y_\delta (\delta_{2f} - \delta_{2a}) \qquad (6.2\text{-}5)$$

Notice first that in the high-speed case, with both propellers thrusting, sideforce, Y , is obtained by <u>difference</u>-cosine cyclic pitch ($\delta_{2f} - \delta_{2a}$), whereas in the hovering case above, with the propellers counter-thrusting, it is obtained by <u>sum</u>-cosine cyclic pitch ($\delta_{2f} + \delta_{2a}$), per Equation (6.2-1). If, in (6.2-5) above $\delta_{2f} = +\delta_2$, $\delta_{2a} = -\delta_2$, and the expression for Y_δ (pg 46 of Reference 1) is substituted:

$$Y_C = 2\delta_2 \left\{ -\tfrac{1}{2}\rho \frac{u_0^2 A N}{\sin\gamma_0} \left[\frac{C_{L_\alpha}}{2} + \cot\gamma_0 \, f_1 C_{L_\alpha}^2 \alpha_0 \right] \right\}$$

Now if the following limits are taken:

as $u_0 \to i \to R\Omega a \delta_0$

$\sin\gamma_0 \cong \gamma_0 \to i/R\Omega$

$\cot\gamma_0 \cong 1/\gamma_0 \to R\Omega/i$

$\alpha_0 = \delta_0 - \gamma_0 \to \delta_0 - i/R\Omega$

the "high-speed" expression for sideforce reduces to

$$Y_C = -2Q C_{L_\alpha} \delta_0 \delta_2 \left(\frac{a}{2} + f_1 C_{L_\alpha} (1-a) \right)$$

which is identical in form to Equation (6.2-3), for the hovering case.

Returning to the hovering case, it is of interest to compute, with the aid of the coefficients of Table 4.1-2, the steady-state y-velocity that can be attained, as well as some of the coupling forces/moments.

Assume that the submarine is initially in a balanced counter-thrusting state (i.e., $\delta_{of} = +\delta_o$, $\delta_{oa} = -\delta_o$) with $\delta_1 = \delta_2 = u = v = w = p = q = r = 0$. If sum-cosine cyclic pitch is applied, that is, $\delta_{2f} = +\delta_2$, and $\delta_{2a} = +\delta_2$, the uncoupled y-force, given by (6.2-1) can be summed with the appropriate, remaining propeller forces in Table 4.1-2 and the hull hydrodynamic force in Table 4.2-1. The result is:*

$$2\delta_o^2 \frac{QC}{\Omega}\left[-\frac{2f_1C}{R}\right]v + 2\delta_o\delta_2\frac{QC}{\Omega}\left[-\Omega f_1 C(1-a) - \frac{1}{2}\Omega a\right] - 4\frac{d}{CR}\frac{QC}{\Omega}v$$

$$+2\delta_2^2\frac{QC}{\Omega}\left[-\frac{3}{2}f_1\frac{C}{R}\right]v - \frac{1}{2}\rho\ell^2(.081)\,v|v| = 0 \qquad (6.2\text{-}6)$$

In keeping with the restriction that $\delta_2 < \delta_o$, the δ_2^2-dependent drag is small compared to the δ_o^2-dependent drag, and can be ignored. The approximate y-force expression then becomes:

$$\frac{QC}{\Omega}\left\{-4\delta_o^2 f_1\frac{C}{R}v - 2\delta_o\delta_2\Omega\left(f_1C(1-a)+\frac{a}{2}\right)\right.$$

$$\left. - \frac{4d}{CR}v\right\} - \frac{1}{2}\rho\ell^2(.081)\,v|v| = 0 \qquad (6.2\text{-}7)$$

On substituting the following physical constants:

$\delta_o = 0.1$; $\delta_2 = 0.02$; $f_1 \cong .1$; $C = 5.7$; $d = .015$; $a = .95$; $N = 16$; $A = 3$; $R = 11$; $\ell = 275$; $\frac{QC}{\Omega} = \frac{1}{2}\rho ANR^2\Omega C$. (6.2-7) becomes:

$$v + .656\Omega + \frac{61.5}{\Omega}v|v| = 0, \qquad (6.2\text{-}8)$$

---

*Since $\dot{v} = 0$ in the steady-state, there are no inertia reaction forces.

for which: $v \cong -.09$ ft/sec. $(\Omega = 1)$

and $v \cong -.48$ ft/sec. $(\Omega = 5)$

For the case $\Omega = 1$, above, the inflow velocity is:

$$\lambda \cong R\Omega\,(.95\delta_0 - \delta_0/\delta_0/)$$
$$\cong .94 \text{ ft/sec.},$$

and the thrust per propeller (neglecting drag) is,

$$X_p \cong \tfrac{1}{2}\rho A N \Omega^2 R^2 C_{l_\alpha} \left(\delta_0 - \frac{\lambda}{R\Omega}\right)$$
$$\cong 496 \text{ lbs.}^*$$

In the calculations just given for the trim y-velocity, it was tacitly assumed that all propeller force/moment couplings to other than the y-axis were zero. These couplings can be identified by using the coefficients of Table 4.1-2.

---

*This is approximately equal to the thrust due to change in momentum given by $2\rho A_d \lambda^2$, where A_d = the projected area of the propeller disc.

On noting that $\delta_1 = 0$, the complete set of δ inputs for the case just treated are:

Line*	Effective δ Inputs		
2	$\delta_{0f} - \delta_{0a}$	=	$2\delta_0$
5	$\delta_{2f} + \delta_{2a}$	=	$2\delta_2$
7	$\delta_{0f}^2 + \delta_{0a}^2$	=	$2\delta_0^2$
12	$\delta_{0f}\delta_{2f} - \delta_{0a}\delta_{2a}$	=	$2\delta_0\delta_2$
15	$\delta_{2f}^2 + \delta_{2a}^2$	=	$2\delta_2^2$
20	$\delta_{0f}^3 - \delta_{0a}^3$	=	$2\delta_0^3$
22	$\delta_{0f}^2\delta_{2f} + \delta_{0a}^2\delta_{2a}$	=	$2\delta_0^2\delta_2$
23	$\delta_{0f}(\delta_{1f}^2 + \delta_{2f}^2)$	=	$\delta_0\delta_2^2$
24	$\delta_{0a}(\delta_{1a}^2 + \delta_{2a}^2)$	=	$-\delta_0\delta_2^2$
25	δ-independent		

On multiplying each δ-input by the corresponding coefficient in each axis, it is seen that the coupled X- and Z-forces due to the propellers are zero. The coupled K- and N-moments are also zero, but the coupled M-moment is (from lines 5, 20 and 22 of Table 4. 1-2),

$$\frac{QC}{\Omega}\left\{2\delta_2\left[-\tfrac{1}{2}\Omega R\right] + 2\delta_0^3\left[-f_1 C a^3\right]v + 2\delta_0^2\delta_2\left[a(1-a)\Omega R f_1 C\right]\right\}$$

*Refer to Table 4. 1-2.

in which the dominant term is the first. This term yields a pitching moment of $-7700\,\Omega^2$ ft-# (approximate) for $\delta_2 = .02$ rad. This moment is not significant at low Ω but would have to be balanced out by appropriate control action for Ω approaching maximum values.

The roll- and yaw-moment couplings resulting from the hydrodynamic characteristics of the hull, are given in Table 4.2-1 as:

$$K_v = -\tfrac{1}{2}\rho l^3\, v|v|\,(.000395)$$

and

$$N_v = -\tfrac{1}{2}\rho l^3\, v|v|\,(.00004)$$

On substituting the two values for $v|_{trim}$ found above, we obtain:

when $\Omega = 1$, and $v \cong -.09$ ft/sec : K-moment $\cong$ 67 ft-#; N-moment $\cong$ 7 ft-#

when $\Omega = 5$, and $v \cong -.48$ ft/sec : K-moment $\cong$ 1900 ft-#; N-moment $\cong$ 190 ft-#

Since these moments are not negligible, at high Ω, it would be necessary to cancel them by appropriate propeller action in order to obtain zero roll/yaw rates.

In summary, we find that for the counter-thrusting hovering case ($u = 0$), lateral* velocities of the order of .1 ft/sec and .5 ft/sec can be attained at low and high propeller speeds, respectively, for a collective pitch of approximately 0.1 radian and cyclic settings of 0.02 radian. The propeller forces coupling into x and z are zero, as are the coupled (propeller) K- and N-moments. The coupled M-moment, due to the propellers, is not large enough to present any problem in achieving a pure side-velocity but the roll and yaw moments (particularly roll) caused by the hydrodynamic characteristics of the hull would have to be cancelled by proper control action.

---

*Since the propeller hydrodynamics in the y-direction and the z-direction are identical, and $Z_w \cong Y_v$, these results would also apply to z-velocities.

6.3 VERY LOW FORWARD SPEED - THRUSTING COLLECTIVE PITCH

In this mode of operation the collective pitch of the forward and aft propellers is trimmed at levels that yield a small, net positive thrust and a resulting forward velocity slightly greater than zero. Consideration of this mode of operation will provide a rough indication of the ability of a TPS configuration to execute very slow translational maneuvers in a single plane. Attention will be confined to the generation of pure sideforce. No examination will be made of the steady-state response to a turning control moment, although rolling and yawing moments may exist because of hydrodynamic coupling.

A small net thrust may be achieved in at least two different ways. In the first way, the δ_0-inputs are symmetrical ($\delta_{0f} = \delta_{0a} = +\delta_0$). δ_0 is small and propeller speeds are equal. Y-force is obtained by superimposing difference-cosine cyclic pitch, $\delta_{1f} - \delta_{1a}$, upon the trim collective pitch. In the second way, large, nearly equal, values of asymmetrical collective pitch are used. If ϵ is small, and $\delta_{0f} = +\delta_0 + \epsilon$ while $\delta_{0a} = -\delta_0 + \epsilon$, the sum, $\delta_{0f} + \delta_{0a}$, is positive and small.

The first method, i.e., using small values of δ_0, is more efficient with respect to power consumption and will be examined below for (1) trimmed forward flight and (2) the generation of a pure sideforce.

The required collective pitch for trimmed, very low forward-speed flight will be determined by equating the propeller X-forces in Table 4.1-1 to the hull drag. If $\delta_{0f} = +\delta_0$, $\delta_{0a} = +\delta_0$ and $\delta_1 = \delta_2 = v = w = p = q = r = 0$, we have:

$$2\rho C_{L_\alpha} \left\{ \delta_0 - \frac{u+i}{R\Omega} \right\} - 2\rho C_{d_0} \left\{ \frac{u+i}{R\Omega} \right\}$$

$$-2\rho f_1 C_{L_\alpha}^2 \left\{ \delta_0^2 \left(\frac{u+i}{R\Omega} \right) \right\} = .001 \ell^2 u|u| \qquad (6.3\text{-}1)$$

in which the squared and cubed terms involving $\frac{u+i}{R\Omega}$ have been ignored. Equation (6.3-1) can be written as:

$$\delta_0 - \frac{u}{R\Omega}\left\{1 + \frac{C_{d0}}{C_{L_\alpha}} + f_1 C_{L_\alpha} \delta_0^2\right\} - \frac{i}{R\Omega}\left\{1 + \frac{C_{d0}}{C_{L_\alpha}} + f_1 C_{L_\alpha} \delta_0^2\right\}$$

$$= 0.001\, \ell^2 \left(\frac{u}{R\Omega}\right)^2 \Big/ \frac{2QC_{L_\alpha}}{R^2\Omega^2} \qquad (6.3\text{-}2)$$

For small δ_0 (i.e., very low forward speeds), the drag terms in the brackets can be expected to be small relative to unity. These terms can be discarded in the $u/R\Omega$ multiplier, since $i/R\Omega$, the inflow "angle of attack", will generally be much smaller than δ_0. On the other hand, for accurate results, the drag terms should not be dropped in the $u/R\Omega$ multiplier because $u/R\Omega$ will usually be very nearly equal to δ_0* (leading to the problem of a small difference of large numbers). Since in the present case we are interested only in arriving at order-of-magnitude results, the drag terms will be dropped in both brackets. The error in computed u will be of the order of 15 or 20 percent.

On substituting the expression for $i/R\Omega$ given in Appendix C (Equation C-5), (6.3-2) becomes:

$$\alpha_u \cong \frac{.001\ell^2\left(\frac{u}{R\Omega}\right)^2}{\frac{2QC_{L_\alpha}}{R^2\Omega^2}\left\{1 - \frac{\frac{u}{2\Omega R} + \frac{1}{4}}{\left(\frac{u}{R\Omega}\right)^2 + \left(\frac{u}{R\Omega}\right) + \frac{1}{4}}\right\}} \qquad (6.3\text{-}3)$$

where $\alpha_u = \delta_0 - \frac{u}{R\Omega}$.

*See computations given below.

For an arbitrarily selected value of $u/R\Omega = .050$, Equation (6.3-3) can be used to compute α_u, while δ_0 and $i/R\Omega$ may be determined from relationships previously given. The following results are obtained:

$$u/R\Omega = .050 \quad \left\{ u = .55 \text{ ft/sec for } \Omega = 1 \right\}$$
$$\alpha_u = \delta_0 - u/R\Omega \cong .0038$$
$$\delta_0 \cong .0538$$
$$i/R\Omega \cong .0034$$

Thus, with $\Omega = 1$, the δ_0 required for $u \cong .55$ ft/sec is, roughly, 2.9°. The inflow velocity is quite small, being about .04 ft/sec (i.e., $\ll u$) and the hydrodynamic angle of attack, $\delta_0 - \frac{u+i}{R\Omega}$, is also quite small. The two-propeller thrust, neglecting drag, is computed to be about 23 lbs*. It is cautioned that this thrust computation, and the calculations preceding it, are admittedly quite crude. In addition to the general limitations previously noted in developing the propeller and inflow velocity equations, and the caution expressed in Section 4.2 concerning the accuracy of the assumed hull drag coefficient, it is possible that significant Reynold's number effects are not being accounted for at the low tip speeds involved (e.g. $\Omega = 1$). In the final analysis, it will probably prove necessary to resort to experimental data in order to carry out the kind of calculations attempted in this section. Accordingly, only a brief qualitative discussion will be given of the generation of sideforce under the conditions specified above.

---

*At this thrust level, many minutes (perhaps hours) would be required to build up to forward speed!

A crude approximation of the sideforce available by means of cyclic pitch can be obtained from the Y-force equation of Table 4.1-1, wherein drag effects are neglected. On using difference-cosine cyclic pitch as the control input (i.e., $\delta_{2f} = +\delta_2$, $\delta_{2a} = -\delta_2$), we obtain:

$$Y_p \cong -QC_{i_\alpha}\delta_2 \frac{u+i}{R\Omega} \qquad (6.3\text{-}4)$$

Since, for the trimmed, forward flight conditions described above, $\frac{u+i}{R\Omega} \cong .0534$, the propeller sideforce is:

$$Y_p = -5820\ \Omega^2 (5.7)(.0534)\ \delta_2 = -1770\ \delta_2 \text{ lbs.}$$

If the above result is compared with the counter-thrusting case of the previous section, namely,

$$Y_p \cong -31400\ \Omega^2 \delta_0 \delta_2 \text{ lbs.}, \qquad (6.2\text{-}3a)$$

it is found that the two forces are about equal when the conditions of the present case are inserted into (6.2-3a), that is, $\delta_0 = .0538$ and $\Omega = 1$. Thus, it should be possible to produce side velocities, in the present case, of about the same order of magnitude as were produced in the counter-thrusting case. In addition, the hydrodynamic couplings for the present case should be quite comparable to the counter-thrusting case, although these couplings are not so easily sorted out in the basic propeller equations of Table 4.1-1, as they are in the matrix of Table 4.1-2.

A significant difference between the counter-thrusting case and the case of very low forward speed is that in the latter, a control input $\delta_{2f} - \delta_{2a}$ produces Y-force, as it does in the high speed case, whereas, the required input is $\delta_{2f} + \delta_{2a}$ when the propellers are counter-thrusting. This difference is due to the fact that δ_0 of the aft propeller is negative for the counter-thrusting case and positive for the thrusting case.

In closing this section, it must be emphasized that, aside from questions of limitations on the analysis and the validity of assumptions, the numerical examples given are not indicative of maximum performance. Relatively low levels of collective and cyclic pitch were used, for reasons which have been explained. More exact performance predictions can be made when the appropriate experimental data become available, or if the analysis presented herein is extended and refined considerably.

VII

STABILITY AND CONTROL

7.1 LOW-SPEED OPERATION

Aside from the analysis of control force/moment interactions and the steady-state translational velocities achievable in trimmed hovering flight (reported in Section VI) it has not been possible to perform any significant work on low-speed stability and control in the present study. A low-speed stability and control analysis is discussed as a future work item in Section VIII.

7.2 HIGH-SPEED OPERATION

As pointed out earlier, the work to be described in this section may be thought of as a continuation of the trim and stability and control studies accomplished and reported in Reference 1. Topics considered in this section are:

(1) Analysis of Diving Performance

(2) Two Propeller, Symmetrical Operation - Yaw Plane

(3) High Speed Operation with One Powered Propeller - Yaw Plane

7.2.1 Analysis of Diving Performance

In order to provide quantitative data for comparing the TPS high speed pitch-plane performance with that of a representative contemporary submarine, a study of the dynamic behavior of the TPS in the pitch plane was performed and the results reported in Reference 1 (pp 73-87). In addition to this small perturbation or linearized analysis, the determination of maximum diving rates consistent with available control range is important for defining the envelope of pitch-plane maneuverability within which the TPS must operate because of limited control forces and moments. In this section, calculations are made to determine limit diving-rate maneuvers at constant forward speed in terms of (1) peak blade angles of attack required to maintain a given steady-state depth rate, and (2) peak blade angles of attack required to achieve transient depth rate changes in response to a sudden change in ordered pitching moment. The results are compared with calculated results for similar maneuvers in a contemporary submarine of the Albacore class.

7.2.1.1 Steady-State Diving Maneuvers

The application of a constant pitching moment to the submarine by means of a cyclic pitch input causing a pure pitching moment results in a steady-state depth rate, $\dot{z}_{ss}$.* On referring to Reference 1 (pg 69), Equations (7-3), we find that the relationships between depth rate, pitch angle, and pitching moment for a steady-state diving-rate maneuver are given by:

$$\begin{aligned} -Z_w \dot{z}_{ss} - Z_w U_o \theta_{ss} &= 0 \\ -[M_w U_o + M_\theta]\theta_{ss} - M_w \dot{z}_{ss} &= M_c = M_\delta \delta_M \end{aligned} \tag{7.2-1}$$

Solving Equations (7.2-1) for $\dot{z}_{ss}$ and θ_{ss}, we have

$$\dot{z}_{ss} = -U_o \theta_{ss} \tag{7.2-2}$$

$$\theta_{ss} = -\frac{M_\delta}{M_\theta} \delta_{M_{ss}} \tag{7.2-3}$$

---

* It is assumed that basic "arrow" stability has been achieved through direct-axis feedback terms in the pitching moment equation, as explained in Reference 1 (pp 71-73).

Equation (7.2-2) shows that the hull angle of attack (or velocity $\dot{w}$ along the submarine z axis) is zero, in contrast to the non-zero steady-state angle of attack that would exist for a conventional submarine. This condition is desirable because it minimizes the hull drag profile, during a steady-state descent.

For purposes of numerical computation, it is assumed that a steady-state pitch angle of the hull equal to twenty degrees is the maximum permissible value. Under this assumption, a longitudinal velocity of u_o = 40 ft/sec (the assumed high-speed value of u_o in Reference 1, Table 6-1) yields a maximum steady-state depth rate of

$$\dot{z}_{ss})_{MAX} = -(40)\left(\frac{20}{57.3}\right) = -14 \text{ FT./sec.}$$

It is desirable to compute the peak values of propeller-blade angles of attack required to generate this steady-state depth rate in order to determine whether propeller stalling will occur; namely, can the specified steady-state pitch-angle be obtained within the linear range of available control forces and moments. On substituting values of M_θ and M_δ taken from Reference 1, Equation (7.2-3) indicates that the y-axis control-moment input necessary to achieve a steady-state pitch angle of twenty degrees is

$$\delta_{M_{ss}} = -\frac{-9.63\times10^6}{30.25\times10^6}(20) = 6.37 \text{ deg.}$$

If a symmetrical control input is assumed, δ_M consists of equal values of the fore and aft sine-cyclic pitch angles, δ_{1f} and δ_{1a}, that is,

$$\delta_{M_{ss}} = \delta_{1a} + \delta_{1f} = 2\delta_{1a} = 2\delta_{1f} \qquad (7.2\text{-}4)$$

Thus, the magnitude of fore and aft cyclic pitch required to produce a steady-state diving rate of 14 ft/sec or a steady-state pitch angle of 20 degrees is

$$\delta_{1f} = \delta_{1a} = \frac{1}{2}(6.37) = 3.18 \text{ deg.}$$

The instantaneous angle of attack of a single propeller blade, for high-speed operation, is given by:

$$\alpha(\sigma) = \alpha_0 + \Delta\delta(t) + \delta_1 \sin\sigma(t) + \delta_2 \cos\sigma(t) \qquad (7.2\text{-}5)$$

Thus the peak angle of attack of any blade, that occurs during one revolution of the propeller, is given by*:

$$|\alpha|_{PEAK} = |\alpha_0 + \Delta\delta| + \sqrt{\delta_1^2 + \delta_2^2} \qquad (7.2\text{-}6)$$

For the vertical-plane maneuver under consideration, Equation (7.2-6) reduces to:

$$|\alpha_{f,a}|_{PEAK} = |\alpha_0| + |\delta_{lf,a}|$$

Reference 1 indicates that the trim angle of attack, α_0, is 0.10 rad (5.73 deg) for u_0 = 20 ft/sec. Therefore,

$$|\alpha_{f,a}|_{PEAK})_{ss} = 5.73 + 3.18 = 8.91 \text{ deg.}$$

Thus, the percentage of available pitching moment required to achieve a steady-state diving rate of fourteen ft/sec (θ_{ss} = 20 deg) is

$$100\frac{M_C}{M_{C_{MAX}}} = \frac{100\delta_{lf,a}}{\alpha_{MAX} - \alpha_0} = \frac{(100)(3.18)}{20 - 5.73} = 22.3\%$$

where α_{MAX} is assumed to be 20 degrees (approximately). Note, however, that the percentage of total available control power, including contributions to both longitudinal thrust and pitching moment is 100 $(\frac{8.91}{20})$ = 44.6 percent. We conclude then, that the peak values of blade angle of attack required to achieve a steady-state pitch angle of 20 degrees fall well within the linear range of the individual propeller lift curves.

---

* If we assume that $\Delta\delta(t)$ varies slowly relative to $\sin\sigma(t)$ and $\cos\sigma(t)$.

7.2.1.2 Transient Maneuvers in the Vertical Plane

Reference 1 recommends that stabilization of the TPS pitch-plane motions be accomplished through direct-axis feedback of pitch angle and pitch rate to the cyclic-pitch control. Accordingly, the y - moment control input, δ_M , is related to an ordered value, δ_{MC} , by:

$$\delta_M = \delta_{MC} - \bar{K}_\theta \theta - \bar{K}_{\dot\theta} \dot\theta \qquad (7.2\text{-}7)$$

If the diving maneuver is considered to be the depth rate resulting from a sudden (step) change in ordered pitching moment, $M_\delta \delta_{MC}$ the variable δ_M will vary with time until the pitch rate decays to zero. If the submarine is flying straight and level, the initial depth rate and pitch angle will be zero. Further, because of the large moment of inertia in pitch, I_{yy} , a period of time must elapse before θ and $\dot\theta$ differ significantly from zero. Consequently, δ_{MC} and δ_M are equal initially, that is,

$$\delta_M(0+) = \delta_{MC}(0+)$$

In Section 7.2.1.1, it was shown that the steady-state pitch angle is related to the y - axis moment control input, δ_M , as follows:

$$\delta_{M_{ss}} = -\frac{M_\theta}{M_\delta}\theta_{ss}$$

Thus, to achieve a steady-state pitch angle of 20 degrees, $\delta_{M_{ss}} = 6.37$ degrees. The magnitude of step-input of δ_{MC} necessary to result in the above value of $\delta_{M_{ss}}$ is obtained by solving Equation (7.2-7) for δ_{MC} .

For

$$\bar{K}_\theta = 5 \qquad \text{(Reference 1, Figure 7-9)}$$

$$\delta_{MC} = 6.37 + (5)(20) = 106.4 \text{ deg}$$

Thus, to perform a dive in which θ goes from zero to twenty degrees, in response to a step-change in δ_{MC}, the fore and aft cyclic pitch required at $t = 0+$ are

$$\delta_{1a} = \delta_{1f} = \frac{1}{2}\delta_M = 53.2 \text{ deg.}$$

Note that these values of cyclic pitch will place the peak angle of attack of individual blades well above the stall limit. Thus the requirement to provide automatic control for dynamic stability does not permit the ordering of a step change in "command" cyclic pitch which, in the steady-state, will result in the cyclic-pitch level required to produce the specified dive angle of twenty degrees. The stabilization process, in effect, reduces the control effectiveness of the submarine during transient conditions but does not influence the control effectiveness in the steady state.

Since the effects of control saturation on the pitch-plane response of the TPS were not included in the analog computer work reported in Reference 1, the degradation of response time due to control saturation is not known. Qualitatively, however, the effect is not expected to be serious because of the inherent pitch instability, wherein the high-speed submarine response is rapidly divergent due to destabilizing hull forces. When an appreciable pitch rate and/or pitch angle does develop, the feedback control system will act to stabilize the remaining portion of the transient response. This fact is clearly illustrated in Reference 1, Figure 7-9, where the fore and aft blade angles of attack reverse almost immediately after application of the step function of ordered pitching moment δ_{MC}. The time constant associated with the linear system responses shown in this figure are about forty seconds and could probably be improved by using pitch acceleration feedback.

7.2.1.3 Albacore Diving Rate

Calculations, similar to those of the previous section, for an Albacore-type submarine indicate that a pitch angle of twenty degrees can be obtained when.

δ_b = - 1.6 deg. the bowplane angle

δ_s = 0.9 deg. the sternplane angle

The Albacore pitch plane response time (here defined as time required to reach 95% of the ordered value of pitch angle) is approximately 80 seconds, according to data from Reference 2. The corresponding response time for the TPS is approximately 40 seconds. The value for the TPS depends on the magnitudes of the feedback gains selected and is not to be considered as optimum. It is concluded that, in comparison with an Albacore-type ship, the TPS can achieve an equivalent steady-state diving rate in an equivalent, or less, time. However, the TPS uses a greater percentage of available control power (Approximate values for this example: TPS - 22%; Albacore-type - 8%).

7.2.2 Two Propeller, Symmetrical Operation - Yaw Plane

In Section VII of Reference 1 a summary is presented of the stability analysis and control-system studies performed to achieve desirable pitch-plane behavior of the TPS. A similar study has since been performed of the yaw-plane behavior of the TPS using both operational-calculus and analog-computer techniques. As before, care was taken to restrict propeller angles of attack to values below an assumed stall point, and an assessment of the division of control power between the required stability augmentation and desired maneuverability was made. The nonlinear control coupling terms (Reference 1, pp 48 and 49) were included in the analog-computer simulation and conclusions are drawn herein, as to their significance.

7.2.2.1 Equations of Motion

The dynamic equations that describe the six-degree-of-freedom response of the TPS to control forces and moments are given in Reference 1 (pg 53). For small perturbations from trim conditions, it is possible to replace the non-linear terms represented by products of variables and trigonometric functions in these equations with the first order terms of Taylor-series expansions, resulting in a set of linear, ordinary-differential equations in the perturbed variables (Reference 1, pg 69). In studying the yaw-plane behavior, the yaw-pitch coupling term M_r is neglected; more exactly, the assumption is made that the proper δ_1 (sine) cyclic-pitch components are applied to the propellers to cause a zero value of pitch rate for all yaw-plane maneuvers. For linear operation, the neglect of M_r or the assumption that pitching moments are available to cancel the effect of M_r are equivalent insofar as yaw-plane results are concerned. With limited control power, however, the δ_1 -cyclic-pitch components required to hold a zero pitch rate subtract from the control power available to perform yaw-plane maneuvers.

The yaw-roll equations are given in matrix form by*:

$$\begin{bmatrix} (m_2 s - Y_v) & (m_1 u_o - Y_r) & -Y_p s \\ -N_v & (I_{zz} s - N_r) & -N_p s \\ -K_v & -K_r & I_{xx} s^2 - K_p s - M_\phi \end{bmatrix} \cdot \begin{bmatrix} \bar{v}(s) \\ \dot{\psi}(s) \\ \phi(s) \end{bmatrix} = \begin{bmatrix} Y_C \\ N_C \\ K_C \end{bmatrix} \quad (7.2\text{-}8)$$

The control terms, Y_C , N_C , K_C originally given in Reference 1, are repeated below for convenience.

---

* The propeller gyroscopic coupling coefficient ($H_f - H_a$) is zero with balanced propeller operation.

$$Y_C = Y_\delta \delta_y + \tfrac{1}{2} Y_{\Delta\delta\cdot\delta} (\delta_x \delta_y + \delta_K \delta_N)$$

$$N_C = N_\delta \delta_N + \tfrac{1}{2} Y_{\Delta\delta\cdot\delta} \ell_2 (\delta_x \delta_N + \delta_K \delta_y) + N_{\Delta\delta\cdot\delta_1} (\delta_x \delta_M + \delta_K \delta_y) + N_{\delta_1} \delta_M$$

$$K_C = K_{\Delta\delta} \delta_K + K_{(\Delta\delta)^2} \delta_x \delta_K + K_{\delta^2} (\delta_y \delta_M + \delta_y \delta_N)$$

(7.2-9)

By forming the characteristic equation* of the yaw-plane dynamics of the TPS and substituting the numerical values tabulated in Reference 1, it is readily determined that the TPS is unstable in the yaw-plane. This result was also noted in the pitch-plane analysis and was explained in Reference 1 (pg 70). Application of Routh's criteria (Reference 3) to the yaw-plane characteristic equation shows the basic requirement for stability to be:

$$N_r (m_1 u_0 - Y_{\dot{r}}) + Y_r N_{\dot{r}} > 0 \qquad (7.2\text{-}10)$$

Substitution of numerical values from Reference 1 into this inequality indicates that the instability exists throughout the high-speed regime. The unstabilized yaw-plane response of the TPS to a small step function of yawing moment command ($\delta_{NC} = \delta_N = 5.73$ deg) is shown in Figure 7.2-1. Note the monotonically divergent response. As a consequence of this instability, an automatic-control system was synthesized to augment the stability of the TPS. This stability augmentation was accomplished by sensing certain yaw-plane motion variables and causing the cyclic and collective pitch angles of the propellers to vary proportional to linear combinations of these motion variables. The cyclic and collective pitch terms combine to produce forces and moments on the submarine in such a direction as to overcome the inherent destabilizing forces and moments, and produce a stable, controllable vehicle.

---

* The characteristic equation is formed by evaluating the determinant of the square matrix of Equations (7.2-8).

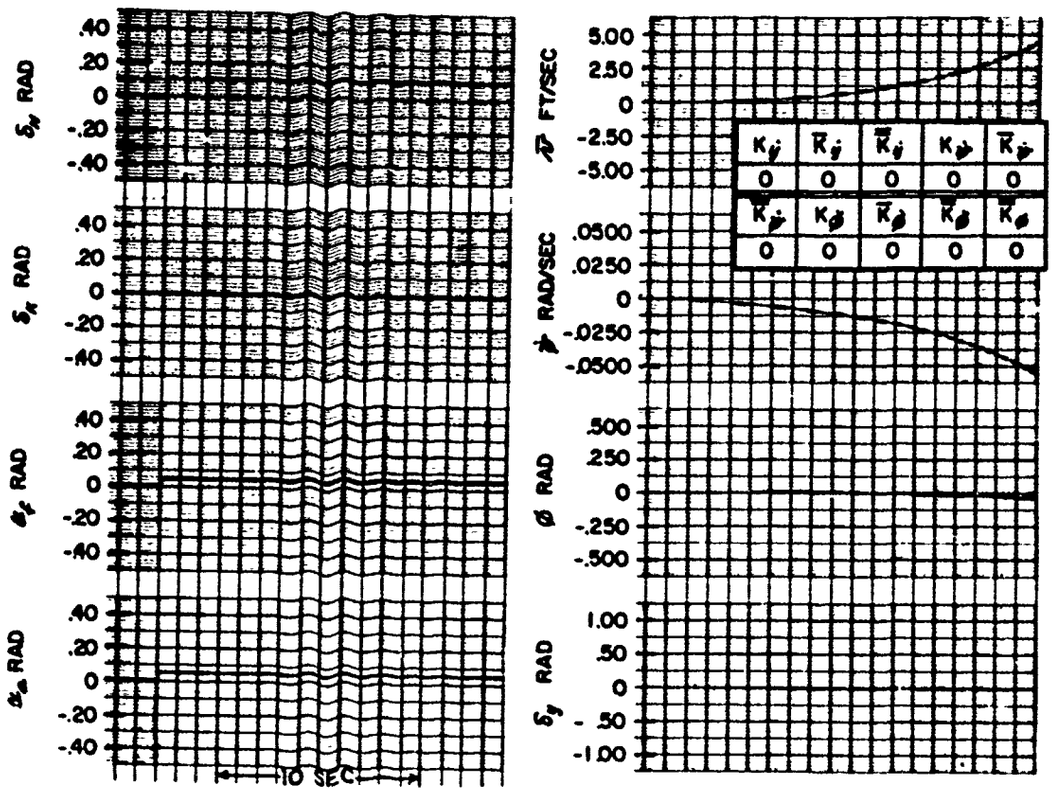

FIGURE NO. 7.2 - 1 BASIC SUBMARINE YAW PLANE RESPONSE TO A SMALL YAWING MOMENT COMMAND (δ_{rc} 0.10 RAD)

Equation (7.2-10) indicates the desirability of increasing the term $Y_{\dot{v}} N_{\dot{\psi}}$ and/or decreasing the term $N_{\dot{v}}(m, z_G - Y_{\dot{v}})$ to produce stable operation. The value of $N_{\dot{\psi}}$ (yaw damping) can be effectively increased, for example, by adding the direct-axis stabilization torque, $-N_{\delta} \bar{K}_{\dot{\psi}} \dot{\psi}$, to the left-hand side of the yawing-moment equation. Similar control terms can be generated to decouple the yaw-sideslip-roll motions of the submarine, through the use of cross-axis feedback terms, thus effectively reducing the terms $(m, z_G - Y_{\dot{v}})$, Y_p, $K_{\dot{v}}$, $K_{\dot{\psi}}$, $N_{\dot{v}}$, N_p, and N_{ϕ} to zero.*

The propeller angles are modified according to Equations (7.2-11) in order to implement the feedback-stabilization technique.

$$\left.\begin{aligned} \delta_y &= \delta_{yc} + K_{\dot{v}} \dot{\bar{v}} - K_{\dot{\psi}} \dot{\psi} - K_{\dot{\phi}} \dot{\phi} \\ \delta_N &= \delta_{Nc} + \bar{K}_{\dot{\psi}} \dot{\psi} - \bar{K}_{\dot{v}} \dot{\bar{v}} - \bar{K}_{\dot{\phi}} \dot{\phi} \\ \delta_K &= \delta_{Kc} + \bar{\bar{K}}_{\dot{\phi}} \dot{\phi} + \bar{\bar{K}}_{\phi} \phi - \bar{\bar{K}}_{\dot{\psi}} \dot{\psi} - \bar{\bar{K}}_{\dot{v}} \dot{\bar{v}} \end{aligned}\right\} \quad (7.2\text{-}11)$$

in which all of the K's are control-system gains. No heading-angle loop was used, because the immediate concern is stabilization for maneuvering and not long-term navigation.** Since the immediate problem was one of stabilizing the TPS, the feedback terms assumed in Equations (7.2-11) were limited to those that contribute directly to producing stable behavior in the yaw plane. Note that yawing acceleration feedback could also be added to improve the transient response of the TPS by effectively reducing, for example, the yawing moment of inertia, I_{zz}. Feedback of this type would have no influence on the

---

* The terms Y_p and N_p are already negligibly small in the TPS, effectively decoupling the roll and yaw-sideslip portion of the fourth order characteristic equation into two independent quadratic factors.

** A navigation loop can be added at any future time with the proper heading angle sensors.

steady-state responses of the submarine. Since acceleration feedback was not included in this study, the transient responses determined herein are probably not optimum. They are, however, optimized with respect to conservation of control power for yaw-plane maneuvers.

7.2.2.2 Direct-Axis Stabilization

The use of direct-axis stabilization in the yawing-moment equation results in an increase in the effective yaw-damping derivative, N_r, which has a stabilizing influence (see Equation 7.2-10). The gain $\bar{K}_{\dot{\psi}}$ is used to achieve this result. It can be shown that dynamic stability is insured through use of this single feedback term provided that the relationship,

$$\bar{K}_{\dot{\psi}} > -\frac{N_r(m, u_o - Y_{\dot{r}}) + N_{\dot{r}} Y_r}{Y_r N_\delta} \qquad (7.2\text{-}12)$$

is satisfied. There is no theoretical upper limit to $\bar{K}_{\dot{\psi}}$, but a practical limit occurs when the individual propeller blade angles of attack approach (approximately) twenty degrees. Because of the metacentric stiffness in roll no stability augmentation is required about the roll axis. However, the roll damping is poor and it appears desirable to improve the dynamic response in roll by augmenting the roll damping and roll stiffness derivatives, K_p and K_ϕ *, by $\bar{K}_{\dot{\phi}}$ and $\bar{\bar{K}}_\phi$, respectively.

By substituting numerical values into the augmented characteristic equation, without yet specifying values of the direct-axis feedback gains, $K_{\dot{v}}$, $\bar{K}_{\dot{\psi}}$, $\bar{K}_{\dot{\phi}}$, and $\bar{K}_\phi$, it is possible to show that the fourth-order characteristic equation, including both products and sums of these feedback terms, neatly factors into two quadratic terms. One quadratic factor contains only the yaw and sideslip direct-axis feedback terms, $\bar{K}_{\dot{\psi}}$ and $K_{\dot{v}}$; the other contains only the roll terms $\bar{K}_{\dot{\phi}}$ and $\bar{K}_\phi$. Further analysis showed that this factoring is permissible because the roll-axis motions are weakly coupled to the yaw and sideslip axes of the submarine, i.e. N_p and Y_p are negligibly small. The converse is not

* Note that the metacentric roll moment has previously been presented as $M_\theta \cos\theta \sin\psi$, which for small angles yields $K_\phi = M_\theta$.

true, however, since yaw and sideslip motions couple into the rolling moment equation through $K_{\dot{\beta}}$ and K_{β}. Carrying this analysis still further in the evaluation of the numerator determinants of Equations (7.2-8), one finds that the numerators of $\frac{\dot{\psi}}{\delta_{NC}}(s)$ and $\frac{\phi}{\delta_{RC}}(s)$ contain common factors with the denominator (i.e., the characteristic equation) resulting in (1) yaw-rate responses that depend on yaw-loop gain and are independent of roll-loop gains, and (2) roll-position responses that depend on roll-loop gains and are independent of yaw-loop gain. This separation of the influence of the four direct-axis feedback gains allows relatively simple analytical evaluation of the yaw-plane dynamics of the augmented TPS.

Examination of the response transforms of direct-axis variables to step functions of corresponding direct-axis control inputs (e.g. $\frac{\dot{\psi}}{\delta_{NC}}(s)$ and $\frac{\phi}{\delta_{RC}}(s)$) indicates that the roll-axis behavior is that exhibited by an underdamped second-order system, with $\bar{K}_{\phi}$ affecting both the undamped natural frequency and the damping ratio, and $\bar{K}_{\dot{\phi}}$ affecting the damping ratio alone. Values of $\bar{K}_{\dot{\phi}}$ and $\bar{K}_{\phi}$ were selected to produce a 6.3 second undamped natural period with a damping ratio of 0.70, thus producing about five percent overshoot in the roll angle response to a step input of roll moment. On the other hand, the yaw rate response to a step-function in yawing moment is always overdamped, for any value of feedback gain $\bar{K}_{\dot{\psi}}$, resulting in two exponential subsidences that approach the steady-state response asymptotically. For example, yaw-rate time constants of 0.65 and 13.5 seconds result when $\bar{K}_{\dot{\psi}} = 100$, as illustrated by Figure 7.2-2.

It is anticipated that some difficulty would occur in sensing sideslip velocity $\bar{v}$, and it can be shown that sensing $\bar{v}$ is not required because satisfactory operation can be obtained without the y-velocity feedback, $K_{\dot{y}}$. Hence, this term is not used.

It can be argued that the most useful controlled variable for high-speed maneuvering is rate of change of heading angle. Lateral translation would very seldom be required, and a commanded roll angle would probably have no utility at high-speeds. For this reason, analog computer responses to yawing

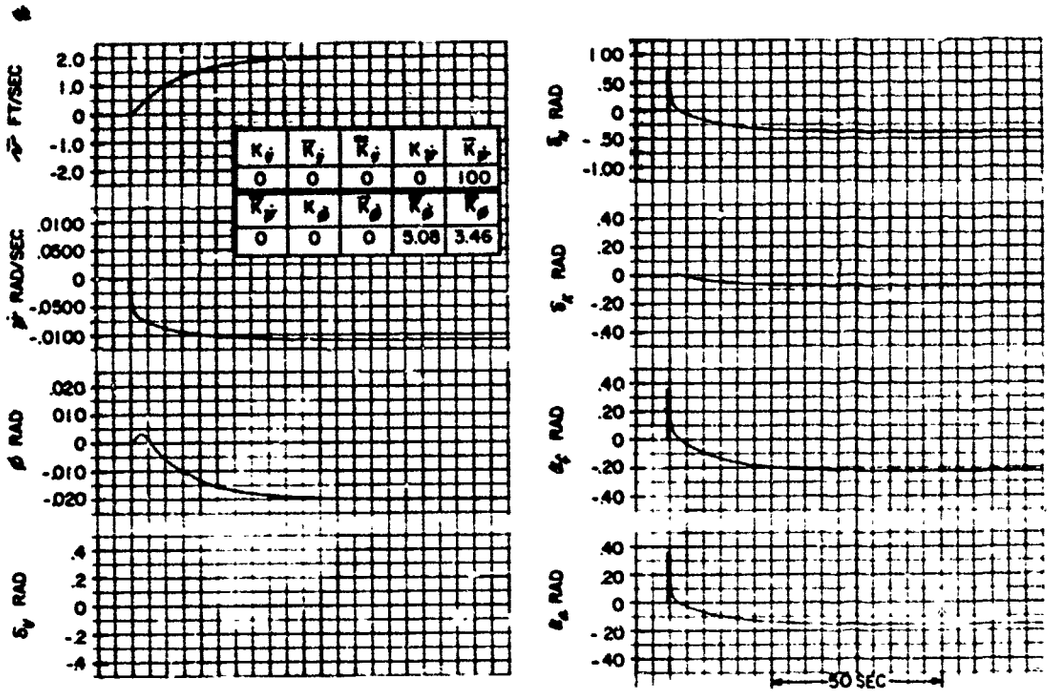

FIGURE NO. 7.2 - 2 DIRECT-AXIS STABILIZATION-YAW PLANE RESPONSE TO A YAWING MOMENT COMMAND (δ_{NC} 0.70 RAD)

moment and side force commands were obtained. Rolling moment feedback terms applied through automatic control were, of course, retained. Both side-force and yawing moment commands were investigated because both yaw and sideslip responses are influenced, through the coupling terms, $m_1 u_0 - Y_r$ and N_r, by either driving function*. It was desired to determine which of the two driving functions is more "economical" in its use of the available control power. Figure 7.2-3 shows the linear system yaw-plane response of the TPS, using roll and yaw direct-axis stabilization, to a step function of side-force resulting from a δ_{yc} command of only 23 degrees.** Although the resulting dynamic responses are reasonable, in that they possess a quasi first-order time constant of approximately fifteen seconds, the peak angle of attack of the front propeller blades increases from 11.5 degrees to 30 degrees as the steady-state condition is approached. Because this figure represents the behavior of a linear dynamic system wherein available control forces and moments are unlimited, whereas in actual fact, saturation of the front propeller occurs beyond blade angles of attack of about twenty degrees, the steady-state responses shown in Figure 7.2-3 must be scaled down by about thirty percent in order to maintain linear control action.

In contrast with the above result, a yawing moment command to the same TPS configuration results in a faster dynamic response with a thirteen percent greater static sensitivity. The peak angles of attack of the propeller blades do not exceed the commanded value at any point in the transient response. These results are illustrated by Figure 7.2-2, where δ_{NC} = 40 degrees. Note that a slight reversal of roll angle occurs at the start of the left turn shown, because the initial yawing moment produces a positive sideforce on the fairwater until the sideslip angle builds up and generates a fairwater angle of attack resulting in a negative steady-state rolling moment. This effect can be removed by decoupling the yaw into roll response (i.e. forcing K_r to zero).

---

* Recall that with direct-axis stabilization both pitch angle and depth rate were influenced by δ_{MC} or δ_{HC} commands in the pitch-plane but that use of pitching moment commands for coordinated depth changes resulted in much lower propeller blade angles of attack for similar transient and steady-state results.

** Note that $\delta_{yc} = \delta_{2fc} - \delta_{2ac}$, thus requiring an initial value of only 11.5 deg. of cyclic pitch on the fore and aft blades with symmetrical operation. This corresponds to approximately 58 percent of the available side force.

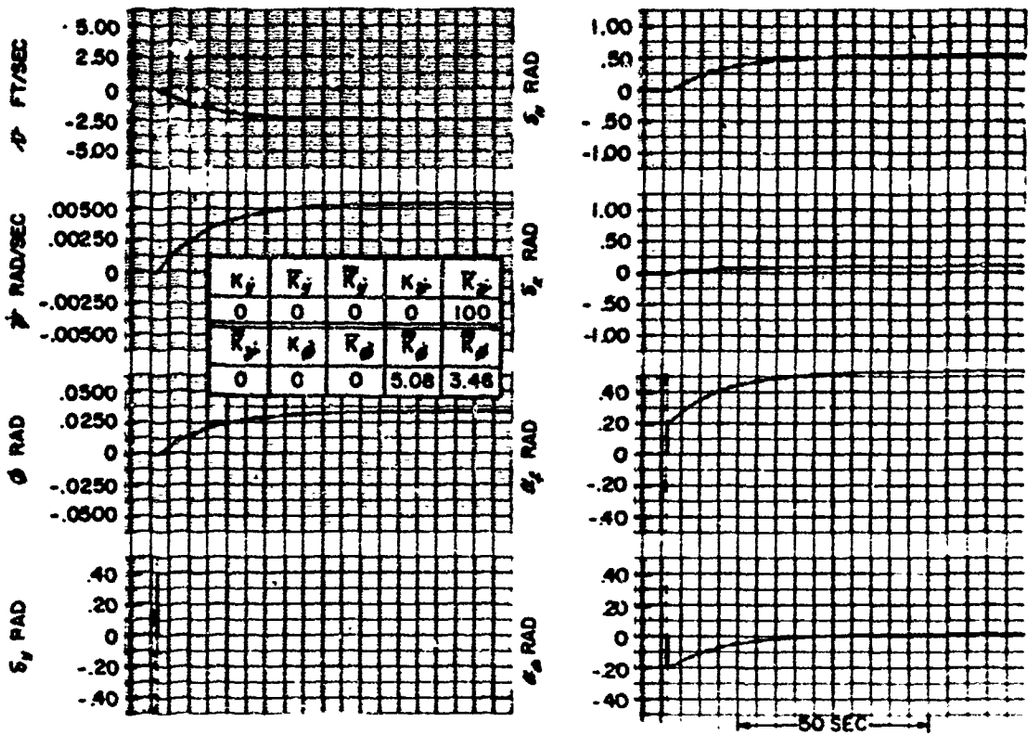

FIGURE NO. 7.2 - 3 DIRECT-AXIS STABILIZATION-YAW PLANE RESPONSE TO A SIDE FORCE COMMAND (δ_{yc} = 0.40 RAD)

7.2.2.3 Decoupling Stabilization

As noted earlier, it is required that $N_v(m, u_o - Y_r) + N_r Y_v > 0$ for dynamic stability in yaw. The direct-axis stabilization techniques described in the previous section were designed to increase the term, $N_r Y_v$, but not to affect the $N_v(m, u_o - Y_r)$ term. By use of decoupling stabilization, the opposite effect is obtained, i.e., $N_r Y_v$ remains unchanged but $N_v(m, u_o - Y_r)$ is made to approach zero. It can be shown that the following relationships define the numerical values of the decoupling feedback gains necessary to null N_v and $m, u_o - Y_r$ respectively*.

$$\bar{K}_{\dot{\psi}} = \frac{N_v}{N_\delta} = 0.239 \frac{\text{RAD.}}{\text{FT/SEC.}} \qquad (7.2\text{-}13)$$

$$K_{\dot{\psi}} \frac{m, u_o - Y_r}{-Y_\delta} = 49.3 \frac{\text{RAD.}}{\text{RAD/SEC.}} \qquad (7.2\text{-}14)$$

Either one, or both of these feedback gains will result in stable behavior in the yaw plane. Figure 7.2-4 for example, illustrates the responses of the TPS to a yawing-moment step function where only $K_{\dot{\psi}}$ and $\bar{K}_{\dot{\psi}}$ are non-zero, thus nulling $(m, u_o - Y_r)$ and K_r. The rolling moment due to yaw rate, $K_r r$, does not affect stability, indicating that the single decoupling feedback gain, $K_{\dot{\psi}}$, will unconditionally stabilize all of the yaw-plane responses. This result is analogous to that achieved with the single direct-axis feedback gain, $\bar{K}_{\dot{\psi}}$, used previously (see Figure 7.2-2). Note, in Figures 7.2-3 and 7.2-4, that the decoupling stabilization requires more control power than direct-axis stabilization, and has a slower yaw-rate response.

If all of the decoupling feedback terms are properly adjusted, it is possible to completely decouple the yaw/sideslip/roll responses. This decoupling process is the only way in which "pure"** submarine control can be accomplished. For example, Figure 7.2-5 shows that the only response of the TPS to a step function of applied rolling moment is the roll angle, ϕ. Nine feedback gains using sensors on four submarine motion variables are required to implement

---

* Note that complete nulling is not required for stability, provided that Equation (7.2-10) is satisfied.

** A single-axis response to a single-axis command.

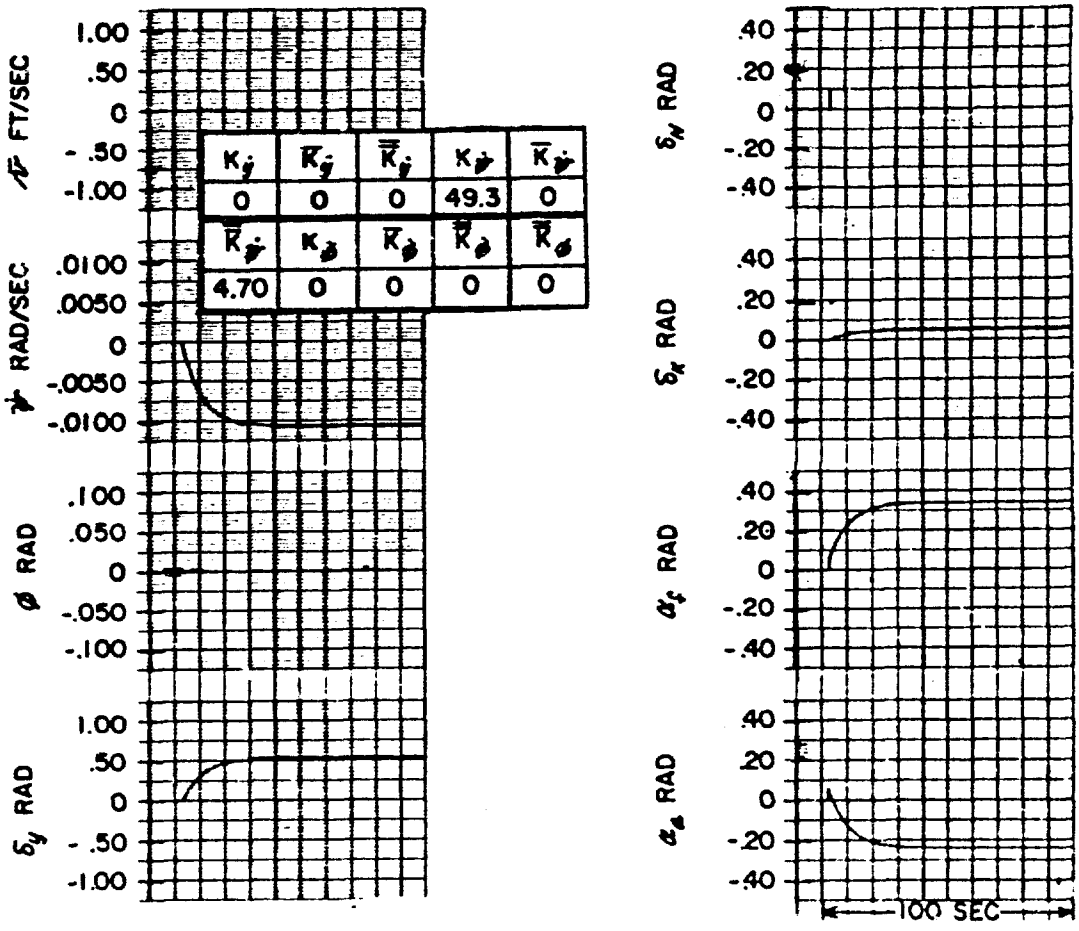

$K_{\dot{y}}$	$\bar{K}_{\dot{y}}$	$\bar{\bar{K}}_{\dot{y}}$	$K_{\dot{\psi}}$	$\bar{K}_{\dot{\psi}}$
0	0	0	49.3	0
$\bar{\bar{K}}_{\dot{\psi}}$	$K_{\dot{\phi}}$	$\bar{K}_{\dot{\phi}}$	$\bar{\bar{K}}_{\dot{\phi}}$	$\bar{\bar{K}}_{\phi}$
4.70	0	0	0	0

FIGURE NO. 7.2 - 4 PARTIAL DECOUPLING STABILIZATION RESPONSE TO A YAWING MOMENT COMMAND (δ_{NC} 0.10 RAD)

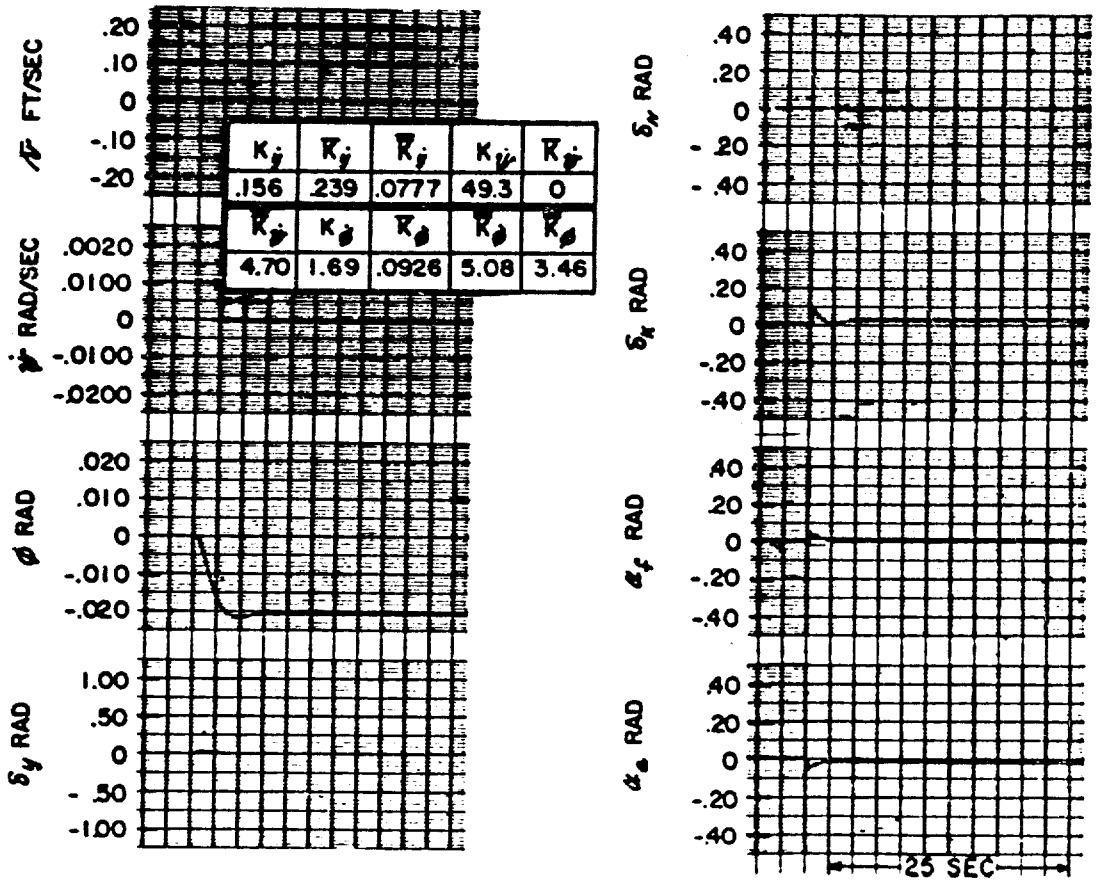

$K_{\dot{y}}$	$K_{\dot{r}}$	$K_{\dot{p}}$	$K_{\dot{\psi}}$	$K_{\dot{\phi}}$
.156	.239	.0777	49.3	0
K_{ψ}	$K_{\dot{\alpha}}$	K_{α}	K_{ϕ}	K_{ϕ}
4.70	1.69	.0926	5.08	3.46

FIGURE NO. 7.2 - 5 FULL DECOUPLING STABILIZATION WITH ROLL RESPONSE SHAPING - YAW PLANE RESPONSE TO A ROLLING MOMENT COMMAND (δ_{RC} 0.10 RAD)

this condition. The utility of using such a complex stabilization system in the high-speed operating regime is questionable but the results are presented in the interests of generality.

7.2.2.4 Combined Decoupling and Direct-Axis Stabilization

An analysis of the characteristics of the two stabilization techniques discussed previously suggests that the best results can be obtained by combining the two methods. This is, in fact, the case. A combination of the two methods tends to increase $N_r Y_v$ and decrease $N_v(mu_o - Y_v)$ simultaneously. Figure 7.2-6 illustrates the result that is obtained when yaw-to-roll and yaw-to-sideslip (i.e., K_v, Y_v) decoupling has been combined with yaw-rate direct-axis stabilization (i.e., an increase in the yaw damping, N_r). The gain $\overline{K\dot{\psi}}$ was adjusted to produce an optimum usage of forward propeller angle of attack. Note that α_f does not vary from twenty degrees throughout the transient response. It is seen that the front propeller generates its maximum available side force continuously during the transient and steady-state portion of the turn; this force essentially contributes to (1) yawing moment initially and, (2) both yawing moment and sideforce in the steady-state.

In the turn shown in Figure 7.2-7, direct-axis stabilization is used to increase the damping in yaw and decoupling stabilization is used to eliminate yaw to roll coupling. The decoupling feedback was included to eliminate the small, initial reversal in roll angle exhibited in Figure 7.2-2. The feedback gain, $\overline{K\dot{\psi}} = 73.5$, was selected to use the full available range of peak blade angle of attack of the forward propeller. The roll response seen in Figure 7.2-7 results from the sideslip-to-roll coupling, K_v, (due to the fairwater) and the sideslip response results from the yaw-to-sideslip coupling, $m, u_o - Y_v$. Note that the incremental collective pitch, $\Delta\delta$, required to shape the roll response of the TPS is small, being less than three degrees. This result is expected because of the relatively small moments required to roll the submarine, and the relatively greater roll-control effectiveness than yaw-control effectiveness*.

---

* A proof of this statement is that $N_\delta/N_r < K_\delta/K_p$, that is, the ratio of the control coefficient to the primary term that requires controlling is greater in the roll axis than in the yaw axis:

$$\frac{N_\delta}{N_r} = .103 \qquad \frac{K_{\Delta\mathcal{E}}}{K_p} = .504$$

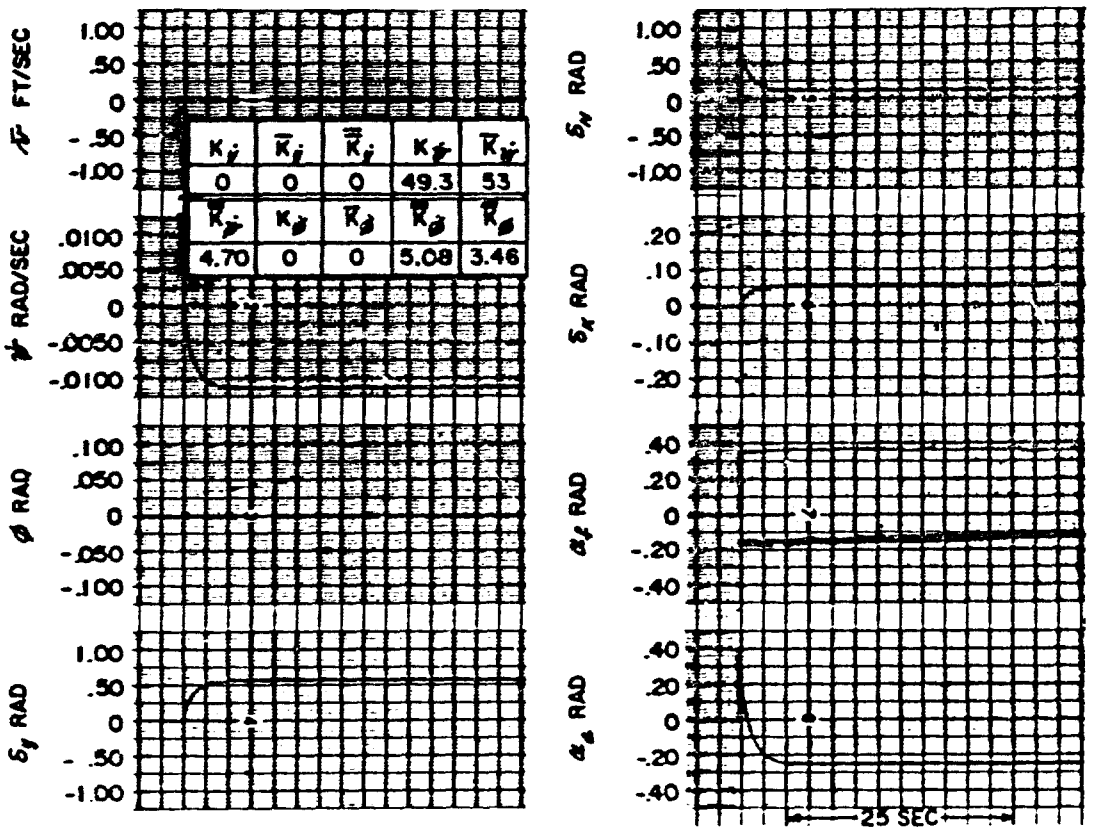

FIGURE NO. 7.2 - 6 COMBINED PARTIAL DECOUPLING PLUS DIRECT-AXIS STABILIZATION-YAW PLANE RESPONSE TO A YAWING MOMENT COMMAND (δ_{mc} 0.70 RAD)

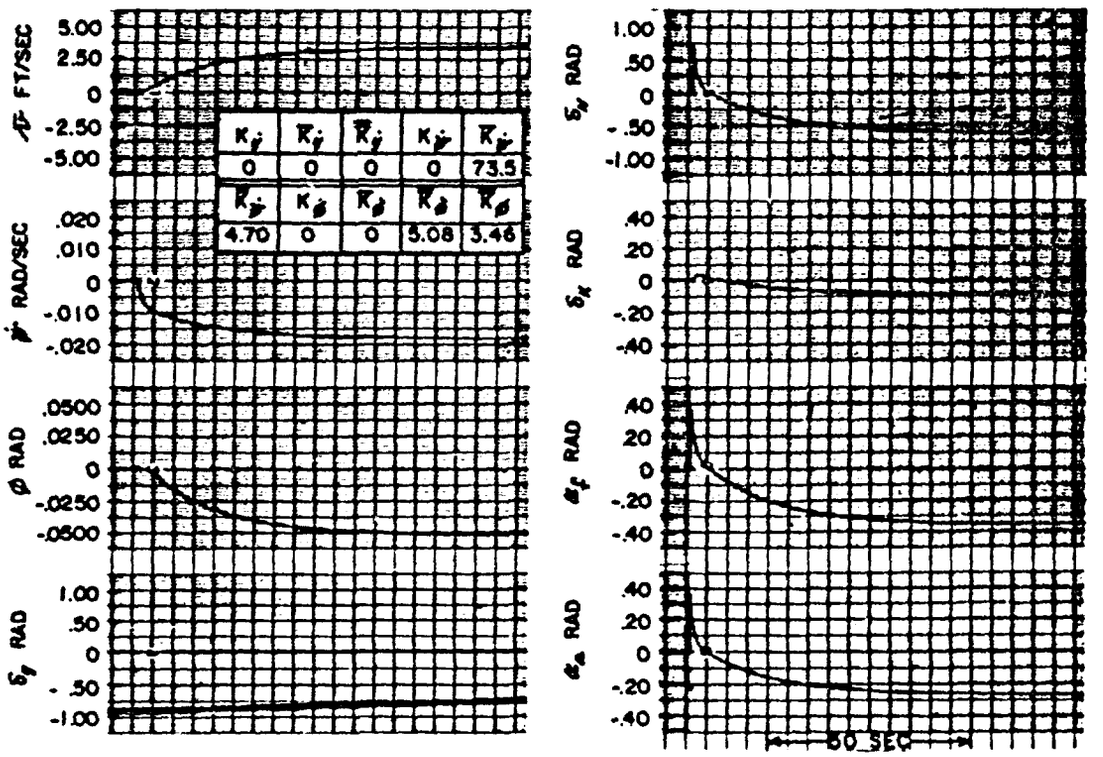

$K_{\dot{y}}$	$\bar{K}_{\dot{y}}$	$\bar{\bar{K}}_{\dot{y}}$	$K_{\dot{\psi}}$	$\bar{K}_{\dot{\psi}}$
0	0	0	0	73.5
$\bar{K}_{\dot{\psi}}$	$K_{\dot{\phi}}$	$\bar{K}_{\dot{\phi}}$	$\bar{\bar{K}}_{\dot{\phi}}$	$\bar{K}_{\phi}$
4.70	0	0	5.08	3.46

FIGURE NO. 7.2 - 7 DIRECT-AXIS STABILIZATION WITH YAW INTO ROLL DECOUPLING-YAW PLANE RESPONSE TO A YAWING MOMENT COMMAND (δ_{Nc} = 0.70 RAD)

Figure 7.2-7 represents the best compromise between (1) loop gain, (2) control-system simplicity, (3) dynamic response and (4) available control power. Here, failure of any or all of the three feedback loops, controlled by $\bar{K}_{\dot{\psi}}$, $\bar{K}_{\psi}$, and $\bar{K}_{\dot{\psi}}$, in the rolling moment equation could occur with no loss of stability. The gain, $\bar{K}_{\dot{\psi}}$, can vary over wide limits, provided that $\bar{K}_{\dot{\psi}} > 34.3$ for $u_o = 40$ ft/sec, without loss of stability and with only small changes in the form of the dynamic responses*. The yaw-rate equivalent time constant (63.2% of final value) for the direct-axis feedback gain of $\bar{K}_{\dot{\psi}} = 73.5$ is approximately seven seconds, compared with an estimated value of about 80 seconds for the Albacore.

7.2.2.5 Influence of Nonlinear, Control-Coupling Terms

The foregoing analysis has been limited to linear system responses, where scaling from one amplitude to another allows a convenient assessment of the maximum capabilities of the control system. If the nonlinear, control-coupling terms from Equations (7.2-9) are included in the analysis, it is no longer allowable to scale responses from one amplitude to another, unless the non-linear effects can be shown to be negligible.

Function generating equipment was used to produce the nonlinear terms of the control force and moment Equations (7.2-9) and key analog computer solutions obtained for the linear system were rerun with the nonlinear control terms included. The nonlinear solutions were obtained at limit values of propeller angles of attack, because the nature of the nonlinearities is such that they are most significant for large control inputs. In every case where limit maneuvers were computed, the effects of the nonlinearities were found to be negligible. The largest effect was the change in forward speed, u_o, resulting from the X_{δ}^2 coefficient and the control terms, δ_g and δ_N (Reference 1, pg 50); this change in speed never exceeded one knot for the most unfavorable combination of blade angles.

---

* For very large values of $\bar{K}_{\dot{\psi}}$, the $\dot{\psi}/\delta_{NC}$ response becomes that of a first-order system with a time constant given by: $T_{\dot{\psi}} = -\frac{I_{zz}}{N_r + N_\delta \bar{K}_{\dot{\psi}}}$

In accordance with the arguments presented earlier favoring the use of yawing- and pitching-moment commands for control of the submarine at high speeds, it can be concluded that the control inputs, δ_z, δ_y, and δ_x, will result almost entirely from control-system feedback signals. Large changes in the thrust command, δ_x, tend to change the effectiveness of the yawing moment command δ_N, and the pitching moment command δ_M, but these are primarily direct-axis effects and are not expected to be serious. In general, except for the most severe high-speed maneuvers, terms involving products of control inputs will be negligible in comparison with the primary control moments, $M_\delta \delta_M$ and $N_\delta \delta_N$.

The computed nonlinear responses of the TPS are in all cases nearly identical to the equivalent, linear-system responses already shown and, accordingly, are not reproduced in this report.

7.2.3 High Speed Operation with One Powered Propeller - Yaw Plane

Because of the relatively complex nature of the propeller control system of the TPS, it is desirable to analyze the influence of various system failures on the stability and control of a partially disabled vehicle. Although the number of possible system failures (without regard to probability) is large, one of the most meaningful studies that can be performed is the study of the loss of driving power to a single propeller, while the remaining propeller maintains normal operation. For the present investigation, this propeller failure is assumed to be represented by a nonrotating propeller ($\Omega = 0$) where control over collective pitch is maintained.

An analysis of submarine stability and control with one nonrotating and one rotating propeller is a logical extension of the single-propeller, trim-operation study of Reference 1. Although it was shown in Reference 1 that the trim force and moment equations can be satisfied simultaneously with a single rotating propeller, no information on the resulting maneuverability of the TPS was presented.

An analysis of single-propeller operation at high speed requires a re computation of the hull and propeller stability derivatives because of (1) a change in the trim operating speed of the submarine and (2) the unbalanced propeller operation. The modified stability derivatives were computed for the optimum single-propeller operating point noted in Reference 1 (pg 60). Analog computer studies were then performed to determine the submarine stability and control behavior for small perturbations from the quiescent point with the aft propeller driving and the forward propeller stationary, and vice versa. As a result of the unbalanced propeller operation it is also necessary to investigate the influence of the yaw-pitch, gyroscopic-coupling torques on submarine motions, in terms of the cyclic pitch angles required to decouple these torques.

Assuming that controllability of collective pitch is maintained in the locked propeller, the trim values that result in the most efficient submarine operation were computed in Reference 1 and are listed below for convenience:

$\gamma_{\text{locked}} = 90°$	$U_o = 24.5$ ft/sec $= 14.5$ knots
$\gamma_{\text{rotating}} = 23°$	$\Omega_{\text{rotating}} = 50$ rpm
$\alpha_{\text{locked}} = 14.7°$	$\Omega_{\text{locked}} = 0$
$\alpha_{\text{rotating}} = 4.8°$	$P_o = 2820$ horsepower

The physical properties of the submarine, viz. weights, inertias, geometry, lift and drag coefficients, and number of propeller blades remain the same as in the study of two-propeller operation. The rotating propeller is assumed to be angular-velocity limited rather than power limited, because it produces only 49% of rated power at rated speed. Note that it is assumed that the trim values hold irrespective of which propeller rotates and which propeller is locked. If, in addition, it is assumed that both propellers possess cyclic-pitch as well as collective-pitch control, a new set of propeller stability derivatives and control coefficients is obtained*. The individual propeller

* The control coefficients computed for a locked propeller are not used in this study because the cyclic pitch control of the locked propeller is assumed to be disabled. However, the numerical values are computed for convenience in possible future studies.

stability derivatives depend upon which propeller rotates and which propeller is locked, whereas the individual control coefficients are invarient for a locked and for a rotating propeller, irrespective of location.

Consider the case where the forward propeller is nonrotating with locked trim collective pitch and the aft propeller rotates at rated speed with adjustable collective and cyclic pitch. The propeller control coefficients for the yaw plane are obtained from the equations for Y_δ and N_δ given in Reference 1 (pp 46 and 48), where account is now taken of the dissymmetry between the trim operating conditions of the fore and aft propellers. Due to this dissymmetry, unequal fore and aft control coefficients are obtained and the yaw-plane control forces and moments are represented by:

$$\left.\begin{aligned} N_C &= N_{\delta f}\,\delta_{2f} + N_{\delta a}\,\delta_{2a} \\ Y_C &= Y_{\delta f}\,\delta_{2f} - Y_{\delta a}\,\delta_{2a} \\ K_C &= K_{\Delta\delta f}\,\Delta\delta_f - K_{\Delta\delta a}\,\Delta\delta_a \end{aligned}\right\} \qquad (7.2\text{-}15)$$

These equations are comparable to the linear terms of Equations (5-15), Reference 1. The nonlinear, control-coupling terms, if they are to be analyzed, must also be separated into the fore and aft components. However, the nonlinear, control-coupling terms have been neglected here because of their small influence on the response of the TPS, as noted previously.

The individual propeller control coefficients indicated in Equation (7.2-15) are given by:

$$
\left.
\begin{aligned}
Y_{\delta a} &= -\tfrac{1}{2}\frac{\rho U_0^2 AN}{\sin^2\gamma_a}\left\{\tfrac{1}{2}C_{L_\alpha}\sin\gamma_a + (f_1 C_{L_\alpha}^2\cos\gamma_a)\alpha_a\right\} \\
Y_{\delta f} &= -\tfrac{1}{2}\rho U_0^2 AN\left\{\tfrac{1}{2}C_{L_\alpha}\right\} \\
N_{\delta a} &= \ell_2 Y_{\delta a} \\
N_{\delta f} &= \ell_2 Y_{\delta f} \\
K_{\Delta\delta a} &= -\tfrac{1}{2}\frac{\rho U_0^2 ANR}{\sin^2\gamma_a}\left\{C_{L_\alpha}\sin\gamma_a + 2f_1 C_{L_\alpha}^2\cos\gamma_a\cdot\alpha_a\right\} \\
K_{\Delta\delta f} &= -\tfrac{1}{2}\rho U_0^2 ANRC_{L_\alpha}
\end{aligned}
\right\} \quad (7.2\text{-}16)
$$

Numerical substitution yields the following results:

$$
\left.
\begin{aligned}
N_{\delta a} &= -16.9 \times 10^6 \text{ ft-lb/rad} \\
N_{\delta f} &= -5.66 \times 10^6 \text{ ft-lb/rad} \\
Y_{\delta a} &= -154 \times 10^3 \text{ lb/rad} \\
Y_{\delta f} &= -51.4 \times 10^3 \text{ lb/rad} \\
K_{\Delta\delta a} &= -3.38 \times 10^6 \text{ ft-lb/rad} \\
K_{\Delta\delta f} &= -1.13 \times 10^6 \text{ ft-lb/rad}
\end{aligned}
\right\} \quad \text{computed for: } \Omega_a = 50 \text{ rpm}, \ \Omega_f = 0
$$

These control coefficients can be compared with the results obtained for symmetrical two-propeller operation as listed in Table 6-3, Reference 1.

When the aft propeller is locked and the forward propeller rotates, the control coefficients are obtained by interchanging the subscripts a and f in the above equations. Thus, for example, $N_{\delta a} = -5.66 \times 10^6$ ft-lb/rad, etc.

It should be recalled that many of the combined fore and aft propeller derivatives were zero for the case of balanced two-propeller operation. This result occurred when the fore and aft propeller forces/moments were equal, but opposite in sign. When single-propeller operation prevails, however, there are additional propeller contributions to the total stability derivatives that must be individually computed. These computations present certain mathematical difficulties that are briefly reviewed in Appendix B.

7.2.3.1 Maneuvering Analysis: Single-Propeller Operation

Since the dynamic stability of the TPS depends on control forces and moments applied through proper modulation of the individual propeller blade angles, it is of interest to examine the behavior of the submarine when the feedback-stabilization gains are not changed from their normal, two-propeller, balanced-operation values but a single propeller is disabled. For the assumed case of single-propeller operation

$$\Omega_f = 0$$

$$\Delta\delta_f = \delta_{1f} = \delta_{2f} = 0$$

Accordingly, the control equations reduce to

$$\left.\begin{aligned} Y_c &= -Y_{\delta a}\,\delta_{2a} \\ N_c &= N_{\delta a}\,\delta_{2a} \\ K_c &= -K_{\Delta\delta a}\,\Delta\delta_a \end{aligned}\right\} \qquad (7.2\text{-}17)$$

Assuming a stabilization mode before breakdown that is equivalent to that employed in obtaining the yaw-rate responses pictured in Figure 7.2-7, the aft propeller blade angles that result from the command signal and the feedback stabilization loops are given by*:

---

* These equations are obtained by solving Equations (7.2-11) simultaneously with the following equations:

$$\delta_y = \delta_{2f} - \delta_{2a} \qquad \delta_{yc} = \delta_{2fc} - \delta_{2ac}$$

$$\delta_N = \delta_{2f} + \delta_{2a} \qquad \delta_{Nc} = \delta_{2fc} + \delta_{2ac}$$

$$\delta_K = \Delta\delta_f - \Delta\delta_a \qquad \delta_{Kc} = \Delta\delta_{fc} - \Delta\delta_{ac}$$

The feedback gains $K\dot{\psi}$, Ky, $K\dot{p}$, $\bar{K}y$, $\bar{K}\dot{p}$, $\bar{\bar{K}}y$ are zero.

$$\left.\begin{aligned} \delta_{2a} &= \delta_{2ac} + \tfrac{1}{2}\bar{K}_{\dot{\psi}}\,\dot{\psi} \\ \Delta\delta_a &= \Delta\delta_{ac} + \tfrac{1}{2}\left[\bar{K}_{\dot{\psi}}\dot{\psi} - \bar{K}_{\dot{\phi}}\dot{\phi} - \bar{K}_{\phi}\phi\right] \end{aligned}\right\} \qquad (7.2\text{-}18)$$

The sine cyclic-pitch angle, δ_{1a}, is available to counteract the yaw to pitch coupling caused by M_r and H_u. If it is assumed that control over cyclic and incremental collective pitch of the forward propeller is lost, the feedback-stabilization terms shown in Equations (7.2-18) above become the sole source for augmenting the stability of the TPS. It remains to be shown (below) that stable operation results when the forward propeller is disabled.

Stable dynamic behavior in yaw is obtained if

$$N_r(m_1 u_0 - Y_{\dot{r}}) + N_{\dot{r}} Y_r > 0$$

as noted in Section 7.2.2.1, Equation (7.2-10). The side force due to yawing velocity derivative, $Y_{\dot{r}}$, is decreased and the yaw-damping derivative, $N_{\dot{r}}$, is increased by the feedback term $\bar{K}_{\dot{\psi}}$. On combining the basic submarine derivatives with the stability augmentation terms, stable operation in yaw results if

$$N_r(m_1 u_0 - Y_{\dot{r}} + \tfrac{1}{2} Y_{\delta a}\bar{K}_{\dot{\psi}}) + (N_{\dot{r}} + \tfrac{1}{2} N_{\delta a}\bar{K}_{\dot{\psi}}) Y_r > 0$$

or $$\bar{K}_{\dot{\psi}} > -2\,\frac{N_{\dot{r}} Y_r + N_r(m_1 u_0 - Y_{\dot{r}})}{N_r Y_{\delta a} + Y_r N_{\delta a}}$$

On substituting numerical values from Table B-1, Appendix B, we find that dynamic stability in yaw places the following requirement on $\bar{K}_{\dot{\psi}}$, namely:

$$\bar{K}_{\dot{\psi}} > 41.7$$

As noted in Figure 7.2-7, $\bar{K}_{\dot{\psi}}$ = 73.5 for "normal" two-propeller operation. Thus, this brief analysis predicts stable single-propeller operation, with the aft propeller thrusting, and no modification of the feedback-stabilization signals required in a transition from two- to one-propeller operation.

An analog computer mechanization of the operational mode discussed above confirms the above conclusion, and demonstrates rapid, well-behaved submarine responses to yawing-moment control inputs. Figure 7.2-7 was previously discussed as representing optimum two-propeller operation of the submarine. The equivalent single-propeller yaw-plane response, with the aft propeller thrusting, is shown in Figure 7.2-8, where the motion variables $\bar{v}$, $\dot{\psi}$, and ϕ of the submarine are plotted with the same vertical scale and time scale sensitivities as in Figure 7.2-7. Since a single propeller, only, is available to generate control forces and moments, the equivalent commanded value of δ_{2a} is 0.15 rad when δ_{NC} = 0.30 rad, with δ_{2f} = 0. It is apparent from Figure 7.2-8 that stable, controllable yaw-plane behavior is obtained in the specified, partially-disabled operating mode.

In order to determine the effects of disabling the aft propeller, an analysis similar to that just presented was performed. In similar fashion, we assume:

$$\Omega_a = 0$$

$$\Delta\delta_a = \delta_{1a} = \delta_{2a} = 0$$

The control forces and moments are given by:

$$\left.\begin{aligned} Y_c &= Y_{\delta_f}\,\delta_{2f} \\ N_c &= N_{\delta_f}\,\delta_{2f} \\ K_c &= K_{\Delta\delta_f}\,\Delta\delta_f \end{aligned}\right\} \qquad (7.2\text{-}19)$$

In the preferred mode of symmetrical two-propeller operation, the cyclic and collective pitch angles of the forward propeller are given by*:

$$\left.\begin{aligned} \delta_{2f} &= \delta_{2fc} + \tfrac{1}{2}\bar{K}_{\dot{\psi}}\,\dot{\psi} \\ \Delta\delta_f &= \Delta\delta_{fc} + \tfrac{1}{2}\left[\bar{K}_{\dot{\phi}}\,\dot{\phi} + \bar{K}_{\phi}\,\phi - \bar{K}_{\dot{\psi}}\,\dot{\psi}\right] \end{aligned}\right\} \qquad (7.2\text{-}20)$$

* See footnote on page 90.

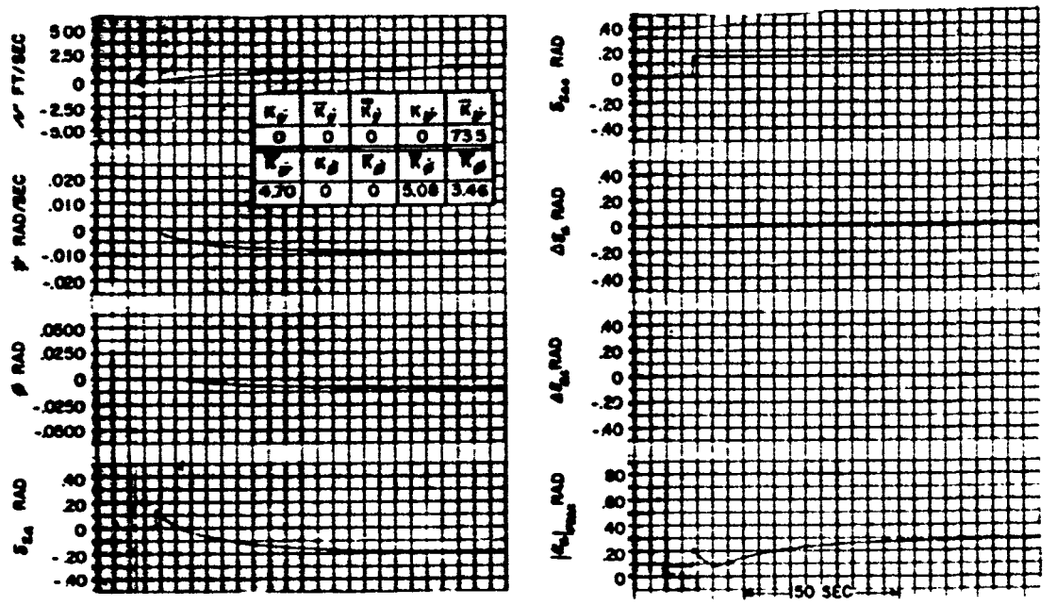

FIGURE NO. 7.2 - 8 SINGLE PROPELLER OPERATION-
AFT PROPELLER THRUSTING

Continuing the analysis in the same manner as before, we have

$$\bar{K}_{\dot{\psi}} > -2\,\frac{N_r Y_v + N_v (m_c u_o - Y_r)^*}{Y_v N_{\delta_f} - N_v Y_{\delta_f}}$$

for stability. Substituting numerical values from Table B-2, we obtain

$$\bar{K}_{\dot{\psi}} > 404.$$

With $\bar{K}_{\dot{\psi}} = 73.5$, the submarine is obviously unstable. The instability is caused by the reversal of sign of the control force, Y_c, that occurs when the thrusting propeller is shifted from the rear to the front of the submarine. Specifically:

$$Y_c = -Y_{\delta_a}\,\delta_{2a}\,, \qquad \text{aft propeller thrusting}$$

$$Y_c = +Y_{\delta_f}\,\delta_{2f}\,, \qquad \text{forward propeller thrusting}$$

Thus, the feedback term, $\bar{K}_{\dot{\psi}}\dot{\psi}$, reduces the destabilizing derivative Y_r when the thrusting propeller is aft but increases Y_r when the thrusting propeller is forward. Because the yawing-moment control term, N_c, does not change sign with location of the thrusting propeller, the yaw-rate feedback increases yaw damping, N_r, in both cases. Thus, if the percentage yaw damping is increased more than the side force due to yawing moment is increased, when the thrusting propeller is forward, an increase in yaw-rate feedback gain in the cosine cyclic pitch, Equation (7.2-20) ultimately stabilizes the submarine response. This requires that $Y_r N_{\delta_f} > N_r Y_{\delta_f}$, a condition that is satisfied with the assumed submarine parameters.

An analog computer simulation confirmed the above predicted instability that results from disabling the aft propeller without modifying the feedback gain, $\bar{K}_{\dot{\psi}}$. It can be shown that a value of feedback gain, $\bar{K}_{\dot{\psi}} = 436$, produces a static sensitivity, $\dot{\psi}/\delta_{2f})_{ss} = -.063\ \frac{\text{rad/sec}}{\text{rad}}$. With the aft propeller thrusting and $\bar{K}_{\dot{\psi}} = 73.5$, the static sensitivity, $\dot{\psi}/\delta_{2a})_{ss}$, is also $-.063\ \frac{\text{rad/sec}}{\text{rad}}$. Thus it is possible to achieve the same static sensitivity simply by increasing the yaw-rate feedback gain used with a thrusting forward

propeller. However, the transient response obtained with a thrusting forward propeller is prohibitively slow, indicating an almost complete lack of maneuverability in this mode. This fact is clearly illustrated by Figure 7.2-9. In order to show the response of the TPS to a step-function of δ_{2fc} in detail, both the vertical and horizontal scales have been changed in Figure 7.2-9 in contrast to the scales used in Figure 7.2-8. Note that the steady-state does not appear in the figure, even though a time period of 30 minutes elapses during the run!

Because cosine cyclic pitch, δ_{2f} , appears directly in both the side-force and yawing-moment control equations, with an opposite effect on submarine stability, depending upon which propeller is being cyclicly controlled, it is apparent that feedback signals that tend to augment stability through the yawing-moment equation will concurrently decrease stability through the side-force equation, and vice versa. We conclude that whenever the aft propeller is disabled (i.e., locked, with control over trim collective pitch only) and control forces and moments can be applied through the forward propeller only, satisfactory transient response cannot be achieved by application of feedback-stabilization signals to control the cyclic pitch of the front propeller. External modification of the pertinent stability derivatives of the TPS through the use of auxiliary control surfaces, for example, would be necessary.

7.2.3.2 Influence of Gyroscopic Coupling on Control Power

In Reference 1 (pg 63) Equations (6-1), the yaw-pitch and pitch-yaw coupling moments, as caused by gyroscopic action, are shown. When balanced operation of the propellers is assumed, the momentum vectors associated with the fore and aft propellers are equal in magnitude and opposite in sign, thus cancelling the effects of each individual propeller on the submarine response. Consequently, these terms are deleted from Equation (7.2-8). If, however, the propeller angular momenta are not equal, as would result from single-propeller operation, a pitching moment due to yaw rate, $(H_f - H_a)\dot{\psi}$, and a yawing moment due to pitch rate, $(H_f - H_a)\dot{\theta}$, are generated. The assumption of pure yaw-plane responses to yaw-moment commands is valid only if sufficient cyclic pitch is available within the control saturation envelope

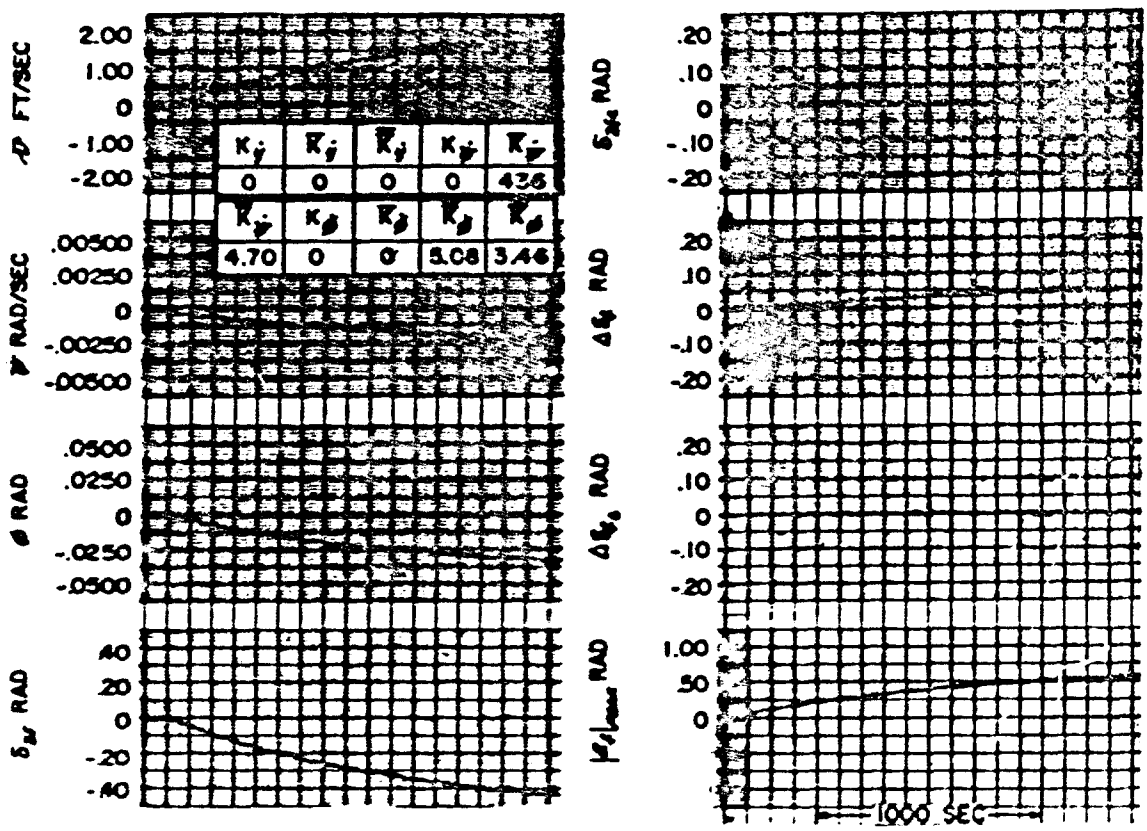

$K_{\dot{v}}$	$K_{\dot{r}}$	$K_{\dot{\phi}}$	$K_{\dot{p}}$	$K_{\dot{\beta}}$
0	0	0	0	436
$K_{\dot{\psi}}$	K_{β}	K_{β}	K_{ϕ}	K_{ϕ}
4.70	0	0	5.08	3.46

FIGURE NO. 7.2 - 9 SINGLE PROPELLER OPERATION - FORWARD PROPELLER THRUSTING

to (1) decouple the yaw to pitch response, (2) decouple the pitch to yaw response, and (3) provide direct yaw and pitch axis control power, simultaneously. Accordingly, it is required that $(H_f - H_a - M_{\dot{\alpha}})\dot{\psi} = M_c$ in the pitching moment equation and $(H_a - H_f - N_{\dot{\beta}})\dot{\theta} = N_c$ in the yawing moment equation. For single propeller operation:

$$\left.\begin{aligned} M_c &= M_{\delta a}\,\delta_{1a} \\ N_c &= N_{\delta a}\,\delta_{2a} \end{aligned}\right\} \quad \text{aft propeller thrusting}$$

$$\left.\begin{aligned} M_c &= M_{\delta f}\,\delta_{1f} \\ N_c &= N_{\delta f}\,\delta_{2f} \end{aligned}\right\} \quad \text{forward propeller thrusting}$$

Consequently, yaw-to-pitch decoupling occurs when

$$\delta_{1a,f} = \frac{H_f - H_a - M_{\dot{\alpha}}}{M_{\delta a,f}}\,\dot{\psi} \qquad (7.2\text{-}21)$$

and pitch-to-yaw decoupling occurs when

$$\delta_{2a,f} = \frac{H_a - H_f - N_{\dot{\beta}}^{*}}{N_{\delta a,f}}\,\dot{\theta} \qquad (7.2\text{-}22)$$

Separate calculations are required for the two single-propeller drive situations. First consider the case of a locked forward propeller. Here, $H_f = 0$ and the remaining terms are listed in Table B-1.

---

* From Reference 1 (pg 28 and 29)

$$N_{\dot{\beta}} = \ell_2\left\{-N_w^{p})_f + N_w^{p})_a + Y_{\dot{\beta}}^{p})_f - Y_{\dot{\beta}}^{p})_a\right\}$$
$$N_w^{p} = M_v^{p}$$
$$Y_{\dot{\beta}}^{p} = Z_{\dot{\alpha}}^{p}$$

Combining these equations with Equation (B-5), it is apparent that $N_{\dot{\beta}} = -M_{\dot{\alpha}}$.

$$\frac{\delta_{1a}}{\dot{\psi}} = \frac{-H_a - M_t}{M_{\delta a}} = \frac{(-2.72 + 5.95) \times 10^6}{16.91 \times 10^6} = .191 \text{ deg/deg/sec}$$

$$\frac{\delta_{2a}}{\dot{\theta}} = \frac{H_a - N_q}{N_{\delta a}} = \frac{(2.72 - 5.95) \times 10^6}{-16.91 \times 10^6} = .191 \text{ deg/deg/sec}$$

When the aft propeller is locked, we find from Table B-2:

$$\frac{\delta_{1f}}{\dot{\psi}} = \frac{H_f - M_r}{M_{\delta a}} = \frac{2.72 + 5.95}{16.1} = .513 \text{ deg/deg/sec}$$

$$\frac{\delta_{2f}}{\dot{\theta}} = \frac{-H_f - N_q}{N_{\delta f}} = \frac{-2.72 - 5.95}{-16.91} = .513 \text{ deg/deg/sec}$$

Maximum values of yaw and pitch rates, when full control power is made available at high speed to perform limit maneuvers with the TPS, are approximately one deg/sec. Consequently, the additional cyclic pitch angles necessary to decouple the yaw and pitch planes never exceed about one-half degree. This amount of cyclic pitch corresponds to 2-3% of the available control power, and is not a significant factor in the TPS stability and control problem.

The general conclusions reached in this section of the report (Section 7.2) are summarized in Section II, Summary of Results and Conclusions.

7.3 BLADE ANGLE RESOLUTION

The trim settings and operating conditions for hovering flight, given in Section VI, and those for the high-speed maneuvers, given in Section VII (Section 7.2) will be discussed briefly with respect to their influence on the resolution* requirements of the collective and cyclic pitch control linkages.

7.3.1 Hovering Flight

In Section VI (6.3) it is shown that, when $\Omega = 1$, the magnitudes of collective and cyclic pitch required for a trimmed forward speed of 0.55 ft/sec and a y-velocity of 0.1 ft/sec are:

$$\delta_0 \cong .05 \text{ rad} \cong 2.9^\circ \quad (u = .55 \text{ ft/sec})$$

$$\delta_2 \cong .02 \text{ rad} \cong 1.1^\circ \quad (v = .1 \text{ ft/sec})$$

These values of δ_0 and δ_2 provide a rough indication of the resolution which would be needed in δ_0 and δ_2, if it is desired to achieve the very low speeds noted.

7.3.2 High-Speed Flight

In high-speed flight a measure of required blade angle resolution can be obtained from the steady-state transmission ratios that define the change in a given motion variable per unit change in the appropriate blade pitch angle.

(a) Forward Speed:

In Reference 1 it is shown that for straight and level flight at high speed ($u_0 \cong 40$ ft/sec) the relationship between change in speed, $\bar{u}$, and change in collective pitch, $\Delta\delta$, is:

$$X_{\Delta\delta}(\Delta\delta_f + \Delta\delta_a) \cong -X_u \bar{u} \quad **$$

---

* Resolution is taken to mean the least amount by which a given variable (e.g. $\dot{\psi}$, δ_0, u, $\dot{z}$ etc.) may be changed by control action.

** The second-order propeller drag term is neglected.

If $\Delta\delta_f = \Delta\delta_a = \Delta\delta$, $X_{\Delta\delta} = 660 \times 10^3$ lb/rad, and $X_u = -17.5 \times 10^3$ lb/ft per sec:

$$\frac{\Delta\delta}{u} \cong .013 \text{ rad/ft per sec, or } .76°/\text{ft per sec}$$

Thus, if a resolution in forward speed of 1 ft/sec is desired, a resolution in collective pitch of .76° is needed.

(b) Dive Angle:

At high speed, the steady-state dive angle (see Section 7.2.1) is given by:

$$\theta = -\frac{M_\delta}{M_\theta}(\delta_{1f} + \delta_{1a})$$

if $\delta_{1f} = \delta_{1a} = \delta_1$, $M_\delta = 30.25 \times 10^6$ ft-lb/rad* and $M_\theta = -9.63 \times 10^6$ ft-lb/rad*:

$$\frac{\theta}{\delta_1} \cong 6.3 \text{ degree/degree.}$$

The corresponding relationship for dive rate is:

$$\frac{\dot{z}}{\delta_1} = -u_0\left(\frac{\theta}{\delta_1}\right) \cong -4.3 \text{ ft/sec/degree}$$

(c) Yaw Rate:

It can be shown that the steady-state yaw rate per unit cosine-cyclic pitch (δ_2 ($\delta_{2f} = \delta_{2a} = \delta_2$) is given by:

$$\frac{\dot{\psi}}{\delta_2} = -\frac{2}{\frac{N_r}{N_\delta} + \frac{N_v}{N_\delta} \cdot \frac{m_1 u_0 - Y_r}{Y_v}}$$

It the proper numerical values for the stability derivatives and the mass*, m_1, are substituted in this expression the result is:

$$\frac{\dot{\psi}}{\delta_2} \cong 0.06 \frac{\text{degree/sec}}{\text{degree}}$$

---

* See Reference 1

If it is assumed that it is not required to operate at hovering speeds much lower than those indicated above, the blade angle resolution requirements will probably be determined by the high-speed flight conditions rather than the hovering conditions. The high-speed case is summarized below:

	Trim Condition	Approximate Resolution Needed
Forward Speed, u	40 ft/sec	0.76° in δ_0 for 1 ft/sec change in u
Dive Angle, θ	20°	0.16° in δ_1 for 1° change in θ
Dive Rate, $\dot{z}$	14 ft/sec	0.23° in δ_1 for 1 ft/sec change in $\dot{z}$
Yaw Rate, $\dot{\psi}$	1°/sec	17.0° in δ_2 for 1°/sec change in $\dot{\psi}$

From these calculations it is evident that the specifications to be placed on the resolution of δ_0, δ_1 and δ_2 will depend upon the minimum change (i.e., the least count) desired in the related motion variable. Based on these preliminary and incomplete* data, one might conclude that reasonable resolution requirements on blade pitch be: $\delta_0 \cong 1°$, $\delta_2 \cong 1°$ and $\delta_1 \cong 0.2°$.

* There may be maneuver requirements, other than dive rate, turn rate, etc., which influence blade angle resolution.

7.4 HANDLING QUALITIES OF THE TPS

A general consideration of handling qualities often include certain aspects of vehicle behavior that are related to the basic open-loop performance of the vehicle. Usually, an attempt is made to set up dynamic-performance criteria in terms of the response of the vehicle to specified control inputs (or a sequence of inputs). In the case of a submarine these criteria may relate, for example, to (1) the ability to perform a given diving rate, (2) the ability to turn at a given rate without exceeding specified limits on induced roll, (3) the specification of time lags or other dynamic measures of maneuvering performance, etc. etc. Efforts have been made to evolve such open-loop performance criteria, both in the case of surface ships* and submarines, by using the concept of definitive maneuvers. It is important to recognize that these performance criteria are limited, in the sense that they can only be used to "test" the vehicle and, possibly, its control linkage, but not the remaining elements of the overall vehicle-control loop (i.e., the pilot; control column dynamics; displays; etc.). Discussion of this type of performance parameter for the TPS is included elsewhere in this report, notably Sections II and VII (Section 7.2).

Although performance parameters of the type discussed above are important in judging the handling qualities of a given vehicle, such a judgment is incomplete without a consideration of other elements in the overall control loop of the vehicle. Here, one becomes involved in the effects of pilot skill, display dynamics, control-column dynamics, etc. on total system performance. Relating total system performance to handling qualities and evolving numerical handling qualities criteria therefrom, is a considerably more difficult task than that of specifying open-loop performance criteria. The reason for this difficulty is the wide variability (and adaptability) of the dynamics of the human operator. Accordingly, attempts at creating a priori criteria for judging total-system performance are usually descriptive in nature, rather than numerical. For example, we find such statements as "the vehicle should be capable of maintaining a straight and level flight path with a minimum of effort

---

* See Reference 9, for example.

on the part of the operator". Thus it is very often necessary to resort to closed-loop simulation techniques, with pilot included, or to full-scale vehicle tests in order to make some headway into the problem of defining the handling qualities of the total system. The extensive experience in the aircraft handling qualities field is notable in this respect.

The above discussion indicates that the objectives of the present program, as undertaken by Cornell Aeronautical Laboratory, Inc., are necessarily limited to a consideration of handling qualities as related to open-loop performance. Considerations of this type have been noted earlier and are treated in various sections of this report.

VIII

FUTURE WORK

Plans for future work are outlined below, in the form of five broad task statements. With the possible exception of the hydrodynamics studies, none of the tasks is considered to be completely independent of the others, and no particular chronological order is implied.

TASK 1: Submarine Hydrodynamics

Review the hydrodynamic theory developed by CAL and compare this with the theoretical and experimental work performed by the Netherlands Ship Model Basin. Attempt to arrive at a useable working theory for the unshrouded propeller hydrodynamics. Examine the applicable experimental results of the work of the NSMB related to shrouded propellers and hull hydrodynamics and, if possible, apply these results, in the form of simple modifications, to the present theory.

TASK 2: Performance Optimization

Investigate the problem of optimizing trimmed-flight operating conditions at zero and low forward speeds and at high speed. Take into account realistic power plant considerations, single and two-propeller performance goals and the trade-offs between these factors and geometric configuration factors.

Arrive at optimum design operating conditions and trim settings with the present configuration (16 blades, 3 ft^2 blade area, 50 rpm max. propeller speed), and an indication of design trade-offs achievable with other configurations.

TASK 3: Stability and Control

Perform such analog computer studies as may be necessary (high-speed case) to assist in the performance optimization task discussed above. Repeat the high-speed single-plane studies reported in Reference 1 and this report, if the results of Task 1 indicate that a revision is necessary in the applicable equations of motion. Perform a six-degree-of-freedom analog or digital computer simulation of the zero and low-speed cases. Investigate the medium speed regime analytically or via single-plane computer studies. Compare TPS performance with a conventional submarine and make final assessments of overall feasibility of the TPS concept as it relates to stability and control. On the basis of all previous work devise an all-speed preliminary control system configuration and attempt to judge the handling qualities of a TPS equipped with such a control system.

TASK 4: Impaired Operation

Select and investigate certain off-trim operating conditions which may arise due to failures or faults in the control system or its components, or to the application of external disturbances to the TPS. Examine such evidences of impaired operation as locked or jammed propellers, power failures, loss of control signals, etc. Utilize the single-plane analog computer mechanizations of Task 3, if necessary, in order to investigate these impaired operating conditions.

TASK 5: Control System Design

Utilizing the theoretical control system configuration of Task 3 as a point of departure, formulate a practical control system design. Specify control system component performance requirements and indicate ways of sensing the necessary stabilization and control signals. Indicate and define the features of automatic modes of operation, including depth-keeping, course-keeping and roll stabilization. Define the elements of the manual control mode of operation. Draw on the stability and control studies to describe manual control of the TPS in one-degree-of-freedom and interaction or coupling with other degrees-of-freedom.

The work-plan outlined above will form a logical continuation of the effort started under Contract Nonr 3659 (00) (FBM). It is designed to provide a sound basis for a final judgement on the feasibility of the tandem propeller concept as it relates to stability and control, and handling qualities. The broad objective of the program is to bring to a satisfactory conclusion the lines of investigation started in the current study and to extend these investigations, where necessary, to achieve the following goals: (1) the determination of overall feasibility, and (2) a preliminary design of a TPS control system.

IX

REFERENCES

1. "First Interim Report on the Hydrodynamics and Stability and Control of a Tandem Propeller Submarine". Cornell Aeronautical Laboratory Report No. AG-1634-V-1, 26 March 1962 by F. Dell'Amico and L. Segel. (U).

2. "Ship Control Information Study-Final Report". Cornell Aeronautical Laboratory Report No. IM-1306-V-2, 31 July 1959 by L. Bogdan, et al.

3. "Network Analysis" by M. E. VanValkenburg, Prentice-Hall, New Jersey, 1955.

4. "First Interim Report on Pitch Changing Systems for the Tandem Propeller". U413-62-092, General Dynamics/Electric Boat, March 31, 1962, (U).

5. "A Two Dimensional Approximation to the Unsteady Aerodynamics of Rotary Wings" by R. G. Loewy. Cornell Aeronautical Laboratory Report No. 75, October 1955. (U).

6. "Computation of Rotary Wing Harmonic Airloads and Comparison with Experimental Results". Proceedings of Eighteenth Annual Forum of the Amer. Helicopter Society, 2-4 May 1962.

7. "Force and Pressure Distribution Measurements on Eight Fuselages" by G. Lange, NACA TM-1194, October 1948.

8. "Effects of Fineness Ratio and Reynolds Number on the Low-Speed Crosswind Drag Characteristics of Circular and Modified Square Cylinders" by L. W. McKinney. NASA TN D-540, October 1960.

9. "Handling Quality Criteria for Surface Ships" by M. Gertler and S. C. Gover, First Symposium on Ship Maneuverability, 24-25 May 1960. David Taylor Model Basin, Washington, D. C.

10. Aerodynamics of the Helicopter (book), Gessow and Myers, The Mac Millan Company, 1952.

11. "Qualitative Discussion of the Hydrodynamic Properties of Tandem Propeller Systems With Cyclic Pitch Control". Netherland Ship Model Basin, February 1962. (U).

APPENDIX A

LOW-SPEED AXIAL-FORCE INTEGRAL

The average axial force is obtained by integrating Equation 4.1-6 over one cycle and dividing by 2π. These integrations can be performed in closed form only if the collective pitch, δ_0, the amplitudes of the cyclic pitch components, δ_1 and δ_2, and the velocities v_t and v_a, are constant. The integration is approximately valid if it is assumed that these variables change slowly with time over any one revolution of the propellers. Unless this assumption is made the vector propeller forces must be calculated for each individual blade, as a function of time, and superposed. A dynamic analysis of the automatically controlled submarine would become extremely difficult because it would be necessary to solve a set of simultaneous integro-differential equations for each set of conditions corresponding to a postulated control system configuration. The steady-state analysis is, of course, unaffected. Also, it can be argued that the conditions under which the assumption noted above is not valid correspond to conditions where unsteady hydrodynamic effects would also be significant.

The effect of the above assumptions on the work described herein, and in Reference 1, is dependent upon the severity of the transient phenomena involved. At high speeds ($\Omega \cong 50$) when, as a result of control action, the peak propeller blade angles of attack change rapidly in one revolution of the propellers, the results may be in considerable error over whatever time interval is involved in the transient. If these variables change relatively slowly, the results are quite accurate. At low speeds the effect of the above assumption is mitigated somewhat by the fact that all transient phenomena will be inherently "slow" phenomena because of the low force/moment levels involved and the large mass/inertia of the submarine.

The equation that predicts the average axial force follows:

$$F_x = +/+\left(\tfrac{1}{2}\rho AN/2\pi\right)\Big\{\int_0^{2\pi} v_t^2 C_{L\alpha}\left[\delta_0 + \delta_1 \sin\sigma + \delta_2 \cos\sigma\right] d\sigma$$

$$- \int_0^{2\pi} \gamma_a v_t \left(C_{L\alpha} + C_{d_0}\right) d\sigma$$

$$- \int_0^{2\pi} v_A v_t f_1 C_{L\alpha}^2 \left[\delta_0^2 + 2\delta_0\delta_1 \sin\sigma + 2\delta_0\delta_2 \cos\sigma + \delta_1^2 \sin^2\sigma\right.$$

$$\left. + 2\delta_1\delta_2 \sin\sigma\cos\sigma + \delta_2^2 \cos^2\sigma\right] d\sigma$$

$$+ \int_0^{2\pi} v_a^2 f_1 C_{L\alpha}^2 \left[2\delta_0 + 2\delta_1 \sin\sigma + 2\delta_2 \cos\sigma\right] d\sigma$$

$$- \int_0^{2\pi} \frac{v_a^3}{v_t} f_1 C_{L\alpha}^2 \, d\sigma \Big\}$$

or

$$F_x = +/+ \tfrac{1}{2}\rho A N \frac{1}{2\pi}\left\{ I_1 + I_2 + I_3 + I_4 + I_5 \right\}$$

Evaluating the integrals over one cycle:

$$I_1 = \int_0^{2\pi} C_{L_\alpha} R^3 \Omega^2 \left[1 + \frac{2p}{\Omega} + \frac{2(v+\gamma l_2)\cos\sigma}{R\Omega} + \frac{2(w-q l_2)\sin\sigma}{R\Omega}\right]\left[\delta_0 + \delta_1 \sin\sigma + \delta_2 \cos\sigma\right] d\sigma$$

$$= 2\pi C_{L_\alpha} R^3 \Omega^2 \left[\left(1 + \frac{2p}{\Omega}\right)\delta_0 + \delta_2 \frac{(v+\gamma l_2)}{R\Omega} + \frac{\delta_1 (w - q l_2)}{R\Omega}\right]$$

$$I_2 = -\int_0^{2\pi} (C_{L_\alpha} + C_{d_0}) R^3 \Omega^2 \left[\frac{u+i}{R\Omega} - \frac{q\cos\sigma}{\Omega} - \frac{r\sin\sigma}{\Omega}\right] d\sigma$$

$$= -2\pi R^3 \Omega^2 (C_{L_\alpha} + C_{d_0})\left(\frac{u+i}{R\Omega}\right)$$

$$I_3 = -\int_0^{2\pi} f_1 C_{L_\alpha}^2 R^3 \Omega^2 \left[\frac{u+i}{R\Omega} - \frac{q\cos\sigma}{\Omega} - \frac{r\sin\sigma}{\Omega}\right]\left[\delta_0^2 + 2\delta_0\delta_1 \sin\sigma\right.$$

$$\left. + 2\delta_0\delta_2\cos\sigma + \delta_1^2 \sin^2\sigma + 2\delta_1\delta_2 \sin\sigma\cos\sigma + \delta_2^2 \cos^2\sigma\right] d\sigma$$

$$= -2\pi f_1 C_{L_\alpha}^2 R^3 \Omega^2 \left[\left(\frac{u+i}{R\Omega}\right)\left(\delta_0^2 + \frac{\delta_1^2}{2} + \frac{\delta_2^2}{2}\right) - \frac{\delta_0\delta_2 q}{\Omega^2}\right.$$

$$\left. - \frac{\delta_0\delta_1 r}{\Omega}\right]$$

$$I_4 = \int_0^{2\pi} R^2\Omega^2 f_1 C_{L\alpha}^2 \left\{\left(\frac{u+\lambda}{R\Omega}\right)^2 - 2\left(\frac{u+\lambda}{R\Omega}\right)\left(\frac{q\cos\sigma}{\Omega} + \frac{r\sin\sigma}{\Omega}\right) + \frac{2qr\sin\sigma\cos\sigma}{\Omega^2} + \frac{q^2\cos\sigma}{\Omega^2} + \frac{r^2\sin^2\sigma}{\Omega^2}\right\}\left\{2\delta_0 + 2\delta_1\sin\sigma + 2\delta_2\cos\sigma\right\} d\sigma$$

$$= R^2\Omega^2 2\pi f_1 C_{L\alpha}^2 \left\{2\left(\frac{u+\lambda}{R\Omega}\right)^2\delta_0 - 2\left(\frac{u+\lambda}{R\Omega}\right)\left(\frac{\delta_1 q}{\Omega} + \frac{\delta_2 r}{\Omega}\right) + \delta_0\left[\frac{q^2+r^2}{\Omega^2}\right]\right\}$$

$$I_5 = -\int_0^{2\pi} R^3\Omega^2 f_1 C_{L\alpha}^2 \left\{\left(\frac{u+\lambda}{R\Omega}\right)^2 - 2\left(\frac{u+\lambda}{R\Omega}\right)\left(\frac{q\cos\sigma}{\Omega} + \frac{r\sin\sigma}{\Omega}\right) + \frac{2qr\sin\sigma\cos\sigma}{\Omega^2} + \frac{q^2\cos^2\sigma}{\Omega^2} + \frac{r^2\sin^2\sigma}{\Omega^2}\right\}\left\{\frac{u+\lambda}{R\Omega}\right\}\left\{1 - \frac{e}{\Omega} - \left(\frac{Rq}{u+\lambda} + \frac{u+rl_2}{R\Omega}\right)\cos\sigma - \left(\frac{Rr}{u+\lambda} + \frac{w-ql_2}{R\Omega}\right)\sin\sigma\right\} d\sigma$$

$$= -2\pi R^2\Omega^2 f_1 C_{L\alpha}^2 \left\{\left(\frac{u+\lambda}{R\Omega}\right)^3\left(1-\frac{e}{\Omega}\right) + \left(\frac{u+\lambda}{R\Omega}\right)\left(1-\frac{e}{\Omega}\right)\left(\frac{q^2+r^2}{2\Omega^2}\right) + \left(\frac{u+\lambda}{R\Omega}\right)^2\left(\frac{Rq}{u+\lambda} + \frac{u+rl_2}{R\Omega}\right)\frac{q}{\Omega} + \left(\frac{u+\lambda}{R\Omega}\right)^2\left(\frac{Rr}{u+\lambda} + \frac{w-ql_2}{R\Omega}\right)\frac{r}{\Omega}\right\}$$

In collecting the integrals all terms involving q^2, r^2, qr, qr and rr are discarded and the substitution $\frac{1}{2}\rho AN\Omega^2R^2 = Q$ is made. F_x then becomes:

$$F_x = W + Q\left\{C_{L_\alpha}\left[\left(1+\frac{2\rho}{\Omega}\right)\delta_0 + \left(\frac{r+rl_2}{R\Omega}\right)\delta_2 + \left(\frac{r-ql_2}{R\Omega}\right)\delta_1 + \left(\frac{u+i}{R\Omega}\right)\right]\right.$$

$$- C_{d_0}\left[\frac{u+i}{R\Omega}\right]$$

$$- f_1 C_{L_\alpha}{}^2\left[\left(\frac{u+i}{R\Omega}\right)\left(\delta_0{}^2 + \frac{\delta_1{}^2}{2} + \frac{\delta_2{}^2}{2} + \frac{2\delta_2 q}{\Omega} + \frac{2\delta_1 r}{\Omega}\right)\right.$$

$$- \left(\frac{u+i}{R\Omega}\right)^2\left(2\delta_0\right)$$

$$+ \left(\frac{u+i}{R\Omega}\right)^3\left(1-\frac{\rho}{\Omega}\right)$$

$$\left.\left. - \left(\frac{\delta_0\delta_2 q}{\Omega} + \frac{\delta_0\delta_1 r}{\Omega}\right)\right]\right\}$$

APPENDIX B

STABILITY DERIVATIVES AND CONTROL COEFFICIENTS - SINGLE PROPELLER OPERATION

Consider the case of a locked forward propeller and a rotating aft propeller. The propeller derivative Y_v^p (i.e. side force due to sideslip velocity) is basic in the calculation of all of the non-zero propeller derivatives. As noted in Reference 1*,

$$Y_v^p)_{f,a} = \frac{-2|M_{xo}|(1-\lambda_{Qf,a})}{R^2 \Omega_{f,a}} \qquad \text{(B-1)}$$

It is apparent that Equation (B-1) cannot be used in its present form to calculate $Y_v^p)_f$, because $\Omega_f = 0$. This problem was resolved by substituting λ_{af}, as defined in Reference 1, page 25, and taking the limit value of the combined expression as Ω_f approaches zero. Further, from Equation (6-7), Reference 1, the trim rolling moment is given by:

$$|M_{xo}| = \tfrac{1}{2}\rho U_o^2 ANRC_{L_\alpha}|\alpha_f| \qquad \text{(B-2)}$$

---

* $|M_{xo}|_f = |M_{xo}|_a$ because the rolling moments are balanced for trimmed operation.

Substituting Equation (B-2) into the limit form of Equation (B-1), the final expression for $Y_{\dot{x}}^{\rho})_f$ is obtained as follows:

$$Y_{\dot{x}}^{\rho})_f = -\tfrac{1}{2}\rho U_o A N\left\{C_{L_\alpha} + C_{d_o} + f_i C_{L_\alpha}^2 \alpha_f^2\right\} \qquad \text{(B-3)}$$

The aft propeller value of $Y_{\dot{x}}^{\rho})_a$ can be computed directly from Equation (B-1) after the required values of $|M_{\dot{x}_o}|$ and λ_{Q_a} are determined.

The combined propeller contributions to the total value of the stability derivatives are computed from the following equations, taken from Reference 1, pages 28 and 29:

$$Y_{\dot{x}}^{\rho} = Y_{\dot{x}}^{\rho})_f + Y_{\dot{x}}^{\rho})_a$$

$$Y_x^{\rho} = \ell_2\left\{Y_{\dot{x}}^{\rho})_f - Y_{\dot{x}}^{\rho})_a\right\}$$

$$Y_\rho^{\rho} = N_\rho^{\rho} = K_{\dot{x}}^{\rho} = K_x^{\rho} = 0$$

$$N_{\dot{x}}^{\rho} = Y_x^{\rho}$$

$$N_x^{\rho} = \ell_2^2 Y_{\dot{x}}^{\rho} + N_x^{\rho})_f^* + N_x^{\rho})_a^* \approx \ell_2^2 Y_{\dot{x}}^{\rho}$$

$$K_\rho^{\rho} = R^2 Y_{\dot{x}}^{\rho}$$

---

*The terms $N_x^{\rho})_f$, a are negligible.

The stability derivatives of the hull are directly proportional to submarine speed. Since the single-propeller trim speed is 61% of the two-propeller value, the corresponding hull derivatives must be reduced to 61% of the values listed in Table 6-2, Reference 1. The modified propeller derivatives must be added to the modified hull derivatives to obtain the total derivatives that apply to the case of single-propeller operation.

In order to estimate the amount of control power required to counteract the gyroscopic coupling resulting from unbalanced operation of the propellers, it is necessary to compute (1) the angular momentum of the rotating propeller, (2) the pitching moment control coefficients, and (3) the propeller stability derivatives, $M_{\dot{w}}$ and N_q . It is shown later in this section, that knowledge of these quantities is both necessary and sufficient for this estimate.

The moment of inertia of the rotating propeller about the longitudinal axis of the submarine was calculated on the assumption that the complete propeller and drive assembly can be approximated by a right circular cylinder with an outside diameter of twenty feet, an inside diameter of fourteen feet, a length of 3.5 feet, and a weight of 125 tons (see Reference 4). The polar moment of inertia of the propeller was computed to be:

$$I_p = 521{,}000 \text{ LB. FT. SEC.}^2$$

For a propeller angular velocity of 50 rpm, the angular momentum is found to be:

$$H = I_p \Omega = (521{,}000)\left(\frac{2\pi}{60}\right)(50) = 2.72 \times 10^6 \text{ FT. LB. SEC.}$$

The pitching moment control term is given by:

$$M_c = M_{\delta_f}\,\delta_{1_f} + M_{\delta_a}\,\delta_{1_a} \tag{B-4}$$

where: $M_{\delta_f} = -N_{\delta_f}$ and $M_{\delta_a} = -N_{\delta_a}$; see Equations (7.2-16).

The yaw-pitch coupling derivative, M_r is defined in Reference 1, (pg 29) to be:

$$M_r = \ell_2\left\{M_v^{\rho})_f - M_r^{\rho})_a - Z_r^{\rho})_f + Z_r^{\rho})_a\right\} \tag{B-5}$$

The individual terms in Equation (B-5) are, in turn, defined in Table 5-2, Reference 1*.

---

*The indeterminate form that results from attempting to compute $M_r^{\rho})_f$, when $\ell_f \to 0$, is resolved by substituting λ_T (Reference 1, pg 25) and taking the limit as ℓ_f approaches zero. In addition, the trim thrusts of the fore and aft propellers are found from:

$$F_{x_0})_f = -\tfrac{1}{2}\rho U_o^2 AN\left(C_{d_0} + f_1 C_{L_\alpha}^2\,\alpha_f^2\right)$$

$$F_{x_0})_a = \tfrac{1}{2}\rho\,\frac{U_o^2 AN}{SIN^2\,\partial_a}\left\{C_{L_\alpha}\alpha_a \cos\partial_a - SIN\,\partial_a\left[C_{d_0} + f_1 C_{L_\alpha}^2\,\alpha_a^2\right]\right\}$$

Table B-1 tabulates the numerical values of the yaw-plane stability derivatives (plus the yaw-pitch plane coupling terms) that prevail for single-propeller operation with the aft propeller thrusting. Note that, unlike the case for balanced operation, Z_r and M_r are non-zero, indicating that yaw-pitch coupling is more severe for the unbalanced operation case.

When the aft propeller is locked and the forward propeller is thrusting, the individual propeller derivatives can be computed by interchanging the subscripts a and f in Equations (7.2-16), (B-2), and (B-3) and substituting numerical values in the expressions for the total derivatives. The results are tabulated in Table B-2.

TABLE B-1

SINGLE PROPELLER OPERATION - AFT PROPELLER THRUSTING

Function	Fwd Prop	Aft Prop	Hull	Total	Units
Ω	0	50	-	-	rpm
α	14.7	4.8	-	-	deg
σ	90	23	-	-	deg
λ_ϕ	1.0	-1.597	-	-	-
λ_T	1.0	-2.11	-	-	-
$\lvert M_{x_0} \rvert$	291,000	291,000	-	-	ft-lb
F_{z_0}	-3320	50,000	-	-	lb
N_δ	-5.66×10^6	-16.91×10^6	-	-	ft-lb/rad
Y_δ	-51,400	-154,000	-	-	lb/rad
$K_{\Delta\delta}$	-1.13×10^6	-3.38×10^6	-	-	ft-lb/rad
M_δ	5.66×10^6	16.91×10^6	-	-	ft-lb/rad
Y_v	-4330	-2390	-38,690	-45,410	lb-sec/ft
Y_r	-476.5×10^3	-262.8×10^3	-763×10^3	-977×10^3	lb-sec/rad
Y_p	0	0	-283×10^3	-283×10^3	lb-sec/rad
N_v	-476.5×10^3	-262.8×10^3	-4.38×10^6	-4.59×10^6	ft-lb-sec/ft
N_r	-52.42×10^6	-28.91×10^6	-101×10^6	-182×10^6	ft-lb-sec/ra
N_p	0	0	-1.70×10^6	-1.70×10^6	ft-lb-sec/ra
K_v	0	0	-286×10^3	-286×10^3	ft-lb-sec/ft
K_r	0	0	-17.3×10^6	-17.3×10^6	ft-lb-sec/ra
K_p	-524×10^3	-289×10^3	-6.54×10^6	-7.35×10^6	ft-lb-sec/ra
Z_r	11,840	18,910	-	30,750	lb-sec/rad
M_v	-1725	59,450	-	57,700	ft-lb-sec/ft
M_r	$-1.4[illegible] \times 10^6$	-4.46×10^6	-	-5.95×10^6	ft-lb-sec/ra
$\lvert H \rvert$	0	2.72×10^6	-	2.72×10^6	ft-lb-sec/ra

TABLE B-2

SINGLE PROPELLER OPERATION - FWD PROPELLER THRUSTING

Function	Fwd Prop	Aft Prop	Hull	Total	Units
Ω	50	0	-	-	rpm
α	4.8	14.7	-	-	deg
σ	23	90	-	-	deg
λ_ρ	-1.597	1.00	-	-	-
λ_T	-2.11	1.00	-	-	-
$\lvert M_{z_0} \rvert$	291,000	291,000	-	-	ft-lb
F_{z_0}	50,000	-3320	-	-	lb
N_δ	-16.91×10^6	-5.66×10^6	-	-	ft-lb/rad
Y_δ	-154,000	-51,400	-	-	lb/rad
$K_{\Delta\delta}$	-3.38×10^6	-1.13×10^6	-	-	ft-lb/rad
M_δ	16.91×10^6	5.66×10^6	-	-	ft-lb/rad
Y_v	-2390	-4330	-38,690	-45,410	lb-sec/ft
Y_r	-262,800	-476,500	-763,000	-549,000	lb-sec/rad
Y_p	0	0	-283,000	-283,000	lb-sec/rad
N_v	-262,800	-476,500	-4.38×10^6	-4.17×10^6	ft-lb-sec/ft
N_r	-28.91×10^6	-52.42×10^6	-101×10^6	-182×10^6	ft-lb-sec/rad
N_p	0	0	-1.70×10^6	-1.70×10^6	ft-lb-sec/rad
K_v	0	0	-286,000	-286,000	ft-lb-sec/ft
K_r	0	0	-17.3×10^6	-17.3×10^6	ft-lb-sec/rad
K_p	-289,000	-524,000	-6.54×10^6	-7.35×10^6	ft-lb-sec/rad
Z_r	-18,910	-11,840	-	30,750	lb-sec/rad
M_v	-59,450	1725	-	-57,700	ft-lb-sec/ft
M_r	-4.46×10^6	-1.49×10^6	-	-5.95×10^6	ft-lb-sec/rad
$\lvert H \rvert$	2.72×10^6	0	-	2.72×10^6	ft-lb-sec/rad

APPENDIX C

PROPELLER-INDUCED AXIAL INFLOW VELOCITY

An expression for the axial component of propeller-induced inflow velocity (derived from combined blade element-momentum theory) that includes the effect of forward velocity, u, is given in Reference 10 as:

$$\lambda = \left(\frac{u}{2} + \frac{NCkC_{L_\alpha}R\Omega}{16\pi R}\right)\left\{-1+\sqrt{1+\frac{2R\Omega\left(\delta_0 - \frac{u}{R\Omega}\right)}{\frac{4\pi u^2}{NCkC_{L_\alpha}\Omega} + u + \frac{NCkC_{L_\alpha}\Omega}{16\pi}}}\right\} \quad \text{(C-1)}$$

in which C_k is the propeller blade chord and all other symbols are as previously defined. If the following substitutions are made:

$$\alpha_u = \delta_0 - \frac{u}{R\Omega}$$

$$B = NCk/2\pi R \cong 2 \quad \text{(for the postulated configuration)}$$

$$C_{L_\alpha} = 5.7$$

(C-1) becomes:

$$\frac{\lambda}{R\Omega} = \left(\frac{u}{2R\Omega} + \frac{1}{4}\right)\left\{-1 + \sqrt{1 + \frac{2\alpha u}{\left(\frac{u}{R\Omega}\right)^2 + \frac{u}{R\Omega} + \frac{1}{4}}}\right\} \qquad \text{(C-2)}$$

The inflow at hovering conditions, Equation (4.1-38), was found by letting $u = 0$ in (C-2) and curve-fitting a quadratic to a plot of $\lambda/R\Omega$ vs δ_0. The following expression:

$$\frac{\lambda}{R\Omega} \cong a\delta_0 + b\delta_0|\delta_0| \qquad \text{(C-3)}$$

was obtained, with $a = .95$ and $b = -1.0$, and yields values of $\frac{\lambda}{R\Omega}$ accurate to within better than 10% for δ_0 up to about 0.3 rad. The values of a and b given in Reference 1(.86 and -.60 respectively) are considered to be less accurate than the values cited above for the conditions that actually prevail.

For the low-forward speed work of Section 6.3 a form of (C-2) is used in which the square-root term is replaced by the first two terms of a binomial expansion. This procedure is fairly accurate if the second term under the radical satisfies the restriction* that

$$\frac{2\alpha u}{\left(\frac{u}{R\Omega}\right)^2 + \left(\frac{u}{R\Omega}\right) + \frac{1}{4}} < \frac{1}{2} \qquad \text{(C-4)}$$

Thus, (C-2) becomes.

$$\frac{\lambda}{R\Omega} \cong \left(\frac{u}{2\Omega R} + \frac{1}{4}\right)\left(\frac{\alpha u}{\left(\frac{u}{R\Omega}\right)^2 + \frac{u}{R\Omega} + \frac{1}{4}}\right) \qquad \text{(C-5)}$$

---

*This condition should be checked for each case being considered.